Pathways for Quality Control of Misfolded Cytosolic Proteins

A DISSERTATION
SUBMITTED TO THE DEPARTMENT OF BIOLOGICAL SCIENCES
AND THE COMMITTEE OF GRADUATE STUDIES
OF STANFORD UNIVERSITY
FOR THE DEGREE OF
DOCTOR IN PHILOSOPHY

Daniel Kaganovich

December 2007

I certify that I have read this dissertation and that in my opinion it is fully adequate, in scope and quality, as a dissertation for the degree of Doctor of Philosophy.

_____
Judith Frydman (Principal Advisor)

I certify that I have read this dissertation and that in my opinion it is fully adequate, in
scope and quality, as a dissertation for the degree of Doctor of Philosophy.

_____
Bill Burkholder

I certify that I have read this dissertation and that in my opinion it is fully adequate, in
scope and quality, as a dissertation for the degree of Doctor of Philosophy.

_____
Tim Stearns

Approved for the University Committee on Graduate Studies:

_____

ABSTRACT

Pathways for Quality Control of Misfolded Cytosolic Proteins

Daniel Kaganovich, PhD
Stanford University, 2007

Advisor: Judith Frydman

Accumulation of misfolded proteins in intracellular amyloid inclusions is a hallmark of many neurodegenerative diseases, including Parkinson's, Huntington's and Prion Disease. These inclusions are proposed to arise upon failure of the Quality Control (QC) mechanisms that prevent the cellular build-up of misfolded proteins. While the inclusions found in each disease often contain structurally and functionally unrelated proteins, they exhibit strikingly similar cellular phenotypes. Specifically, inclusions found in affected tissues contain aggregated polypeptides, often in the amyloid form, and stain positive for ubiquitin and molecular chaperones. It is thought that all these disease-causing proteins share a propensity to aggregate and adopt non-native conformations that exhibit a toxic gain-of-function interaction with essential cellular processes. Though inclusion formation is now understood to be a highly regulated process essential for cell viability and homeostasis, little is known about the cellular pathways that direct aggregated proteins to inclusions. The strong correlation between the accumulation of aggregated proteins in inclusions and the onset of disease calls for a better understanding of the mechanisms and functions of inclusion formation. Here we examine the formation of protein inclusions in the eukaryotic cytosol. We demonstrate that there is a general cellular pathway that distinguishes between soluble misfolded proteins and insolubly aggregated proteins, and directs their transport to one of two inclusions. Soluble ubiquitinated misfolded proteins that can be degraded by the proteasome or refolded are

targeted to a juxtanuclear quality control compartment that co-localizes with proteasomes and other quality control components, while insoluble aggregates are sequestered in a cytosolic inclusion that may later be processed by the autophagic pathway. Strikingly, disease-associated Huntingtin and prion proteins are preferentially directed to the perivacuolar compartment. Enhancing ubiquitination of a prion protein suffices to promote its delivery to the juxtanuclear inclusion. The mis-targeting of the amyloidogenic prion renders it toxic to the cell, suggesting that proper sorting of aggregated proteins to inclusions is essential for preventing toxicity. The identification of ubiquitination as a signal directing misfolded proteins to distinct subcellular quality control compartments provides a framework for understanding the preferential accumulation of amyloidogenic proteins linked to human disease.

Approved for publication:

By:_____
For The Department of Biological Sciences

Acknowledgements

I am grateful to my thesis advisor, Judith Frydman, for so many things including her unwavering support and her constant encouragement and good will. Besides being a truly excellent advisor, Judith has also been a true mentor for me, and I am happy to have been a student in her lab. Judith has always expressed strong, and sometimes unjustified, confidence in my abilities as a scientist; she was also extremely patient and supportive for the period of time that it took me to get my thesis project going. The fact that we were able to get some interesting results is not only due to her direction and advice, but in no small part to her patience and her belief in this project. Judith has also always been very kind to me, and seems to always have my best interests in mind. I am thankful for the many things I've learned from her and for our exciting and productive work together.

Members of my thesis committee, in particular Bill Burkholder and Tim Stearns, have been extremely helpful and supportive over the duration of my thesis. I would like to thank both of them for valuable guidance and assistance. Bill has always had his door open for me to talk and get important advice, and he has provided both valuable scientific and technical help, as well as words of encouragement and moral support.

I would like to thank co-workers and collaborators who have helped me in countless ways with this work and with the thesis. Jeremy England has provided extensive valuable discussion and editorial help with this entire project, in fact he is by now at least as familiar with it as I am. Mark Kaganovich provided substantial assistance and valuable comments and discussion. I have gotten a lot of help from Ron Geller in the Frydman lab, both in terms of technical support and discussion. All of the members of the Frydman lab have provided a wonderful environment to work in, and have given me much assistance. Members of the Nelson lab, particularly So Yamada and Shirin Bahmanyar, have also been extremely helpful and have added to the exciting research environment. I would also like to thank other collaborators for experimental guidance and assistance, especially Ron Kopito and Jon Mulholland.

I owe a debt of gratitude to RSI and CEE which has been incredibly supportive of my scientific development from the very beginning, and which has been a source of friends and community for me since before college. My family has also been very helpful with this project, and my parents have provided many valuable things including their generous gift of chromosomal DNA. I hope to continue collaborating with them on many future projects.

Finally, I will always be in the debt of my close friend and wonderful mentor, Harold Amos. Harold has had the most influence of anyone on the way I think about science and about my career as a scientist. He had the gift of only seeing the best in people, and everyone who interacted with him or worked with him came away with the impression that they were extraordinary and brilliant individuals. In fact, it was Harold who was extraordinary and I hope to live up to his expectations of me and my scientific career. He is my model and inspiration for being a scientist as well as decent person.

I initially learned to do microscopy working with Harold. Though he had already been retired for many many years, upon reading somewhere that certain transporters in human cells re-distribute under certain conditions, he was compelled to immediately test their behavior under his own experimental conditions, so we took over a new microscope of someone in the department and started doing immune-fluorescence.

He still plays an important role in how I design and carry out experiments, and how I approach science and mentorship.

Table of Contents

Abstract iv

Acknowledgements vi

List of Figures x

Publication of chapters and role of author xi

CHAPTER 1
Introduction: Protein Misfolding and Aggregation

Section 1.1: Protein Folding Homeostasis 2

Section 1.2: Ubiquitin Proteasome System 2

Section 1.3: Chaperones and Quality Control of Protein Folding 4

Section 1.4: Modular Proteins Link Chaperones to Degradation 5

Section 1.5: Quality control E3 Ligases 6

Section 1.6: Protein Misfolding and Molecular Chaperones 9

Section 1.7: Protein Aggregation and Inclusion Formation 11

Section 1.8: Effect of Protein Aggregates on Cellular Protein Folding Homeostasis 14

Section 1.9: References 19

CHAPTER 2
Ubiquitination determines the partitioning of misfolded proteins between two distinct subcellular quality control compartments

Section 2.1: Summary 28

Section 2.2: Introduction 28

Section 2.3: Results 30

Section 2.4: Discussion 42

Section 2.5: Methods 45

Section 2.6: Acknowledgements 50

Section 2.7: References 80

CHAPTER 3

Failure to Sequester Amyloidogenic Proteins in Insoluble Inclusion Underlies Toxicity of Aggregated Proteins in Yeast

Section 3.1: Summary 87
Section 3.2: Introduction 88
Section 3.3: Results 93
Section 3.4: Discussion 95
Section 3.5: Methods 98
Section 3.6: Acknowledgements 101
Section 3.7: References 115

CHAPTER 4

Conclusion and Future Directions

Section 4.1: Summary 120
Section 4.2: Future Directions 122
Section 4.3: References 126

List of Figures

Figure 1.1: Quality control of protein folding in the cytosol……18

Figure 2.1: A thermally destabilized QC substrate accumulates in two distinct inclusions upon proteasome impairment……51

Figure 2.2: A panel of QC substrates defines two distinct compartments for the sequestration of misfolded cytosolic proteins……57

Figure 2.3: Mammalian cells differentially sequester misfolded proteins in two distinct compartments……59

Figure 2.4: Differential solubility of misfolded substrates in the distinct quality control compartments……62

Figure 2.5a-c: JUNQ co-localizes with NE and ER……...65

Figure 2.5d: JUNQ co-localizes with proteasomes……66

Figure 2.5e: JUNQ and IPOD co-localize with Hsp104……...67

Figure 2.5f-g: IPOD may have autophagic function……68

Figure 2.5h-i: IPOD may have autophagic function……69

Figure 2.6a-f: Ubiquitination determines partitioning to JUNQ or IPOD...……72

Figure 2.6g-i: Ubiquitination determines partitioning to JUNQ or IPOD……73

Figure 2.6j-n: The Sti1 chaperone is required for VHL ubiquitination and degradation..74

Figure 2.6o-r: Ubiquitination suffices to promote prion delivery to the JUNQ ……75

Figure 2.6s-t: Recovery of diffuse cytosolic fluorescence by thermally denatured GFP-Ubc9^{ts} accumulated in the JUNQ……...76

Figure 3.1: Ubiquitination re-routs Rnq1 to the JUNQ where it causes cytotoxicity…102

Figure 3.2: HttQ103ΔP toxicity correlates to its redistribution from IPOD to JUNQ..104

Figure 3.3: Toxic aggregation-prone proteins inhibit VHL degradation, while labile aggregates do not……106

Figure 3.4: JUNQ and IPOD show differential interaction with cellular chaperones.109

Figure 3.5: Hsp70 suppresses Ub-Rnq1 toxicity……111

Figure 3.6: Hsp104 and Atg8 localize to an IPOD-like structure in the absence of ectopic expression of an aggregation-prone protein……113

Figure 4.1: Using reporters to assess which stages of the quality control pathway are inhibited by toxic misfolded proteins……..125

PUBLICATION OF CHAPTERS AND ROLE OF AUTHOR

All experiments described in this dissertation were performed by me. The experiments were developed and designed by me together with my advisor, Judith Frydman. Several experiments were also designed and carried out together with Ron Kopito.

Parts of Chapter 1 are published as a review:

McClellan, A. J., Tam, S., Kaganovich, D. & Frydman, J. Protein quality control: chaperones culling corrupt conformations. Nat Cell Biol 7, 736-41 (2005).
It was co-written by all of the authors.

Chapter 2 has been submitted and is currently under review in *Nature*.

Kaganovich, D., Kopito, R., Frydman, J. Ubiquitination determines the partitioning of misfolded proteins between two distinct subcellular quality control compartments.

Chapter 1

Introduction

Protein Misfolding and Aggregation

Section 1.1: Protein Folding Homeostasis

The misfolding of proteins in the cell, and the resulting accumulation of non-native polypeptides disrupts cellular homeostasis and can eventually lead to toxicity and cell death. Accordingly, cells contain an elaborate enzymatic machinery of molecular chaperones that bind non-native polypeptides and promote their folding into the native state in an ATP-dependent manner (Hartl, 2002; McClellan and Frydman, 2001). However, many cellular events such as genetic mutation, biosynthetic errors, heat-denaturation, oxidative damage, or the absence of a necessary post-translational binding partner result in protein misfolding. Abundance of non-native proteins is thought to cause toxicity in several ways: (1) by titrating out cellular factors necessary for viability, (2) by inhibiting protein function, (3) by inhibiting protein turnover and other homeostatic processes, and (4) by forming insoluble oligomeric aggregates which may have harmful gain-of-function effects (Bennett et al., 2005; Dobson, 2004; Muchowski, 2002; Sakahira et al., 2002; Schaffar et al., 2004). Consequently, protein misfolding and protein aggregation are closely linked to many human disease states, including many neurodegenerative diseases (Caughey and Lansbury, 2003).

For these reasons, the cell devotes a significant amount of energy to ensuring that proteins reach their native state upon translation, maintaining the folded state of intracellular proteins, and preventing the accumulation of aberrant proteins. Two main classes of regulators – the chaperone system, which recognizes and binds to misfolded proteins, and the ubiquitin-proteasome system (UPS), which destroys them – function to maintain the balance between protein folding and degradation, and together constitute the cellular quality control system (Fig. 1.1) (Hohfeld et al., 2001).

Section 1.2: Ubiquitin Proteasome System

In eukaryotic cells, the UPS is the major pathway for cellular protein turnover, including the elimination of misfolded proteins (Hershko and Ciechanover, 1998; Wolf and Hilt, 2004). As a result, blocking its function pharmacologically or genetically inhibits the

clearance of misfolded proteins and eventually leads to the formation of intracellular aggregates (Goldberg, 2003). The proteolytic system is comprised of the 26S proteasome, a 2.4 MDa complex which includes a 20S catalytic core particle (CP) housing three sets of active sites for proteolysis, and one or two 19S regulatory particle (RP) complexes responsible for the recognition, de-ubiquitination, unfolding, and processive threading of the substrate into the core for degradation (Pickart and Cohen, 2004; Zwickl et al., 1999). The 20S CP comprises 4 rings with seven subunits each, with β subunits containing threonine protease active sites on the two interior rings, and α subunits which bind the 19S RP on the two exterior rings. The 20S complex contains an axial channel, through which all degradation substrates must be translocated in order to gain access to the active sites, and which is gated by the N-termini of the α subunits (Kisselev et al., 2002). The 19S RP consists of a base complex which acts as a AAA ATPase, which unfolds proteins and translocates linear polypeptites into the CP, and a lid complex which recognizes ubiquitinated substrates, edits or removes the ubiquitin chain, and mediates substrate delivery and recognition.

A separate system regulates the targeting of substrates to the proteasome through the addition of a poly-ubiquitin tag to a substrate lysine through an isopeptide bond, and consists of a growing number of factors including an E1 ubiquitin-activating enzyme, several E2 ubiquitin-conjugating enzymes, and a vast array of E3 ligases which target the ubiquitination machinery to specific substrates (Hershko and Ciechanover, 1998). A sub-class of regulators such as E4 ubiquitin ligases and de-ubiquitinating (DUB) enzymes with isopeptidase activity regulate the length and structure of the poly-ubiquitin chain (Hoppe, 2005). A family of ubiquitin-like (UBL) and ubiquitin-associated (UBA) domain-containing proteins are thought to facilitate substrate transfer to the 26S proteasome and the coupling of ubiquitination, de-ubiquitination, and proteolysis (Hartmann-Petersen et al., 2003).

Proteins are earmarked for UPS-mediated degradation by the covalent attachment of a poly-ubiquitin chain(s), which is recognized by the 26*S* proteasome (Hershko and Ciechanover, 1998; Wolf and Hilt, 2004). With few exceptions, only substrates targeted to the proteasome by poly-ubiquitination are able to gain access to its proteolytic core. Ubiquitination is a multi-step process involving an E1 ubiquitin-activating enzyme, E2

ubiquitin-conjugating enzymes, and E3 ubiquitin ligases which select the substrate and facilitate ubiquitination. Polyubiquitination of some proteins also requires so-called E4 enzymes that cooperate with E3 ligases to extend the polyubiquitin chain (Hoppe, 2005). A group of ubiquitin-binding proteins which includes Rad23(hHR23), Rpn10(S5a), and Dsk2 (hPlic-2) have also been shown to facilitate ubiquitinated substrate delivery to the 26S, binding the poly-ubiquitin chain via a ubiquitin associated (UBA) domain, and the proteasome via a ubiquitin-like (UBL) domain, which usually docks at the Rpn1 subunit of the RP. While it has long been known that the yeast E2s Ubc4/5 and Ubc6/7 are involved in the ubiquitination of misfolded proteins (Cyr et al., 2002), specific E3s for these proteins have been more elusive. However, a number of candidate E3 ligases for quality control of cytosolic proteins have been described in recent years.

Section 1.3: Chaperones and Quality Control of Protein Folding

Chaperones are the first buffer between misfolded proteins and aggregated or toxic species (Dobson, 2003). Various chaperones are thought to be involved in every aspect of the quality control pathway. Some, like Hsp70, which recognizes exposed hydrophobic stretches, and Hsp90, can bind misfolded proteins and attempt to refold them and help restore their native state (Cashikar et al., 2005). Other chaperones, such as Hsp104, a AAA ATPase, and Hsp40, may in some cases disaggregate large or intermediate-sized aggregates (Muchowski, 2002). Chaperone function is also coupled to the elimination of non-native conformers by the proteasome in at least two ways. First, chaperones are thought to be essential for unfolding a substrate protein so that it can enter the narrow axial channel of the 20S proteolytic subunit (Kopito, 2000). In *E. coli*, the ATPase rings of ClpAP and ClpXP , Hsp104 homologues ClpA and ClpX, mediate ATP-dependent unfolding of target proteins before they are transferred to the proteolytic complex for degradation (McGinness et al., 2007; Wickner et al., 1999). In eukaryotes, the 19S proteasome subunit is thought to have the same substrate unfolding activity, and also possesses AAA ATPase function (Pickart and Cohen, 2004).

The second role chaperones are thought to play in degradation of misfolded proteins is that of modulators between folding and destruction (Esser et al., 2004). There is a growing body of evidence that systems of chaperones act together with UPS machinery to target aberrant proteins for degradation by the proteasome (McClellan and Frydman, 2001). In ERAD (endoplasmic reticulum associated degradation) the activity of ER chaperones and the AAA ATPase Cdc48 are essential for the retro-translocation of misfolded protein that necessarily precedes ubiquitination (Ellgaard and Helenius, 2003). In the yeast cytosol, Hsp70 and Hsp90, as well as coordination between them, are both required for the degradation of the misfolded form of the von Hippel-Landau (VHL) tumor suppressor protein (McClellan, 2005). In mammalian systems, chaperones interact with various co-chaperones, such as CHIP, which serves as a modulator between chaperone-assisted folding and ubiquitination (Cyr et al., 2002). Both Hsp70 and Hsp90 can bind to CHIP which in turn can regulate the ATPase activity of Hsp70 via its BAG domain, and confers E3 ligase activity via its RING finger (Wiederkehr et al., 2002). CHIP has been shown to ubiquitinate several Hsp70 folding substrates in vitro and in cell culture (Wiederkehr et al., 2002). Furthermore, over-expression of Hsp70 and Hsp40 increases degradation of certain aggregation-prone proteins, such as polyQ expanded proteins and alpha-synuclein, by the proteasome (Esser et al., 2004; Jana et al., 2005).

Section 1.4: Modular Proteins Link Chaperones to Degradation:

The identification of E3 ligases and chaperone cofactors that physically link chaperones to the UPS further supports the idea of direct communication between the folding and degradation machineries (Cyr et al., 2002; Esser et al., 2004). A trademark of these emerging families of modular proteins is the presence of a combination of chaperone-interaction domains with domains that function in the UPS.

Two proteins with these structural features, CHIP and BAG1, were initially identified in chaperone-interaction screens and have since emerged as linkers between chaperones and the proteasome (McClellan and Frydman, 2001). CHIP contains three chaperone-interacting tetratricopeptide (TPR) domains at the N-terminus, which confer

binding to Hsp70 and Hsp90, and a U-Box with E3 ligase activity at the C-terminus. BAG1, a member of a larger family of proteins containing a BAG domain with Hsp70 nucleotide exchange activity, also contains a UBL (ubiquitin-like) domain which binds the 26*S* proteasome (Esser et al., 2004). While CHIP has been established as an E3 capable of associating with chaperones and poly-ubiquitinating their bound substrates (Cyr et al., 2002; Esser et al., 2004), BAG1 has been shown to link Hsp70 to the 26*S* proteasome, presumably to facilitate delivery of Hsp70-bound targets to the proteasome for degradation (Esser et al., 2004). Because BAG1 and CHIP also regulate the ATPase activity of Hsp70 they may not only physically link chaperones and UPS enzymes but may also modulate the transition between the two pathways (Esser et al., 2004; McClellan and Frydman, 2001).

Section 1.5: Quality Control E3 Ligases:

Several groups have shown that CHIP over-expression in cultured cells promotes clearance of Hsp70/Hsp90 substrates such as CFTR, the glucocorticoid receptor, and the ErbB2 receptor (Cyr et al., 2002; Xu et al., 2002). Purified CHIP, along with recombinant Hsp40 and Hsp70 can ubiquitinate CFTR *in vitro* (Younger et al., 2004); chaperone association is a prerequisite for CHIP-mediated CFTR ubiquitination as CFTR poly-ubiquitination by CHIP requires both its TPR and U-box domains (Meacham et al., 2001). A similar *in vitro* approach demonstrated that a CHIP-Hsp70 complex, together with E1, E2, ATP and ubiquitin, can ubiquitinate heat-denatured luciferase bound to either Hsp70/Hsp40 or Hsp90 (Murata et al., 2001). These experiments indicate that CHIP can ubiquitinate chaperone clients *in vitro* and, when over-expressed, can shift the quality control equilibrium from folding to ubiquitination and degradation. (Hoppe, 2005). In some cases, CHIP itself exhibits E4 activity such as in facilitating poly-ubiquitination of unfolded Pael-R receptor in collaboration with the RING-finger E3 ligase Parkin. CHIP can also associate with aggregation-prone proteins, including tau and polyQ-expanded proteins (Esser et al., 2004; Jana et al., 2005), and in some cases facilitates their ubiquitination and clearance from the cell. Thus, CHIP may alleviate the

toxicity of aggregation-prone proteins in disease states. While the cumulative data indicate that CHIP is a strong candidate for a quality control ligase, the physiologically relevant substrates of this pathway remain to be found (Xu et al., 2002).

Two additional E3 ligases, Parkin and Dorfin, have also been implicated in the clearance of disease-related misfolded proteins. The role of these E3s in quality control and their connection to the chaperone machinery is less well understood than for CHIP (Kitada et al., 1998). Parkin inactivation is a major cause of early onset PD (Kitada et al., 1998). Parkin contains both a RING-finger domain with E3 ligase activity and a UBL domain (Kitada et al., 1998), and can promote the ubiquitination of three PD-associated proteins, alpha-synuclein, Pael-R, and synphilin-1, both *in vitro* and *in vivo* (Tanaka et al., 2004). However, it is unclear whether defective ubiquitination of these proteins underlies PD. Interestingly, the intracellular aggregates, called Lewy bodies, commonly associated with PD are absent in the Parkin-deficient form of the disease, indicating that their formation requires Parkin function (Shimura et al., 2001).

Parkin can bind to, and cooperate with CHIP and Hsp70, as CHIP over-expression enhances Parkin's ubiquitin ligase activity towards the PD-associated receptor Pael-R (Imai et al., 2002). Like CHIP, Parkin also binds to polyQ expanded Huntingtin *in vitro* and localizes to Huntingtin inclusions in human HD brains (Tsai et al., 2003). Furthermore, over-expressing Parkin in cultured cells improves clearance of polyQ expanded proteins and increases the survival rate of these cells (Tsai et al., 2003). Conversely, BAG5, an inhibitor of both Parkin and Hsp70, accelerates neuronal degeneration in rat brains (Kalia et al., 2004). Parkin may also shuttle certain aggregation-prone substrates to the proteasome, since it interacts with the 26*S* proteasome, presumably via its UBL domain (Tsai et al., 2003). Thus, similar to CHIP, Parkin may link Hsp70-bound substrates and the proteasome while also acting as an E3. However, many questions remain about the functions of CHIP and Parkin in quality control. For instance, while CHIP and Parkin are able to ubiquitinate misfolded or aggregating substrates *in vitro* and when over-expressed *in vivo*, neither has been shown to distinguish between wild type and folding-defective mutants of its substrates as would be expected for quality control components. Moreover, though CHIP has been suggested to act in heat shock response (Dai et al., 2003), neither CHIP nor Parkin are stress-

inducible, unlike other quality control components including ubiquitin, the E2s Ubc4 and Ubc5, many chaperones, and proteasome subunits (Gasch et al., 2000). Because stress produces a massive accumulation of misfolded proteins that need to be cleared, it is likely that there are additional E3s that function in quality control. Indeed, deletion or knockdown of CHIP does not prevent the degradation of its known substrates *in vivo* (Xu et al., 2002), suggesting the existence of redundant pathways to ubiquitinate chaperone-bound proteins.

Dorfin, yet another mammalian E3 implicated in quality control, associates with and selectively ubiquitinates mutant but not wild-type SOD1 (Niwa et al., 2002). Dorfin colocalizes with SOD1 inclusions in transgenic mice expressing an aggregation-prone SOD1 mutant (Niwa et al., 2002) and with Lewy bodies in PD brains (Ito et al., 2003). Dorfin overexpression increases the viability of cells expressing aggregation-prone SOD1 (Niwa et al., 2002); it also promotes ubiquitination of the Parkin substrate synphilin-1 in cultured cells (Ito et al., 2003). Dorfin, like Parkin, contains two RING domains, but associates with its known substrates without an obvious link to Hsp70 or other chaperones.

While ongoing characterization of these E3s provides a glimpse into the mechanism of protein quality control and strengthens the idea that the chaperone machinery directly communicates with the UPS, more components of the quality control system remain to be described. For instance, CHIP, Parkin and Dorfin lack homologues in *Saccharomyces cerevisiae*, which nonetheless carry out efficient quality control of misfolded proteins. Interestingly, a novel nuclear quality control E3, San1p, has recently been identified in yeast (Dasgupta et al., 2004; Gardner et al., 2005). San1p selectively targets misfolded nuclear proteins for proteasome-mediated degradation but it does not recognize the native proteins (Gardner et al., 2005). How San1p recognizes and interacts with its misfolded substrates remains to be determined. It may bind non-native structures directly or through an intermediary recognition factor, such as a chaperone, although San1p does not contain any canonical chaperone interaction domains.

Section 1.6: Protein Misfolding and Molecular Chaperones

Cells must perpetually contend with a misfolded protein load, normally arising from mistakes in transcription/translation or from mutated proteins. Roughly one third of all nascent proteins are thought to be targeted to the 26S proteasome upon exiting the ribosome (Kopito, 2000). Blocking proteasome function causes the accumulation of DRIPs (defective ribosomal products) and, conversely, increasing the frequency of translational mistakes by introducing amino-acid analogs leads to an increased turnover of newly synthesized proteins (Goldberg, 2003). Folded proteins can also lose their native structure spontaneously as a result of heat denaturation, oxidative stress, or chemical modification. These post-synthetically damaged proteins are also subject to degradation by the 26*S* proteasome (Goldberg, 2003). In times of stress, such as heat shock, exposure to pharmacological agents, or oxidative damage, cells adjust to an increased misfolded protein load by increasing the expression of certain stress-inducible genes (Goldberg, 2003). In yeast, heat stress induces the expression of components of the ubiquitination machinery such as the E2 Ubc4, Ubiquitin, proteasome subunits, chaperones such as Hsp70, Hsp90, and Hsp26, as well as other factors involved in quality control (Hahn et al., 2004).

Protein misfolding leading to either loss-of-function of the affected protein or gain-of-function due to toxicity of the misfolded species has been linked to human disease. For instance, loss-of-function mutations impairing the correct folding of the tumor suppressors p53 and von Hippel-Lindau (VHL) lead to their enhanced degradation and concomitant tumor development (Scott and Frydman, 2003). Similarly, mutations affecting folding of the cystic fibrosis transmembrane conductance regulator (CFTR) affect the trafficking of mature CFTR to the plasma membrane, thus resulting in cystic fibrosis (Amaral, 2005).

Selective recognition of non-native proteins is the first step toward their elimination. Based on their ability to interact with non-native folding intermediates, molecular chaperones are prime candidates to aid in the triage of misfolded proteins. Once potentially damaging conformers have been identified, the cell can respond to their presence in three ways. First, cellular factors may attempt to rescue the misfolded

conformations by refolding them to a functional native state. Second, the cell can sequester misfolded proteins in an attempt to prevent toxic interactions. Accordingly, chaperones alleviate the toxicity associated with aberrant protein conformations in neurodegenerative disease models (Muchowski and Wacker, 2005). For instance, over-expressing Hsp70 suppresses the toxicity associated with various proteins including Aß and tau in AD, alpha-synuclein in PD, superoxide dismutase (SOD1) in ALS, and polyQ-expanded proteins in HD, SBMA and ataxias (Muchowski and Wacker, 2005). It appears that chaperones alter the conformation of these pathogenic proteins, as Hsp70, together with its cofactor Hsp40, induces a conformational rearrangement in mutant Huntingtin (Schaffar et al., 2004) and disfavors the accumulation of specific soluble polyQ fibril intermediates (Wacker et al., 2004). An intriguing trend emerging from these studies is that chaperone-mediated neuroprotection is not a consequence of reduced inclusion body formation. Instead, chaperones appear to alleviate toxicity by sequestering the soluble toxic oligomeric species or by modulating their conformation (Muchowski and Wacker, 2005; Wacker et al., 2004).

Finally, proteins that cannot be refolded must be eliminated by the UPS. Different studies have pointed to a role for cytosolic chaperones in misfolded protein degradation. Hsp70 is required for the *in vitro* degradation of some misfolded proteins (Bercovich et al., 1997), while *in vivo* experiments implicate the yeast Hsp40 Ydj1p (Lee et al., 1996). Hsp70 and Hsp90 are required for degrading CFTR (Meacham et al., 2001; Youker et al., 2004) and misfolded VHL variants (McClellan, 2005). In addition, over-expressing Hsp70 and Hsp40 increases the proteasome-mediated degradation of alpha-synuclein and polyQ-expanded proteins (Muchowski and Wacker, 2005).

The precise role of chaperones in eliminating misfolded proteins is still unclear. In the simplest model, chaperones would be primarily dedicated to stabilizing and refolding non-native polypeptides. In this case, their role in quality control could be an extension of their primary role in folding, i.e. to maintain the solubility of misfolded intermediates and facilitate sampling by the ubiquitination machinery. On the other hand, recent analysis of the quality control mechanisms of misfolded variants of the VHL tumor suppressor suggests that chaperones have an active role selecting proteins for degradation (McClellan, 2005). The observation that some chaperones specifically

interact with E3s raises the possibility that, at least in some cases, chaperones could recognize misfolded proteins and subsequently mediate their poly-ubiquitination by directly recruiting an E3 ligase (Cyr et al., 2002; Esser et al., 2004; Verma et al., 2000). In addition, a post-ubiquitination function for chaperones has been proposed (Esser et al., 2004). For instance, the neuronal Hsp70 cofactor HSJ1, stimulates the ubiquitination of Hsp70-bound proteins via its UIM (ubiquitin-interaction motif) domains and their subsequent sorting to the proteasome (Westhoff et al., 2005). Furthermore, Hsp90 associates with the proteasome in an ATP-dependent manner (Verma et al., 2000). Thus, Hsp70 or Hsp90-bound substrates may be directed to proteasomes by virtue of direct or indirect chaperone-UPS interactions.

Section 1.7: Protein Aggregation and Inclusion Formation

When the misfolded protein load exceeds the degradative capacity of the quality control system and non-native proteins accumulate in excess of chaperones, their abundance can result in a toxic gain of function state known as protein aggregation (Dobson, 2004). This is caused by the inclination of exposed hydrophobic groups to associate with one another to form oligomeric insoluble aggregates. Whether large aggregates themselves or the accumulation of aggregation-prone non-native conformers are the cause of toxicity remains unclear (Kopito, 2000). It is thought that aggregates may inhibit the proteasome, damage membrane structure, and recruit other proteins, such as transcription factors, which are required for viability (Bennett et al., 2005; Muchowski, 2002; Sakahira et al., 2002; Schaffar et al., 2004). However, failure to eliminate aggregation prone intermediates is thought to be the underlying cause of aggregation, as well as of the numerous disease states which are marked by aggregate formation (Ciechanover and Brundin, 2003). Diseases in which non-native polypeptides gain a toxic function also result from misfolding (Dobson, 2004; Muchowski and Wacker, 2005). These diseases are characterized by the accumulation of intracellular aggregates

or inclusion bodies, often consisting of insoluble heat-stable beta-sheet amyloid deposits. Aggregation-based diseases disproportionately affect post-mitotic cells, such as neurons, presumably because they cannot dilute the toxic species during cell division, and underlie various neurodegenerative disorders, including Alzheimer (AD), Parkinson's (PD), and Amyotrophic Lateral Sclerosis (ALS). (Muchowski and Wacker, 2005). A number of amyloid diseases are caused by the expansion of a polyglutamine (polyQ) tract, usually beyond a critical threshold of approximately 40 repeats. PolyQ tract-containing proteins are soluble when the tract contains less than a threshold value (around 40) of glutamine residues (Morley et al., 2002). Proteins containing a polyQ tract above this value aggregate at a rate proportional to the number of glutamines, and onset of disease also correlates linearly with polyQ repeat length (Taylor et al., 2002). These glutamine-expansion diseases include Huntington's disease (HD), Spinocerebellar Ataxia, and Spinal Bulbar Muscular Atrophy (SBMA) (Muchowski and Wacker, 2005). Despite a lack of amino acid sequence similarity, these aberrant proteins appear to adopt a common toxic conformation that affects cell viability. Amyloidogenic oligomers of proteins associated with AD, PD, and polyQ diseases share a common structural signature that can be recognized by the same antibody (Glabe, 2004). While soluble early intermediates in the aggregation pathway appear to be toxic (Bucciantini et al., 2002), the larger amyloid deposits themselves are not pathogenic (Arrasate et al., 2004). Ultimately, aggregation-based diseases reflect a failure of the quality control system, either in surveillance or in elimination, and an imbalance between protein synthesis, folding, and degradation.

Studies following misfolded protein accumulation in different model systems suggest that formation of cellular inclusions is an organized process conserved from yeast to mammalian cells (Chiti and Dobson, 2006; Rubinsztein, 2006; Sherman and Goldberg, 2001). Distinct inclusions with specific characteristics have been observed using different quality control substrates (Huyer et al., 2004; Kamhi-Nesher et al., 2001; Krobitsch and Lindquist, 2000; Matsumoto et al., 2006; Matsumoto et al., 2005). For example, insoluble forms of polyQ-expanded proteins, as well as CFTRΔF508 or SOD-1 mutants, accumulate upon proteasome inhibition in a perinuclear structure, termed the aggresome, that co-localizes with the microtubule organizing center (MTOC) (Johnston et al., 2000; Johnston et al., 2002). Aggresome formation is a dynamic process which depends on

minus-end-directed transport along microtubules to the MTOC (Kopito, 2000). However, different aggregation-prone proteins have been shown to form similar peri-nuclear inclusions with different solubility properties (Matsumoto et al., ; Matsumoto et al., 2005). In a recent study, polyQ and SOD1 inclusions from two different SOD1 mutants were shown to form different inclusions, some completely insoluble and impermeable to native proteins and chaperones, and some exhibiting a porous structure through which other proteins can diffuse. Other studies suggest that the autophagic pathway aids in the removal of aggregated protein through the aggresome formation mechanism, forming an autophagic structure around the inclusion (Rideout et al., 2004). It is not clear whether aggresome formation is a protective response to an otherwise harmful phenomenon, or simply the byproduct of an abundance of aggregated species. However, recent work shows that aggresome formation may be protective and increase the probability of cell survival (Arrasate et al., 2004).

Another perinuclear inclusion, termed the quality control compartment, contains soluble misfolded substrates of the ERAD pathway (Kamhi-Nesher et al., 2001). Yet another class of perinuclear inclusions containing autophagic markers and sometimes co-localizing with lysosomes have also been observed with polyQ-expanded proteins (Iwata et al., 2005; Taylor et al., 2003). Because in mammalian cells many of the observed inclusions, as well as the ER, Golgi, and lysosomes, are all located in the perinuclear region, it is unclear whether all these observations pertain to the same compartment. It is also unclear what underlies the distinct solubility characteristics and long term fates observed for different quality control substrates in these inclusions.

Accumulation of intracellular inclusions is not restricted to disease states such as Huntington's or Prion disease but can also arise during cellular stress, for instance following proteasome inhibition (Johnston et al., 2000). While the aggregation of disease-related amyloidogenic proteins (Duennwald et al., 2006; Kopito, 2000) and ERAD substrates (Huyer et al., 2004; Kamhi-Nesher et al., 2001; Kruse et al., 2006b) has been extensively studied, little is known about the fate of “normal” misfolded cytosolic globular proteins (McClellan et al., 2005b). In the cell, misfolding of “normal” cytosolic proteins can arise as a consequence of either stress-induced denaturation, destabilizing missense mutations, or lack of oligomeric assembly partners. It is puzzling that, while all

proteins can form amyloid-like inclusions upon misfolding, (Bucciantini et al., 2002), only a handful of proteins cause amyloidosis and disease (Chiti and Dobson, 2006). In principle, it is possible that these amyloid disease-related proteins interact differently with the cellular quality control machinery. Furthermore, although aggregated protein inclusions associated with different neurodegenerative diseases contain otherwise unrelated aggregated proteins, many of these inclusions share cell-biological features such as co-staining with components of the quality control machinery. All this implies a general cellular pathway for recognition of misfolded and aggregated proteins and their sorting and delivery to intracellular inclusions associated with amyloidosis and disease. Accordingly, characterization of the pathways and mechanisms leading to inclusion formation is critical for understanding the molecular basis of protein conformational disorders.

Section 1.8: Effect of Protein Aggregates on Cellular Protein Folding Homeostasis

An intriguing characteristic of conformational disorders is that, in most cases, disease pathology is manifested only upon aging of an organism, despite the continued presence of the aggregation-prone species for decades without apparent harmful effects (Cohen et al., 2006; Dobson, 2003). Several models have been formulated to explain this late-onset feature of many neurodegenerative diseases. One possibility is that the quality control system (and in particular the cellular chaperone network), which for most of the organism's lifespan is able to keep aggregation at bay and maintain aggregation-prone proteins in a soluble state or degrade them via the UPS, eventually experiences a decline in capacity, thus allowing for wide-scale aggregation to occur and for the pathology to be manifested. Alternatively, aggregation-prone proteins and toxic intermediates may gradually accumulate over time, evading the quality control system, until their levels are substantial enough to inhibit essential processes or titrate out factors needed for viability. Aside from exerting these toxic "gain-of-function" effects on cellular processes, it has also been suggested that meta-stable conformations of mutant and poly-morphic alleles of essential genes exist perpetually in the cytosol and that their native state is buffered by

the cellular chaperone network. When significant levels of aggregation-prone proteins build up in the cell, the chaperone networks could be re-directed to cope with these misfolded species, leading to a perturbation of the cellular protein folding homeostasis and the subsequent misfolding, de-activation, or even co-aggregation of the previously buffered meta-stable protein pool.

Some clues about the effect of aging on protein aggregation and cellular protein folding homeostasis have come from work in the *C. elegans* model for Huntington's and Alzheimer diseases (Cohen et al., 2006; Morley et al., 2002; Morley and Morimoto, 2004). Given that in *C. elegans* the pathways regulating aging and lifespan are well understood (Guarente and Kenyon, 2000; Wolkow et al., 2000), worms provide an ideal system to explore the relationship between aging and late-onset neurodegenerative disease (Brignull et al., 2006). In worms, as well as flies and mammals, aging is regulated mainly by insulin/insulin growth factor-1-like (IIS) pathway signaling (Hsu et al., 2003). The insulin/IGF-1 receptor in *C. elegans*, DAF-2, negatively regulates the DAF-16 transcription factor, and in its absence DAF-16 initiates the expression of factors that drastically extend lifespan. Among DAF-16 transcriptional targets are many chaperones and quality control components, and its lifespan-extending activities are also dependent on the activity of the heat shock factor 1 (HSF-1) transcription factor, which itself regulates the expression of chaperones and UPS components (Arantes-Oliveira et al., 2003; Hsu et al., 2003; Muchowski et al., 2002). Not surprisingly, over-expressing certain quality control components, chaperones, and anti-oxidants can also extend lifespan in a DAF-16 dependent manner, though not as significantly as a *daf-2* mutation which activates DAF-16 (Hsu et al., 2003; Murphy et al., 2003).

Several studies have now shown that there is a link between the DAF-16/HSF-1 regulated aging pathway in *C. elegans*, and the proteotoxicity caused by the aggregation of polyQ Huntingtin and Aβ peptide. Extending the lifespan of worms was found to both increase the threshold of polyQ aggregation (by delaying the onset of aggregation for Q40-expanded proteins, which would otherwise form aggregates earlier in life), and to alleviate the toxicity associated with prolonged expression of aggregation prone polyQ-expanded proteins (Morley et al., 2002). Over-expressing HSF-1 reproduced these protective effects, suggesting that factors within the DAF-16 and HSF-1 transriptomes

actively protect cells from aggregate toxicity and in some cases buffer the onset of aggregation (Morley and Morimoto, 2004). A more recent study suggested a mechanism for the aggregation-induced toxicity protection conferred by the lifespan extension pathway, by using an Alzheimer disease model in *C. elegans*. $A\beta_{1-42}$ peptide-induced toxicity was lowered by *daf-2* knockdown (lifespan extension), and this protection was dependent on both HSF-1 and DAF-16 (Cohen et al., 2006). However, the DAF-16 and HSF-1 transcriptomes appeared to have separate and seemingly opposing roles in mediating the aggregation and clearance of aggregation-prone proteins. While HSF-1 induced factors that regulated the disaggregation of small toxic intermediates and assist in their clearance, DAF-16 targets appeared to actively promote the formation of higher molecular weight aggregates that were no longer toxic. Interestingly, *daf-16* knockdown was less harmful than knockdown of *hsf-1*, indicating that the directed aggregation pathway is secondary to the HSF-1 mediated detoxification of small aggregated intermediates. Consistent with this, accumulation of higher molecular weight aggregates did not correlate with toxicity.

While these interesting findings do not fully explain the late-onset of neurodegenerative diseases and their hallmark inclusion formation and toxicity, they do support the model that the aging process actively reduces the ability of cells to disaggregate, detoxify, and clear aggregating species. The molecular basis of toxicity, however, remains an open question. Although models for aggregate-induced toxicity exist in organisms including *S. cerevisiae, C. elegans, D. melanogaster*, as well as mammalian tissue culture systems (Brignull et al., 2006; Hsu et al., 2003; Outeiro and Lindquist, 2003; Warrick et al., 1999), there is little consensus regarding the precise adverse effects of amyloidogenic protein aggregation that eventually results in cell death. In yeast, amyloidogenic proteins such as certain types of polyQ Htt, alpha-synuclein, and synphillin-1 have been suggested to interfere with the actin cytoskeleton, inhibit intracellular trafficking, and perhaps inhibit some parts of the quality control/ UPS system (Muchowski and Wacker, 2005; Outeiro and Lindquist, 2003). In fly and mammalian models over-expression of the Hsp70 chaperone alone was shown to alleviate toxicity of polyQ aggregation (Warrick et al., 1999), suggesting that perhaps cytotoxicity was due to a sequestration of the chaperone by the aggregate from the

cytosol; indeed work in tissue culture models of aggregation showed that Hsp70 binds irreversibly to some polyQ inclusions but not to inclusions from other amyloidogenic proteins. A more conclusive study in *C. elegans* showed that the toxicity of polyQ aggregation correlated with adverse effect of these aggregates on the protein folding capacity of the worm cytosol (Gidalevitz et al., 2006). Aggregation of these expanded polyQ fragments resulted in the trans co-aggregation of meta-stable temperature-sensitive alleles, which had presumably previously been kept soluble by the buffering capacity of the cellular chaperone network. Once polyQ aggregates had formed and had directed part of the chaperone network to the aggregated protein inclusions, or possibly the lower molecular weight intermediates, the buffering capacity was reduced and other proteins also began to aggregate. It is possible that this process can eventually become fatal to the cell, as more and more essential factors that may exist in meta-stable polymorphic states, or that otherwise require the presence of chaperones for folding and function, begin to misfold and aggregate. Together, these studies from different models of neurodegeneration point to the conclusion that the process of sorting misfolded and aggregation prone proteins by the quality control system into inclusions is intimately connected to keeping the toxic effects of aggregation at bay. How the quality control system interacts with aggregating proteins and directs them to inclusions, and what underlies the toxicity associated with conformational disorders remain interesting open questions.

Figure 1.1

Quality control of protein folding in the cytosol

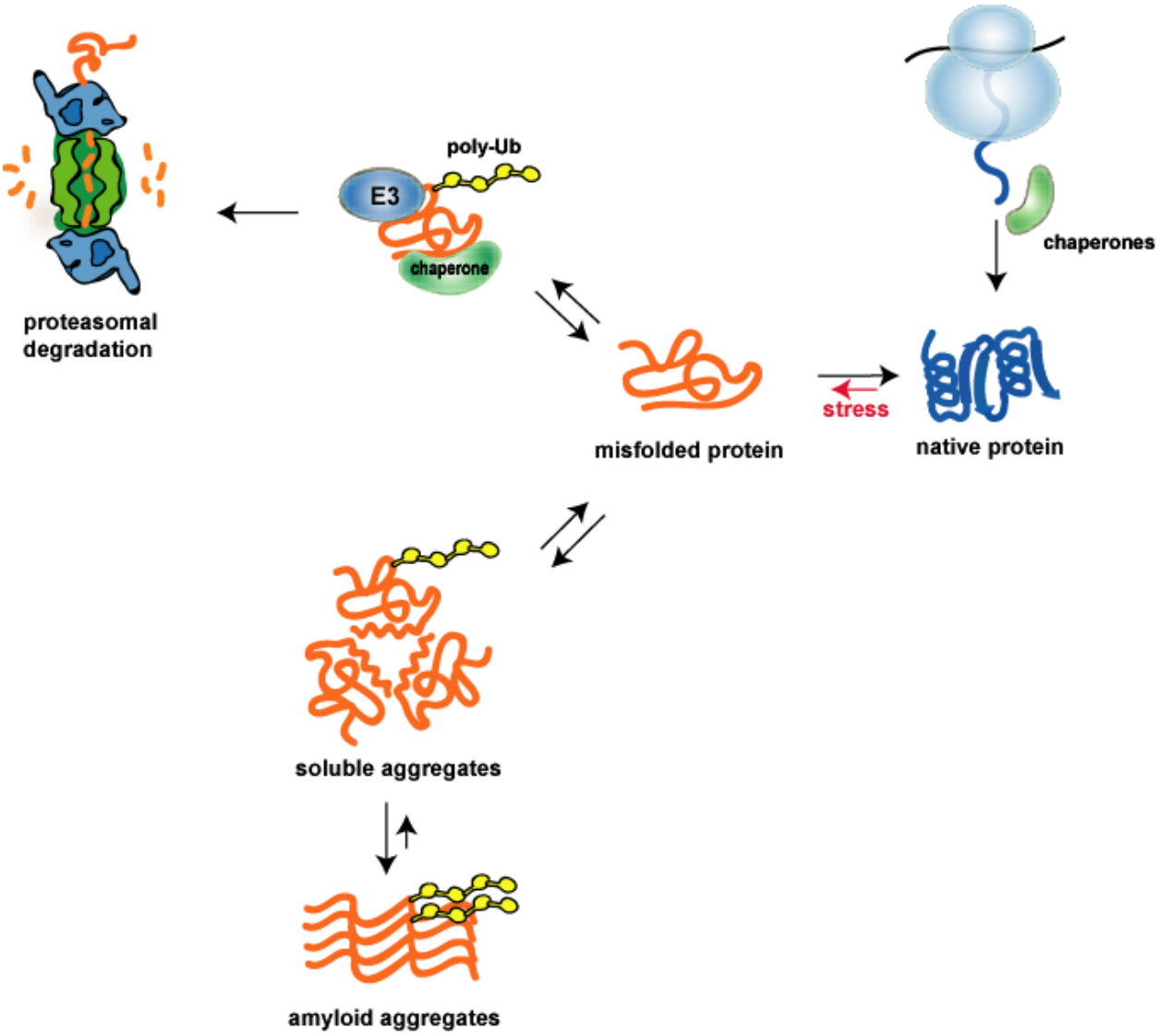

Section 1.9: References

Amaral, M.D. (2005). Processing of CFTR: Traversing the cellular maze-How much CFTR needs to go through to avoid cystic fibrosis? Pediatr Pulmonol.

Arantes-Oliveira, N., Berman, J.R., and Kenyon, C. (2003). Healthy animals with extreme longevity. Science *302*, 611.

Arrasate, M., Mitra, S., Schweitzer, E.S., Segal, M.R., and Finkbeiner, S. (2004). Inclusion body formation reduces levels of mutant huntingtin and the risk of neuronal death. Nature *431*, 805-810.

Bennett, E.J., Bence, N.F., Jayakumar, R., and Kopito, R.R. (2005). Global impairment of the ubiquitin-proteasome system by nuclear or cytoplasmic protein aggregates precedes inclusion body formation. Mol Cell *17*, 351-365.

Bercovich, B., Stancovski, I., Mayer, A., Blumenfeld, N., Laszlo, A., Schwartz, A.L., and Ciechanover, A. (1997). Ubiquitin-dependent degradation of certain protein substrates in vitro requires the molecular chaperone Hsc70. J Biol Chem *272*, 9002-9010.

Brignull, H.R., Morley, J.F., Garcia, S.M., and Morimoto, R.I. (2006). Modeling polyglutamine pathogenesis in C. elegans. Methods in enzymology *412*, 256-282.

Bucciantini, M., Giannoni, E., Chiti, F., Baroni, F., Formigli, L., Zurdo, J., Taddei, N., Ramponi, G., Dobson, C.M., and Stefani, M. (2002). Inherent toxicity of aggregates implies a common mechanism for protein misfolding diseases. Nature *416*, 507-511.

Cashikar, A.G., Duennwald, M., and Lindquist, S.L. (2005). A chaperone pathway in protein disaggregation. Hsp26 alters the nature of protein aggregates to facilitate reactivation by Hsp104. J Biol Chem *280*, 23869-23875.

Caughey, B., and Lansbury, P.T. (2003). Protofibrils, pores, fibrils, and neurodegeneration: separating the responsible protein aggregates from the innocent bystanders. Annu Rev Neurosci *26*, 267-298.

Chiti, F., and Dobson, C.M. (2006). Protein misfolding, functional amyloid, and human disease. Annu Rev Biochem *75*, 333-366.

Ciechanover, A., and Brundin, P. (2003). The ubiquitin proteasome system in neurodegenerative diseases: sometimes the chicken, sometimes the egg. Neuron *40*, 427-446.

Cohen, E., Bieschke, J., Perciavalle, R.M., Kelly, J.W., and Dillin, A. (2006). Opposing activities protect against age-onset proteotoxicity. Science *313*, 1604-1610.

Cyr, D.M., Hohfeld, J., and Patterson, C. (2002). Protein quality control: U-box-containing E3 ubiquitin ligases join the fold. Trends Biochem Sci *27*, 368-375.

Dai, Q., Zhang, C., Wu, Y., McDonough, H., Whaley, R.A., Godfrey, V., Li, H.H., Madamanchi, N., Xu, W., Neckers, L., *et al.* (2003). CHIP activates HSF1 and confers protection against apoptosis and cellular stress. Embo J *22*, 5446-5458.

Dasgupta, A., Ramsey, K.L., Smith, J.S., and Auble, D.T. (2004). Sir Antagonist 1 (San1) is a ubiquitin ligase. J Biol Chem *279*, 26830-26838.

Dobson, C.M. (2003). Protein folding and misfolding. Nature *426*, 884-890.

Dobson, C.M. (2004). Principles of protein folding, misfolding and aggregation. Semin Cell Dev Biol *15*, 3-16.

Duennwald, M.L., Jagadish, S., Giorgini, F., Muchowski, P.J., and Lindquist, S. (2006). A network of protein interactions determines polyglutamine toxicity. Proc Natl Acad Sci U S A *103*, 11051-11056.

Ellgaard, L., and Helenius, A. (2003). Quality control in the endoplasmic reticulum. Nat Rev Mol Cell Biol *4*, 181-191.

Esser, C., Alberti, S., and Hohfeld, J. (2004). Cooperation of molecular chaperones with the ubiquitin/proteasome system. Biochim Biophys Acta *1695*, 171-188.

Gardner, R.G., Nelson, Z.W., and Gottschling, D.E. (2005). Degradation-mediated protein quality control in the nucleus. Cell *120*, 803-815.

Gasch, A.P., Spellman, P.T., Kao, C.M., Carmel-Harel, O., Eisen, M.B., Storz, G., Botstein, D., and Brown, P.O. (2000). Genomic expression programs in the response of yeast cells to environmental changes. Mol Biol Cell *11*, 4241-4257.

Gidalevitz, T., Ben-Zvi, A., Ho, K.H., Brignull, H.R., and Morimoto, R.I. (2006). Progressive disruption of cellular protein folding in models of polyglutamine diseases. Science *311*, 1471-1474.

Glabe, C.G. (2004). Conformation-dependent antibodies target diseases of protein misfolding. Trends Biochem Sci *29*, 542-547.

Goldberg, A.L. (2003). Protein degradation and protection against misfolded or damaged proteins. Nature *426*, 895-899.

Guarente, L., and Kenyon, C. (2000). Genetic pathways that regulate ageing in model organisms. Nature *408*, 255-262.

Hahn, J.S., Hu, Z., Thiele, D.J., and Iyer, V.R. (2004). Genome-wide analysis of the biology of stress responses through heat shock transcription factor. Mol Cell Biol *24*, 5249-5256.

Hartl, F.U.a.M.H.-H. (2002). Molecular Chaperones in the Cytosol: from Nascent Chain to Folded Protein. Science *295*, 1852-1858.

Hartmann-Petersen, R., Seeger, M., and Gordon, C. (2003). Transferring substrates to the 26S proteasome. Trends Biochem Sci *28*, 26-31.

Hershko, A., and Ciechanover, A. (1998). The ubiquitin system. Annu Rev Biochem *67*, 425-479.

Hohfeld, J., Cyr, D.M., and Patterson, C. (2001). From the cradle to the grave: molecular chaperones that may choose between folding and degradation. EMBO Rep *2*, 885-890.

Hoppe, T. (2005). Multiubiquitylation by E4 enzymes: 'one size' doesn't fit all. Trends Biochem Sci *30*, 183-187.

Hsu, A.L., Murphy, C.T., and Kenyon, C. (2003). Regulation of aging and age-related disease by DAF-16 and heat-shock factor. Science *300*, 1142-1145.

Huyer, G., Longsworth, G.L., Mason, D.L., Mallampalli, M.P., McCaffery, J.M., Wright, R.L., and Michaelis, S. (2004). A striking quality control subcompartment in Saccharomyces cerevisiae: the endoplasmic reticulum-associated compartment. Mol Biol Cell *15*, 908-921.

Imai, Y., Soda, M., Hatakeyama, S., Akagi, T., Hashikawa, T., Nakayama, K.I., and Takahashi, R. (2002). CHIP is associated with Parkin, a gene responsible for familial Parkinson's disease, and enhances its ubiquitin ligase activity. Mol Cell *10*, 55-67.

Ito, T., Niwa, J., Hishikawa, N., Ishigaki, S., Doyu, M., and Sobue, G. (2003). Dorfin localizes to Lewy bodies and ubiquitylates synphilin-1. J Biol Chem *278*, 29106-29114.

Iwata, A., Christianson, J.C., Bucci, M., Ellerby, L.M., Nukina, N., Forno, L.S., and Kopito, R.R. (2005). Increased susceptibility of cytoplasmic over nuclear polyglutamine aggregates to autophagic degradation. Proc Natl Acad Sci U S A *102*, 13135-13140.

Jana, N.R., Dikshit, P., Goswami, A., Kotliarova, S., Murata, S., Tanaka, K., and Nukina, N. (2005). Co-chaperone CHIP associates with expanded polyglutamine protein and promotes their degradation by proteasomes. J Biol Chem *280*, 11635-11640.

Johnston, J.A., Dalton, M.J., Gurney, M.E., and Kopito, R.R. (2000). Formation of high molecular weight complexes of mutant Cu, Zn-superoxide dismutase in a mouse model for familial amyotrophic lateral sclerosis. Proc Natl Acad Sci U S A *97*, 12571-12576.

Johnston, J.A., Illing, M.E., and Kopito, R.R. (2002). Cytoplasmic dynein/dynactin mediates the assembly of aggresomes. Cell Motil Cytoskeleton *53*, 26-38.

Kalia, S.K., Lee, S., Smith, P.D., Liu, L., Crocker, S.J., Thorarinsdottir, T.E., Glover, J.R., Fon, E.A., Park, D.S., and Lozano, A.M. (2004). BAG5 inhibits parkin and enhances dopaminergic neuron degeneration. Neuron *44*, 931-945.

Kamhi-Nesher, S., Shenkman, M., Tolchinsky, S., Fromm, S.V., Ehrlich, R., and Lederkremer, G.Z. (2001). A novel quality control compartment derived from the endoplasmic reticulum. Mol Biol Cell *12*, 1711-1723.

Kitada, T., Asakawa, S., Hattori, N., Matsumine, H., Yamamura, Y., Minoshima, S., Yokochi, M., Mizuno, Y., and Shimizu, N. (1998). Mutations in the parkin gene cause autosomal recessive juvenile parkinsonism. Nature *392*, 605-608.

Kisselev, A.F., Kaganovich, D., and Goldberg, A.L. (2002). Binding of hydrophobic peptides to several non-catalytic sites promotes peptide hydrolysis by all active sites of 20 S proteasomes. Evidence for peptide-induced channel opening in the alpha-rings. J Biol Chem *277*, 22260-22270.

Kopito, R.R. (2000). Aggresomes, inclusion bodies and protein aggregation. Trends Cell Biol *10*, 524-530.

Krobitsch, S., and Lindquist, S. (2000). Aggregation of huntingtin in yeast varies with the length of the polyglutamine expansion and the expression of chaperone proteins. Proc Natl Acad Sci U S A *97*, 1589-1594.

Kruse, K.B., Brodsky, J.L., and McCracken, A.A. (2006). Characterization of an ERAD gene as VPS30/ATG6 reveals two alternative and functionally distinct protein quality control pathways: one for soluble Z variant of human alpha-1 proteinase inhibitor (A1PiZ) and another for aggregates of A1PiZ. Mol Biol Cell *17*, 203-212.

Lee, D.H., Sherman, M.Y., and Goldberg, A.L. (1996). Involvement of the molecular chaperone Ydj1 in the ubiquitin-dependent degradation of short-lived and abnormal proteins in Saccharomyces cerevisiae. Mol Cell Biol *16*, 4773-4781.

Matsumoto, G., Kim, S., and Morimoto, R.I. (2006). Huntingtin and mutant SOD1 form aggregate structures with distinct molecular properties in human cells. J Biol Chem *281*, 4477-4485.

Matsumoto, G., Stojanovic, A., Holmberg, C.I., Kim, S., and Morimoto, R.I. (2005). Structural properties and neuronal toxicity of amyotrophic lateral sclerosis-associated Cu/Zn superoxide dismutase 1 aggregates. J Cell Biol *171*, 75-85.

McClellan, A.J., and Frydman, J. (2001). Molecular chaperones and the art of recognizing a lost cause. Nat Cell Biol *3*, E51-53.

McClellan, A.J., Scott, M. D., Frydman, J. (2005). Folding and Quality Control of the VHL Tumor Suppressor Proceed Through Distinct Chaperone Pathways. Cell *121*, 739-748.

McClellan, A.J., Tam, S., Kaganovich, D., and Frydman, J. (2005). Protein quality control: chaperones culling corrupt conformations. Nat Cell Biol *7*, 736-741.

McGinness, K.E., Bolon, D.N., Kaganovich, M., Baker, T.A., and Sauer, R.T. (2007). Altered tethering of the SspB adaptor to the ClpXP protease causes changes in substrate delivery. J Biol Chem *282*, 11465-11473.

Meacham, G.C., Patterson, C., Zhang, W., Younger, J.M., and Cyr, D.M. (2001). The Hsc70 co-chaperone CHIP targets immature CFTR for proteasomal degradation. Nat Cell Biol *3*, 100-105.

Morley, J.F., Brignull, H.R., Weyers, J.J., and Morimoto, R.I. (2002). The threshold for polyglutamine-expansion protein aggregation and cellular toxicity is dynamic and influenced by aging in Caenorhabditis elegans. Proc Natl Acad Sci U S A *99*, 10417-10422.

Morley, J.F., and Morimoto, R.I. (2004). Regulation of longevity in Caenorhabditis elegans by heat shock factor and molecular chaperones. Mol Biol Cell *15*, 657-664.

Muchowski, P.J. (2002). Protein misfolding, amyloid formation, and neurodegeneration: a critical role for molecular chaperones? Neuron *35*, 9-12.

Muchowski, P.J., Ning, K., D'Souza-Schorey, C., and Fields, S. (2002). Requirement of an intact microtubule cytoskeleton for aggregation and inclusion body formation by a mutant huntingtin fragment. Proceedings of the National Academy of Sciences of the United States of America *99*, 727-732.

Muchowski, P.J., and Wacker, J.L. (2005). Modulation of neurodegeneration by molecular chaperones. Nat Rev Neurosci *6*, 11-22.

Murata, S., Minami, Y., Minami, M., Chiba, T., and Tanaka, K. (2001). CHIP is a chaperone-dependent E3 ligase that ubiquitylates unfolded protein. EMBO Rep *2*, 1133-1138.

Murphy, C.T., McCarroll, S.A., Bargmann, C.I., Fraser, A., Kamath, R.S., Ahringer, J., Li, H., and Kenyon, C. (2003). Genes that act downstream of DAF-16 to influence the lifespan of Caenorhabditis elegans. Nature *424*, 277-283.

Niwa, J., Ishigaki, S., Hishikawa, N., Yamamoto, M., Doyu, M., Murata, S., Tanaka, K., Taniguchi, N., and Sobue, G. (2002). Dorfin ubiquitylates mutant SOD1 and prevents mutant SOD1-mediated neurotoxicity. J Biol Chem *277*, 36793-36798.

Outeiro, T.F., and Lindquist, S. (2003). Yeast cells provide insight into alpha-synuclein biology and pathobiology. Science *302*, 1772-1775.

Pickart, C.M., and Cohen, R.E. (2004). Proteasomes and their kin: proteases in the machine age. Nat Rev Mol Cell Biol *5*, 177-187.

Rideout, H.J., Lang-Rollin, I., and Stefanis, L. (2004). Involvement of macroautophagy in the dissolution of neuronal inclusions. Int J Biochem Cell Biol *36*, 2551-2562.

Rubinsztein, D.C. (2006). The roles of intracellular protein-degradation pathways in neurodegeneration. Nature *443*, 780-786.

Sakahira, H., Breuer, P., Hayer-Hartl, M.K., and Hartl, F.U. (2002). Molecular chaperones as modulators of polyglutamine protein aggregation and toxicity. Proc Natl Acad Sci U S A *99 Suppl 4*, 16412-16418.

Schaffar, G., Breuer, P., Boteva, R., Behrends, C., Tzvetkov, N., Strippel, N., Sakahira, H., Siegers, K., Hayer-Hartl, M., and Hartl, F.U. (2004). Cellular toxicity of polyglutamine expansion proteins: mechanism of transcription factor deactivation. Mol Cell *15*, 95-105.

Scott, M.D., and Frydman, J. (2003). Aberrant protein folding as the molecular basis of cancer. Methods Mol Biol *232*, 67-76.

Sherman, M.Y., and Goldberg, A.L. (2001). Cellular defenses against unfolded proteins: a cell biologist thinks about neurodegenerative diseases. Neuron *29*, 15-32.

Shimura, H., Schlossmacher, M.G., Hattori, N., Frosch, M.P., Trockenbacher, A., Schneider, R., Mizuno, Y., Kosik, K.S., and Selkoe, D.J. (2001). Ubiquitination of a new form of alpha-synuclein by parkin from human brain: implications for Parkinson's disease. Science *293*, 263-269.

Tanaka, K., Suzuki, T., Hattori, N., and Mizuno, Y. (2004). Ubiquitin, proteasome and parkin. Biochim Biophys Acta *1695*, 235-247.

Taylor, J.P., Hardy, J., and Fischbeck, K.H. (2002). Toxic proteins in neurodegenerative disease. Science *296*, 1991-1995.

Taylor, J.P., Tanaka, F., Robitschek, J., Sandoval, C.M., Taye, A., Markovic-Plese, S., and Fischbeck, K.H. (2003). Aggresomes protect cells by enhancing the degradation of toxic polyglutamine-containing protein. Hum Mol Genet *12*, 749-757.

Tsai, Y.C., Fishman, P.S., Thakor, N.V., and Oyler, G.A. (2003). Parkin facilitates the elimination of expanded polyglutamine proteins and leads to preservation of proteasome function. J Biol Chem *278*, 22044-22055.

Verma, R., Chen, S., Feldman, R., Schieltz, D., Yates, J., Dohmen, J., and Deshaies, R.J. (2000). Proteasomal proteomics: identification of nucleotide-sensitive proteasome-interacting proteins by mass spectrometric analysis of affinity-purified proteasomes. Mol Biol Cell *11*, 3425-3439.

Wacker, J.L., Zareie, M.H., Fong, H., Sarikaya, M., and Muchowski, P.J. (2004). Hsp70 and Hsp40 attenuate formation of spherical and annular polyglutamine oligomers by partitioning monomer. Nat Struct Mol Biol *11*, 1215-1222.

Warrick, J.M., Chan, H.Y., Gray-Board, G.L., Chai, Y., Paulson, H.L., and Bonini, N.M. (1999). Suppression of polyglutamine-mediated neurodegeneration in Drosophila by the molecular chaperone HSP70. Nature genetics *23*, 425-428.

Westhoff, B., Chapple, J.P., Spuy, J.v.d., Höhfeld, J., and Cheetham, M.E. (2005). HSJ1 Is a Neuronal Shuttling Factor for the Sorting of Chaperone Clients to the Proteasome. Current Biology *15*, 1058-1064.

Wickner, S., Maurizi, M.R., and Gottesman, S. (1999). Posttranslational quality control: folding, refolding, and degrading proteins. Science *286*, 1888-1893.

Wiederkehr, T., Bukau, B., and Buchberger, A. (2002). Protein turnover: a CHIP programmed for proteolysis. Curr Biol *12*, R26-28.

Wolf, D.H., and Hilt, W. (2004). The proteasome: a proteolytic nanomachine of cell regulation and waste disposal. Biochim Biophys Acta *1695*, 19-31.

Wolkow, C.A., Kimura, K.D., Lee, M.S., and Ruvkun, G. (2000). Regulation of C. elegans life-span by insulinlike signaling in the nervous system. Science *290*, 147-150.

Xu, W., Marcu, M., Yuan, X., Mimnaugh, E., Patterson, C., and Neckers, L. (2002). Chaperone-dependent E3 ubiquitin ligase CHIP mediates a degradative pathway for c-ErbB2/Neu. Proc Natl Acad Sci U S A *99*, 12847-12852.

Youker, R.T., Walsh, P., Beilharz, T., Lithgow, T., and Brodsky, J.L. (2004). Distinct roles for the Hsp40 and Hsp90 molecular chaperones during cystic fibrosis transmembrane conductance regulator degradation in yeast. Mol Biol Cell *15*, 4787-4797.

Younger, J.M., Ren, H.Y., Chen, L., Fan, C.Y., Fields, A., Patterson, C., and Cyr, D.M. (2004). A foldable CFTR{Delta}F508 biogenic intermediate accumulates upon inhibition of the Hsc70-CHIP E3 ubiquitin ligase. J Cell Biol *167*, 1075-1085.

Zwickl, P., Voges, D., and Baumeister, W. (1999). The proteasome: a macromolecular assembly designed for controlled proteolysis. Philos Trans R Soc Lond B Biol Sci *354*, 1501-1511.

Chapter 2

Ubiquitination determines the partitioning of misfolded proteins between two distinct subcellular quality control compartments

Daniel Kaganovich, Ron Kopito and Judith Frydman

Department of Biological Sciences and BioX Program,
Stanford University, Stanford, CA 94305, USA

Section 2.1: Summary

The accumulation of misfolded proteins in intracellular amyloid inclusions, typical of many neurodegenerative disorders including Huntington's and Prion Disease, is thought to arise upon failure of the cellular protein Quality Control (QC) mechanisms (Chiti and Dobson, 2006; McClellan et al., 2005b; Rubinsztein, 2006). Here we examine the formation of misfolded protein inclusions in the eukaryotic cytosol. We identify two intracellular compartments for the sequestration of misfolded cytosolic proteins. Partition of QC substrates to either compartment appears to depend on their ubiquitination status and aggregation state. Soluble ubiquitinated misfolded proteins accumulate in a juxtanuclear compartment where proteasomes are concentrated. In contrast, terminally aggregated proteins are sequestered in a perivacuolar inclusion possibly linked to the autophagic pathway. Strikingly, disease-associated Huntingtin and prion proteins are preferentially directed to the perivacuolar compartment. Enhancing ubiquitination of a prion protein suffices to promote its delivery to the juxtanuclear inclusion. Our findings provide a framework for understanding the preferential accumulation of amyloidogenic proteins in inclusions linked to human disease.

Section 2.2: Introduction

The strong correlation between the accumulation of aggregated proteins in inclusions and the onset of several neurodegenerative diseases calls for a better understanding of the mechanisms and functions of inclusion formation. Previous research has indicated that soluble aggregation intermediates have a toxic "gain of function" activity, suggesting that the regulated formation of protein inclusions serves a cytoprotective function, namely to sequester misfolded species (Bence et al., 2001; Chiti and Dobson, 2006; Gidalevitz et al., 2006; Lesne et al., 2006; Muchowski and Wacker, 2005; Outeiro and Lindquist, 2003; Schaffar et al., 2004). Because aggregated proteins may be poor substrates for either chaperones or the proteasome they may also be

concentrated in inclusions for clearance by the autophagic pathway(Iwata et al., 2005; Rideout et al., 2004; Rubinsztein, 2006; Taylor et al., 2003; Yorimitsu and Klionsky, 2005). However, it is unknown whether inclusions contain only terminally aggregated proteins or whether there are mechanisms to also sequester soluble misfolded conformations(Matsumoto et al., 2006). It is puzzling that, while all proteins can form amyloid-like inclusions upon misfolding[1,] (Bucciantini et al., 2002), only a handful of proteins cause amyloidosis and disease(Chiti and Dobson, 2006). In principle, it is possible that these amyloid disease-related proteins interact differently with the cellular QC machinery. Accordingly, characterization of the pathways and mechanisms leading to inclusion formation is critical for understanding the molecular basis of protein conformation disorders.

Studies following misfolded protein accumulation in different model systems suggest that formation of cellular inclusions is an organized process conserved from yeast to mammalian cells (Chiti and Dobson, 2006; Rubinsztein, 2006; Sherman and Goldberg, 2001). Distinct inclusions with specific characteristics have been observed using different QC substrates(Huyer et al., 2004; Kamhi-Nesher et al., 2001; Krobitsch and Lindquist, 2000; Matsumoto et al., 2006; Matsumoto et al., 2005). For example, insoluble forms of polyglutamine (polyQ)-expanded proteins, as well as CFTRΔF508 or SOD-1 mutants, accumulate upon proteasome inhibition in a perinuclear structure, termed the aggresome, that co-localizes with the microtubule organizing center (MTOC)(Johnston et al., 2002; Kopito, 2000). Another perinuclear inclusion, termed the QC compartment, contains soluble misfolded substrates of the ERAD pathway(Kamhi-Nesher et al., 2001). Yet another class of perinuclear inclusions containing autophagic markers and sometimes co-localizing with lysosomes have also been observed with polyQ-expanded proteins(Iwata et al., 2005; Taylor et al., 2003). Because in mammalian cells many of the observed inclusions, as well as the ER, Golgi, and lysosomes, are all located in the perinuclear region, it is unclear whether all these observations pertain to the same compartment. It is also unclear what underlies the distinct solubility characteristics and long term fates observed for different QC substrates in these inclusions.

Accumulation of intracellular inclusions is not restricted to disease states such as Huntington's or Prion disease but can also arise during cellular stress, for instance

following proteasome inhibition(Kopito, 2000). While the aggregation of disease-related amyloidogenic proteins(Duennwald et al., 2006; Kopito, 2000) and ERAD substrates(Huyer et al., 2004; Kamhi-Nesher et al., 2001; Kruse et al., 2006b) has been extensively studied, little is known about the fate of "normal" misfolded cytosolic globular proteins(McClellan et al., 2005b). In the cell, protein misfolding can arise as a consequence of either stress-induced denaturation, destabilizing missense mutations, or lack of oligomeric assembly partners. To examine how cytosolic QC proceeds in these different scenarios we chose a panel of model substrates corresponding to each case (Fig. 1a, d) and compared their fate to that of model amyloidogenic proteins (Fig. 2a). Our findings reveal that cells contain two distinct compartments for the accumulation of misfolded proteins. The QC machinery uses the ubiquitination state and solubility of its substrates as primary determinants to partition misfolded proteins among these compartments. Soluble misfolded proteins destined for degradation by the proteasome or refolding by the chaperone machinery are directed to a perinuclear compartment. A second compartment, apparently linked to the autophagic pathway, accumulates terminally aggregated proteins. Interestingly, our data indicates that unlike normal misfolded polypeptides, amyloidogenic proteins are preferentially sorted to this compartment. We propose that these distinct QC compartments represent two cellular strategies for the sequestration of aggregation-prone, potentially toxic polypeptides.

Section 2.3: Results

A thermally destabilized QC substrate accumulates in two distinct inclusions

To determine the interplay between the QC machinery and cytosolic misfolded substrates, we initially followed the fate of a previously characterized Ubc9 variant that misfolds above 30 °C (Betting and Seufert, 1996; Tongaonkar et al., 1999)(Fig. 2.1a). Ubc9^{ts}, fused to GFP to facilitate detection (GFP-Ubc9^{ts}) was expressed under the control of a galactose-regulated promoter. Glucose addition repressed expression, allowing us to

follow the fate of GFP-Ubc9^{ts} from the earliest stages of protein misfolding upon shift to 37 °C (Fig. 2.1a). At permissive temperatures, GFP-Ubc9^{ts} was native and exhibited the diffuse distribution observed for wild type GFP-Ubc9 (Fig. 2.1b, 0 min compare with WT panel 120 min). GFP-Ubc9^{ts} misfolding led to degradation by the ubiquitin-proteasome pathway, as previously reported for the untagged protein (Fig. 2.1b, compare 5 min and 60 min and Fig. 2.1d, left panel) (Betting and Seufert, 1996; Tongaonkar et al., 1999). The time-course of degradation revealed a transient accumulation of Ubc9^{ts} in distinct cytosolic inclusions that were eventually cleared (e.g. Fig. 2.1 b 30 min and Fig. 2.1c). Most cells contained a juxtanuclear inclusion as well as smaller puncta distributed throughout the cytosol, although some cells contained only the juxtanuclear inclusion (Fig. 2.1 b, c). Impairment of proteasome-mediated degradation, either in *cim3-1* cells or by treatment with the proteasome inhibitor MG132, stabilized GFP-Ubc9^{ts} and led to its reproducible accumulation in two distinct inclusions in virtually every cell (Fig. 2.1b, 60 and 120 min and Fig. 2.1h). At early time-points following misfolding in proteasome-defective cells, GFP-Ubc9^{ts} accumulated in structures resembling those observed during degradation in control cells (compare 15 and 30 min in Figs. 2.1b). Quantification indicated that the juxtanuclear inclusion appeared to form first, closely followed by additional cytosolic puncta (Fig. 2.1c). However, at later incubation times at 37 °C the juxtanuclear inclusion remained but the puncta were no longer observed. Instead, a second large perivacuolar inclusion was now formed at the periphery of the cell (Fig. 2.1 b, c). Once formed, both inclusions persisted well beyond the time-course shown in Fig. 2.1. These two inclusions may represent distinct compartments for the sequestration of misfolded proteins.

The temporal regulation of misfolded protein accumulation first in puncta and then in larger inclusions, led us to examine whether microtubule polymerization was required for inclusion assembly (Fig. 2.1k-m). Treatment with the microtubule polymerization inhibitor Benomyl arrested this process at the stage of puncta formation (Fig. 2.1k), even when added after 15 min at 37 °C, once the puncta were already formed (Fig. 2.1k, l). Strikingly, washing out Benomyl after 30 min at 37 °C allowed the puncta to coalesce into two inclusions (Fig. 2.1m), suggesting that the Benomyl induced arrest was reversible. Together these data reveal that the misfolded protein initially

accumulates in small oligomeric structures that are then actively transported to two distinct inclusions.

Two distinct compartments for the sequestration of misfolded cytosolic proteins.

We next examined whether other types of cytosolic quality control substrates are directed to the same subcellular compartments as our model for thermal denaturation. To this end, we initially followed the fate of the unassembled VHL tumor suppressor (McClellan et al., 2005a; Vang et al., 2005). VHL can only fold upon binding to its cofactor complex elongin BC(Feldman et al., 1999) (Fig. 2.1d). Tumor-causing mutations impairing elongin BC binding, or VHL expression in the absence of elongin BC, lead to VHL misfolding followed by ubiquitination and degradation (McClellan et al., 2005a) (Fig. 2.1d). Accordingly, under normal growth conditions misfolded GFP-VHL was degraded, resulting in reduced levels of diffuse fluorescence (Fig. 2.1e, left panel compare with folded VHL in right panel). Inhibition of the proteasome in *cim3-1* cells (Fig. 2.1f) or with MG132 (Fig. 2.1h) led to formation of a single juxtanuclear GFP-VHL inclusion. Importantly, proteasome impairment did not produce GFP-VHL inclusions under conditions leading to productive VHL folding (Fig. 2.1e +elongin BC, right panel).

It was intriguing that at 30 °C VHL consistently formed only a single juxtanuclear inclusion while Ubc9^{ts} formed two distinct inclusions. Since Ubc9^{ts} destabilization requires conditions of stress, we hypothesized that the formation of two inclusions may result from the increased load of denatured QC substrates at 37 °C. Indeed, when unassembled VHL was expressed at 37 °C it also accumulated in two inclusions as observed for Ubc9^{ts} (Fig. 2.1f; see also Fig. 2.1c). Three-dimensional fluorescence deconvolution microscopy demonstrated that the inclusions formed by VHL and Ubc9^{ts} overlap spatially in the same compartments (Fig. 2.1g).

We next used a similar approach to examine the fate of a previously characterized missense mutation of actin, that is also degraded via the ubiquitin-proteasome pathway (McClellan et al., 2005a). As observed for VHL, misfolded actin-E364K accumulated in

the same two inclusions as Ubc9^{ts} (Fig. 2.1g). Since clearance of misfolded Ubc9, VHL and actin requires ubiquitination, we considered whether proteasome impairment or stress lead to widespread aggregation of ubiquitinated protein (Fig. 2.1i). This is not the case since native substrates of the ubiquitin-proteasome pathway(Mateus and Avery, 2000), such as Ub-Arg-GFP (Ub-R-GFP), Ub-G76A-GFP (Ub-GFP), and Deg1-GFP (not shown) remained soluble and diffuse upon proteasome impairment, even under conditions of stress (Supplementary Fig. 2.1i and Fig. 2.4e). We conclude that different classes of misfolded cytosolic proteins accumulate in two defined inclusions, one juxtanuclear and one perivacuolar at the periphery of the cell. The juxtanuclear inclusion appears to form first and is more prevalent under cellular conditions with a milder load of misfolded proteins. However, stress conditions lead to protein accumulation in the second peripheral inclusion. We hypothesize that these inclusions may represent distinct subcellular compartments for the sequestration of misfolded QC substrates. In principle, the differential partitioning of non-native QC substrates between these two compartments may be determined by a change in their intrinsic properties, such as aggregation state, or by their interaction with saturatable QC components, or both.

We next explored the relationship between the inclusions formed by these disease-related amyloidogenic proteins and those characterized here for misfolded cytosolic proteins (Figs. 2.2a-d). The relative spatial localization of the aggregates formed by the yeast prion proteins Rnq1 and Ure2, as well as the disease-related HttQ103 relative to the Ubc9^{ts} inclusions was determined by deconvolution microscopy. Strikingly, all the amyloidogenic proteins tested formed a single major inclusion, which consistently co-localized with the perivacuolar peripheral inclusion of Ubc9^{ts} (Figs. 2.2b, c). We did not observe any cases of co-localization of either the prion proteins or Htt with the juxtanuclear inclusion.

Unlike normal QC substrates, amyloidogenic proteins including Huntingtin (Htt) and prions, form large insoluble inclusions even in the absence of stress or proteasome inhibition (Fig. 2.2a) (Duennwald et al., 2006; Horwich and Weissman, 1997; Krobitsch and Lindquist, 2000; Matsumoto et al., 2006; Rajan et al., 2001; Taylor et al., 2003). Thus, amyloidogenic proteins were also analyzed in the absence of proteasome inhibition and under normal growth temperatures (Fig. 2.2j, k). Unlike misfolded globular proteins,

such as VHL or Ubc9, glutamine-rich Rnq1, Ure2, and HttQ103 also accumulated under these normal conditions in aggregates localized exclusively in the peripheral compartment (Fig. 2.2e, f), although Rnq1 was also found in small puncta throughout the cell (Fig 2.2b). The accumulation of amyloidogenic proteins in the perivacuolar, peripheral inclusion in the absence of either stress or proteasome impairment (Fig. 2.2e, f) indicates that this compartment can also form under normal conditions. Notably, Rnq1 always surrounded the Ure2 and HttQ103 deposits in the peripheral inclusion (red fluorescence in Fig. 2.2e, f) suggesting that Rnq1 is targeted to the perivacuolar compartment with slower kinetics than the other amyloidogenic proteins. These observations, together with the finding that misfolded globular proteins are preferentially targeted to the juxtanuclear inclusion at 30 °C, suggests some unique feature of amyloidogenic proteins earmarks them for delivery to the peripheral inclusion.

Mammalian cells sequester misfolded proteins in two distinct compartments

We next determined whether the two distinct QC compartments that differentially sequester misfolded and amyloidogenic proteins are conserved in mammalian cells. To this end, we compared the subcellular distribution of misfolded forms of $Ubc9^{ts}$ and VHL with that of the amyloidogenic HttQ103, in the presence or absence of proteasome inhibition (Fig. 2.3). Both $Ubc9^{ts}$ and VHL showed diffuse fluorescence when expressed in untreated HeLa cells (Fig. 2.3a, upper panel), with VHL more prominent around the ER and nucleus. Upon proteasome inhibition both proteins co-localized completely in the peri-nuclear region, as observed in yeast cells (Fig. 2.3, middle panel). Importantly, wild-type folded Ubc9 did not co-aggregate with VHL under these conditions (Fig. 2.3, lower panel). We next, compared the distribution of HttQ103 and misfolded VHL. Our experiments in yeast predict that, in the absence of stress these QC substrates should be directed to different compartments. Strikingly, this was the case in mammalian cells, since HttQ103 and misfolded VHL were sequestered in two clearly different inclusions upon proteasome inhibition (Fig. 2.3b, middle and lower panels). Absent proteasome

impairment, VHL was degraded while the HttQ103 inclusion was still observed. It thus appears that the differential sequestration of misfolded proteins in two QC compartments is conserved from yeast to mammals.

Misfolded proteins in the two quality control compartments exhibit distinct diffusion properties

To better characterize the two quality control compartments, we next examined the solubility state of misfolded proteins accumulating in either inclusion. As a measure of solubility for misfolded proteins in these compartments we determined their diffusion properties using Fluorescence Loss In Photobleaching (FLIP) (Lippincott-Schwartz and Patterson, 2003). Briefly, a laser pulse was used to photobleach GFP-Ubc9^{ts} from a small section of cytosol outside of the two GFP-Ubc9^{ts} inclusions (box in Fig. 2.4a). The ensuing changes in fluorescence intensity of the different cellular compartments, assessed as a function of time, provide a measure of their relative exchange rate with the bleached cytoplasmic portion (Fig. 2.4a). As a result of bleaching, the diffuse cytosolic fluorescence corresponding to soluble GFP-Ubc9^{ts} was rapidly lost (Fig. 2.4a, black trace). A rapid fluorescence loss was also observed for the juxtanuclear inclusion (Fig. 2.4a, red trace), indicating that a substantial fraction of GFP-Ubc9^{ts} in this compartment is soluble and can exchange with the cytosolic pool. We therefore refer to this inclusion as the *JuxtaNuclear Quality Control* compartment, or JUNQ. In contrast, following a small initial reduction in fluorescence, the peripheral perivacuolar compartment retained most (>70%) of its fluorescent signal (Fig. 2.4a, cyan trace). This suggests that this inclusion contains a large fraction of non-diffusing, possibly insoluble GFP-Ubc9^{ts}. Accordingly, we named this inclusion the *Insoluble Protein Deposit* or IPOD. In principle the conservation of fluorescent signal within the IPOD during bleaching could result from a barrier to exchange with the cytosolic pool, for instance due to a membrane, rather than to the insolubility of the protein in the inclusion. Accordingly, we examined the internal mobility of the protein within the IPOD using Fluorescence Recovery After Photobleaching (FRAP) (Lippincott-Schwartz and Patterson, 2003). In this case we

directly bleached a small sector within the IPOD inclusion. Because we failed to observe any redistribution of the fluorescent signal within the IPOD from the non-bleached part of the inclusion it appears that the protein in this structure is immobile, consistent with this compartment containing aggregated species (Fig. 2.4b).

The conclusion that the JUNQ and IPOD accumulate proteins in distinct solubility states was supported by biochemical analyses (Fig. 2.4c-e, see also Fig. 2.6c). Thus, when VHL localized only to the JUNQ, all of the protein was in a Triton-soluble form (Fig. 2.4c), whereas VHL accumulation in the IPOD correlated with a shift to the insoluble fraction (Fig. 2.4c, see also Fig. 2.6c and Fig. 2.6f for Ubc9 and Htt). Together, these results suggest that one compartment, the JUNQ, contains a large fraction of soluble misfolded protein, while the IPOD compartment contains non-diffusing, insoluble species. Furthermore, the observation that amyloidogenic proteins appear to be targeted exclusively to the IPOD suggests that this compartment is the preferred cellular destination for protein aggregates.

Characterization of the JUNQ and IPOD as defined subcellular compartments.

Because different quality control substrates reproducibly accumulated in the same two compartments, we next examined the relationship of both JUNQ and IPOD with known cellular structures and quality control components using fluorescence deconvolution microscopy and EM (Fig. 2.5). Analysis of the relative spatial localization of the nucleus and the inclusions formed by $Ubc9^{ts}$ and VHL indicated that the JUNQ is formed in an indentation of the nucleus (Fig. 2.5a, nuclear DNA, blue, stained with DAPI, nucleoplasm, red, with NLS-TFP). Interestingly, in dividing cells both the JUNQ and IPOD were invariably retained in the mother cell, raising the possibility that these compartments provide a mechanism to retain misfolded proteins in the mother cells during cell division (Fig. 2.5a) (Rujano et al., 2006). Notably, neither the JUNQ nor the IPOD were localized to the spindle pole body (visualized with Spc42, Fig. 2.5b) unlike the aggresome which co-localizes with the MTOC (Johnston et al., 2002).

A similar analysis using the ER marker Sec63 (Huyer et al., 2004) indicated that the JUNQ is in close proximity to the ER. Sec63 redistributed around the JUNQ relative to the remaining nuclear envelope (Fig. 2.5c), although there was no direct overlap between Sec63 and either VHL or $Ubc9^{ts}$, consistent with the FLIP experiments indicating that the proteins in the JUNQ exchange freely with the cytosol. Since Sec63 usually marks the ERAC structures that accumulate ERAD substrates, these results suggest that the JUNQ forms at a defined cellular location in close proximity to the region that participates in the degradation of misfolded ER proteins. Perhaps the localization of cytosolic and ER misfolded proteins to one cellular location serves to concentrate chaperones and other QC components with their substrates to both enhance the efficiency of misfolded protein clearance and remove misfolded proteins from the cellular milieu.

Given the central role of proteasomal degradation in misfolded protein turnover, we next examined the cellular distribution of using previously characterized GFP tagged proteasomes (Enenkel et al., 1998) (in either the regulatory particle, Cim5 subunit or the core particle, Pre6 subunit) (Fig. 2.5d). Deconvolution microscopy revealed that most proteasomes in the cells localize to the ER, even though there is a fraction of diffuse tagged proteasomes. Strikingly, for all misfolded proteins examined we observed a marked re-distribution of proteasomes to the site of JUNQ protein accumulation both at 30 °C and 37 °C (Fig. 2.5d). On the other hand, proteasomes did not co-localize with the IPOD, This indicates that, surprisingly, soluble misfolded proteins rather than insoluble amyloid aggregates cause a re-distribution of cellular proteasomes. Furthermore, it appears that the peri-nuclear JUNQ compartment acts as a major site of proteasome concentration and misfolded protein degradation.

The localization of another quality control component that interacts with misfolded and aggregated proteins, the chaperone Hsp104 (Cashikar et al., 2005), was assessed using a previously characterized functional GFP-tagged Hsp104 (Tkach and Glover, 2004). Unlike the 26S proteasome, which co-localized only with the JUNQ, Hsp104 co-localized with both JUNQ and IPOD (Fig. 2.5e). However, the majority of Hsp104 accumulated around the IPOD compartment, often in a striking circular arrangement (Fig. 2.5e). Because, Hsp104 often accumulated in an IPOD-like inclusion,

and sometimes also in a JUNQ-like inclusion, in the absence of an ectopically expressed misfolded protein (Fig. 2.5e, middle panel, and unpublished data) it appears that these QC compartments are normally present in cells. The co-localization of Hsp104 with the IPOD resonates with its role in disaggregating prion proteins, which also localize to this compartment. On the other hand, we hypothesize that the co-localization of Hsp104 may serve to keep JUNQ proteins soluble for either refolding or degradation (as shown below in Fig. 2.6t).

Autophagy has been implicated in the clearance of protein aggregates(Sarkar et al., 2007). We found that the IPOD, but not the JUNQ, co-localized with the autophagic marker Atg8(Yorimitsu and Klionsky, 2005) (Fig. 2.5f, see also Fig. 2.6m for EM). Although neither Atg8 nor Atg7, both essential components of the autophagic pathway, were required for IPOD formation (Fig. 2.5i), the proximity of the IPOD to the vacuole (see Fig. 2.5g) and its association with an autophagic marker (Fig. 2.5h for EM) suggest that the IPOD may sequester aggregated proteins for their eventual elimination by autophagy.

The sub-cellular structure of the JUNQ and IPOD compartments was further defined by Immuno-EM analysis (Fig. 2.5g, h). This analysis confirmed that the JUNQ is closely associated with the nucleus, and may be flanked by proliferations of the nuclear membrane (Fig. 2.5g, upper panels). The JUNQ-containing sections of the nucleus exhibited a very consistent co-localization with vacuolar lobes. The IPOD (Fig. 2.5g, lower panels) was made up of electron-dense material, consistent with our FRAP and biochemical characterization. Although we rarely observed IPODs completely surrounded by membranes, they were frequently seen associated with membranous structures including double-membrane autophagic vesicles (Fig. 2.5g, h). Strikingly, EM analysis of prion IPODs showed heavy GFP immune-gold labeling in a circular shape around a densely packed core (Fig. 2.5g for Ure2) consistent with our fluorescence microscopy images where the IPODs formed by prions (including Ure2-GFP: inset) occasionally appears hollow. Since the Hsp104 analysis indicates that cells normally contain an IPOD structure formed with endogenous proteins, we hypothesize that the ectopically expressed aggregation prone prion, like Ure2, is directed to the IPOD and layered on top of the existing aggregates.

Ubiquitination modulates partitioning of QC substrates to the JUNQ or IPOD compartments.

Proteasomal degradation of misfolded proteins requires their prior tagging with a poly-ubiquitin tail(Sherman and Goldberg, 2001) (Fig. 2.6a). We next considered whether ubiquitination of misfolded proteins plays a role in their partitioning to either JUNQ or IPOD. Since degradation of misfolded VHL, Ubc9, and actin requires ubiquitination by the E2 pair Ubc4/5 (Betting and Seufert, 1996; McClellan et al., 2005a; Vang et al., 2005) we expressed these proteins in cells lacking Ubc4/5 (Fig. 2.6a, b for VHL, Fig. 2.6g for $Ubc9^{ts}$, not shown for actin). Ubiquitination was also reduced by over-expression of Ubp4 (Swaminathan et al., 1999) (Fig. 2.6h). Similar results were obtained using either strategy for all misfolded proteins (Fig. 2.6b, Fig. 2.6h, i). Strikingly, impairing misfolded protein ubiquitination blocked their accumulation in the JUNQ and resulted instead in their exclusive accumulation in the IPOD compartment, even at 30°C and in the absence of proteasome inhibition (Fig. 2.6b, g, h, i). The IPOD formed by the misfolded proteins under these conditions exhibited the same morphology as those observed previously, and were also Atg8 and Hsp104-positive (Fig. 2.6n, o, not shown for EM).

It was intriguing that blocking the ubiquitination of misfolded proteins caused them to behave in a manner reminiscent of aggregation-prone amyloidogenic proteins such as HttQ103. Because formation of detergent insoluble aggregates is a hallmark of amyloid formation, we next examined the effect of blocking ubiquitination on the solubility of misfolded VHL (Fig. 2.6c) and Ubc9 (Fig. 2.6f). While misfolded VHL remained Triton-soluble under conditions where it only forms the JUNQ (Fig. 2.6c, left panel), it was almost entirely insoluble when targeted to the IPOD upon blocking ubiquitination (Fig. 2.6c, right panel). Similar results were obtained with $Ubc9^{ts}$; indeed blocking its ubiquitination rendered it as insoluble as aggregated HttQ53 (Fig. 2.6f). On the other hand, blocking the ubiquitination of the native degradation substrate Ub-GFP in the same Δ*ubc4/5* cells did not impair the solubility (Fig. 2.4c). These results indicate that ubiquitination is an important determinant for maintaining solubility and sorting proteins to the JUNQ and that non-ubiquitinated species are directed to the IPOD.

To gain insight into how the quality control machinery helps partition misfolded proteins between JUNQ and IPOD, we exploited the observation that the chaperone Sti1 is required for VHL degradation but not for VHL folding (McClellan et al., 2005a). Biochemical analysis indicates that Sti1 is required for efficient VHL ubiquitination (Fig. 2.6j). Importantly, deletion of Sti1 has no growth defects. Furthermore, Sti1 is not required for $Ubc9^{ts}$ clearance, confirming that degradation of misfolded proteins exhibits different chaperone requirements (McClellan et al., 2005a; Park et al., 2007) (Fig. 2.6k). Strikingly, Sti1 deletion also directed VHL to the IPOD, as observed in Δ*ubc4/5* cells (Fig. 2.6m, n), but had no effect on the localization of $Ubc9^{ts}$ (Fig. 2.6l). This result indicates that ubiquitination and partitioning of misfolded proteins between JUNQ and IPOD is modulated by specific interactions with the cellular chaperone network. Accordingly, the finding that amyloidogenic proteins are primarily targeted to the IPOD may reflect their inefficient interaction with quality control chaperone and ubiquitination components. This property could distinguish prions and other amyloidogenic proteins from the bulk of misfolded QC substrates that normally do not accumulate in amyloids.

We next tested whether enhancing the ubiquitination of a prion protein by addition of a synthetic ubiquitination signal suffices to promote partitioning to the JUNQ (Fig. 2.6p-r). We therefore engineered an N-terminal UFD ubiquitination signal onto the prion Rnq1, which normally only accumulates in IPOD inclusions (Fig. 2.2b-f and Fig. 2.6p, left panel). Strikingly, enhancing its ubiquitination (Fig. 2.6r) directed a fraction of Ub-Rnq1 to the JUNQ (Fig. 2.6p, right panel). Biochemical analysis supported this idea by showing that addition of a poly-ubiquitin tag to the Rnq1 prion resulted in its partial re-distribution to the detergent soluble fraction (Fig. 2.6r). Thus, whereas Rnq1 is predominantly found in the insoluble fraction (Fig. 2.6r, left panel), the Ub-Rnq1 is nearly evenly distributed between the soluble and insoluble fractions (Fig. 2.6r, right panel). Notably, higher molecular weight poly-ubiquitinated Ub-Rnq1 was found only in the soluble fraction. Since non-ubiquitinated Ub-Rnq1 nevertheless has one N-terminal ubiquitin, it appears that poly-ubiquitination is required for enhancing the solubility of Ub-Rnq1. Indeed, co-expressing the de-ubiquitinating enzyme Ubp4 together with Ub-Rnq1 abolished its targeting to the JUNQ (data not shown), and produced an IPOD-only localization, indicating that Rnq1 delivery to the JUNQ requires a poly-ubiquitin tag.

Together, these experiments indicate that poly-ubiquitination is a key determinant for partitioning proteins between the two quality control compartments as it is necessary for sorting misfolded proteins to the JUNQ and sufficient to redirect a prion protein from the IPOD to the JUNQ.

Reversible accumulation of misfolded proteins in the JUNQ but not the IPOD

We next examined the functional consequences of accumulating proteins in the JUNQ or the IPOD by exploiting the observation that a globular misfolded protein can be directed to either compartment by changing its ubiquitination state. We generated misfolded GFP-Ubc9^{ts} at 37 °C and directed it to either the JUNQ or the IPOD. Since the thermal denaturation of Ubc9^{ts} is reversible (data not shown) (Tongaonkar et al., 1999) this strategy allowed us to follow the fate of the protein in either compartment upon return to the permissive temperature at 25 °C (Fig. 2.6s, scheme). While cells containing Ubc9^{ts} in the JUNQ gradually recovered diffuse cytoplasmic GFP-Ubc9^{ts} fluorescence (Fig. 2.6s, top), cells containing misfolded GFP-Ubc9^{ts} in the IPOD did not recover diffuse fluorescence (Fig. 2.6s, bottom for co-expression of Ubp4, not shown for Δ*ubc4/5*). Notably, Ubc9 refolding from the JUNQ required Hsp104 and was inhibited by 5mM Guanidine, consistent with our hypothesis that Hsp104 maintains the solubility of proteins in the JUNQ. Thus, thermally denatured Ubc9 that is ubiquitinated and sorted into the JUNQ can be refolded by the cellular chaperone machinery, while Ubc9 sorted to the IPOD is terminally sequestered from the cytoplasm, consistent with our finding regarding the differential diffusion properties of proteins in the JUNQ and IPOD.

Section 2.4: Discussion

The age-dependent onset of most amyloid diseases highlights the key role of the QC networks in maintaining protein homeostasis. Since different cytosolic QC substrates examined here localized to the JUNQ, the IPOD, or both, we propose that these compartments carry out general but distinct functions in the management of misfolded and aggregated proteins (Fig. 2.6t). Upon misfolding, most proteins will be recognized and ubiquitinated by the chaperone and QC machinery, which directs them to the JUNQ. Proteins in the JUNQ remain competent for either refolding or proteasomal degradation (Fig. 2.1 and 2.6). The JUNQ appears to be a region that concentrates disaggregating chaperones and 26S proteasomes and is in close proximity to the perinuclear ER region involved in ERAD (Fig. 2.5). The localization of both misfolded proteins and QC components at the ER membrane may serve to facilitate both degradation and refolding by increasing their local concentrations and enhancing their encounter rates by restricting diffusion. Conditions that increase the misfolded protein load, such as stress or aging, may saturate the QC machinery needed for sorting to the JUNQ, leading to the accumulation of aggregated and potentially toxic species. These misfolded proteins are directed to the IPOD, which appears to terminally sequester protein aggregates. The spatial sequestration of these aggregates from the site where most proteasomal degradation takes place may serve a protective function (Rubinsztein, 2007). The IPOD co-localization with Atg8 supports previous proposals that insoluble aggregates are eventually delivered to the autophagic pathway (Arrasate et al., 2004; Kopito, 2000; Rubinsztein, 2006) . Notably, the differential sorting of misfolded proteins into these compartments is conserved from yeast to mammalian cells.

The identification of two distinct QC compartments resonates with a number of previous observations in various model systems. For instance, studies in a *C. elegans* model for Alzheimer suggest the existence of two hierarchical pathways for the degradation of different types of Aβ amyloidogenic species (Cohen et al., 2006; Siegel et al., 2007). Furthermore, it has been observed that both ERAD substrates (Kruse et al., 2006b) and cytosolic alpha-synuclein (Webb et al., 2003) can be degraded by alternate pathways, with soluble species of the same protein degraded via the proteasome and

insoluble aggregates by autophagy (Kruse et al., 2006a; Webb et al., 2003). Additionally, for mammalian cells, there have been disparate reports on the solubility and structural properties of protein inclusions (Kamhi-Nesher et al., 2001; Matsumoto et al., 2006; Matsumoto et al., 2005; Szeto et al., 2006). Our findings provide a framework for integrating these observations into a conserved cellular mechanism of quality control. Importantly, our results identify solubility and the ubiquitination state of a QC substrate as key determinants of its delivery to either the JUNQ or the IPOD. The finding that adding a synthetic ubiquitination signal to Rnq1 promotes delivery to the JUNQ argues for a direct role of poly-ubiquitination as a trafficking signal (Fig. 2.6p-r). The analysis of $Ubc9^{ts}$ recovery from heat-shock further indicates that poly-ubiquitination not only targets proteins for degradation, but may also contribute to their re-folding competence (Fig. 2.6s). Future studies should determine whether poly-ubiquitination exerts these effects through interactions with ubiquitin receptors and chaperone components or whether the presence of a poly-ubiquitin tail directly enhances the solubility of misfolded proteins.

A striking finding in our study is that unlike the bulk of cellular misfolded proteins, amyloidogenic proteins are targeted directly to the IPOD. This distinguishing characteristic may arise from either enhanced aggregation rates or reduced affinity for cytosolic QC components involved in sorting to the JUNQ, which may lead to higher levels of toxic misfolded conformations in the cytosol. This idea is consistent with findings that the toxicity of amyloidogenic proteins resides in small soluble species (Arrasate et al., 2004). Over-expression of chaperones and ubiquitination components, known to reduce toxicity could compensate for their reduced affinity for the amyloidogenic species (Barral et al., 2004; Bukau et al., 2006; McClellan et al., 2005b; Muchowski and Wacker, 2005; Tam et al., 2006). The decline in chaperone capacity due to aging could account for the increased occurrence of aggregate formation and cytotoxicity in older patients (Cohen et al., 2006).

In summary, we find that eukaryotic cells contain two distinct compartments that manage misfolded proteins depending on their solubility and ubiquitination state. Amyloidogenic and globular misfolded proteins are differentially engaged by these pathways. Our finding provides new perspectives on the molecular basis of protein

conformation diseases, which may have profound implications for the understanding of neurodegeneration, aging and stress.

Section 2.5: Methods

Yeast Media, Plasmids, and Strains

Yeast media preparation, growth, transformations, and manipulations were performed according to standard protocols(Adams et al., 1997). The protein substrates used in this study were visualized as fusions to fluorescent proteins derived from Green Fluorescent Protein (GFP). GFP-Ubc9^{ts}, GFP-Ubc9^{wt}, GFP-VHL, Act1-E364K-GFP, Rnq1-GFP, Ure2-GFP, Ub-G76A-GFP, Ub-Arg-GFP, Ub-G76A-Rnq1-GFP, CHFP-Apg8, NLS-tdTomato (Shaner et al., 2004) (TFP) were cloned into pESC (GAL1 *URA3*; Stratagene, La Jolla, California). Each of the above was also cloned into pESC GAL1 LEU2 vectors, and identical fusion proteins were made with mCherry (Shaner et al., 2004) Fluorescent Protein (CHFP) instead of GFP. The pESC plasmid expressing elongin B and elongin C from a GAL-inducible promoter is described elsewhere (McClellan et al., 2005a; Melville et al., 2003). All proteins were cloned by PCR from yeast genomic DNA or a template plasmid and verified by sequencing. Spc42-GFP and Spc42-CHFP were cloned downstream of the Tub2 promoter into the pRS316 vector. Sec63-CHFP was cloned by excising the GFP from pSM1462 (Prinz et al., 2000) and replacing it with mCherry. GFP-Hsp104 (Tkach and Glover, 2004) was a generous gift from John Glover.

The yeast strains used in this study are as follows: wt *CIM3* (YPG499; MAT**a** *ura3-52 leu2-Δ1 his3-Δ200 trp1-Δ63 lys2-801 ade2-101*) and *cim3-1* (CMY762; *ura3-52 leu2-Δ1 his3-Δ200 cim3-1*)(Ghislain et al., 1993); MHY501 (MATα *his3-Δ200 leu2-3, 112 ura3-52 lys2-801 trp1-1*) and the isogenic mutant strains MHY508 *(ubc4::HIS3 ubc5::LEU2*) and MHY570 (*ubc4::TRP1 ubc5::LEU2 ubc6::HIS3 ubc7::LEU2*)(Chen et al., 1993); GCE6 (*MAT***a** *his3-11,15 leu2-3,112 ura3 PRE6-GFPHA::HIS3::URA3*), GAL5 (*MAT***a** *his3-11,15 leu2-3,112 ura3 CIM5-GFPHA::HIS3::URA3*)(Enenkel et al., 1998); YKO wt, *Δsti1*, *Δpdr5* (MAT**a**/MATα *orfΔ::kanMX4/orfΔ::kanMX4 ura3Δ0/ura3Δ0 leu2Δ0/leu2Δ0 his3Δ1/his3Δ1 met15Δ0/MET15 lys2Δ0/LYS2* (*Saccharomyces* Genome Project) (Winzeler et al., 1999). For experiments using MG132, the YKO (B4147) strains lacking the Pdr5 transporter were used as wild-type. Deletion of Pdr5 sensitizes cells to the proteasome inhibitor MG132. When indicated, cells were treated with 80μM MG132

(Sigma) dissolved in DMSO for 1hr. For all experiments, expression was shut off prior to temperature shift and microscopy by addition of 2% Glucose.

Mammalian Cell Culture and Plasmids

HeLa cells were cultured according to standard procedures. HeLa S3 cells were maintained in DMEM/F12 (Gibco, Carlsbad, CA), supplemented with 10% FCS and L-glutamine. Confluent cells were transfected using Lipofectamine 2000 (Invitrogen) according to manufacturer's protocol. Cells were treated with MG132 (or DMSO control) 24 h post-transfection and analyzed 4-8 h later by microscopy. HeLa cells were split onto coverslips, washed twice with PBS, fixed with 4% paraformaldehyde (in PBS) for 20 min and washed twice with PBS. GFP-Ubc9^{ts}, GFP-Ubc9^{wt}, and CHFP-VHL were sub-cloned from their original pESC vectors into pcDNA3.1 (Invitrogen) vectors.

Fluorescence Microscopy

Conventional epifluorescence micrographs were obtained from live yeast cells on a Zeiss Axiovert microscope with a 100× oil lens (NA1.4; Zeiss). Digital (12-bit) images were acquired with a cooled CCD (Princeton Instruments, Trenton, NJ) and processed by using METAMORPH software (Universal Imaging, Media, PA). The excitation filters used for conventional microscopy were 500DF20 (GFP), 540DF20 (Rhodamine), and 570DF20 (Texas red). Emission filters were 535DF20 (GFP), 560DF20 (Rhodamine), and 630DF25 (Texas red). The dichroics were: 505 DCLP (GFP), and 595 DCLP (Texas red). For deconvolution microscopy, yeast cells were fixed on glass coverslips in 4% paraformaldehyde. Deconvoluted images were acquired by using an Olympus microscope with 436 DF10 (CFP) and 500DF20 (YFP) filters for excitation and 470 DF30 (CFP) and 535 DF30 (YFP) filters for emission. Digital images (12 bit) were digitally deconvoluted by using DELTAVISION hardware and software (Applied Precision, Issaquah, WA). Live-cell imaging was performed using the Marianas system from Intelligent Imaging Innovations equipped with the MicroPoint FRAP laser system (Photonic Instruments, Inc.).

VHL Solubility and Ubiquitination Assay

Yeast were grown, collected, and lysed according to standard protocols as described in(McClellan et al., 2005a). Cells expressing VHL were grown at 30 °C or 37 °C, harvested, washed once with sterile double-distilled H_2O, and resuspended in 1X native yeast lysis buffer (30 mM HEPES [pH 8.0], 150 mM NaCl, 1% glycerol, 1 mM DTT, 1 mM PMSF, and 1 μg/ml pepstatin-A; and 1mM NEM for ubiquitination assays). Where indicated, lysis buffer also contained 0.5% Triton. Pellets were frozen in liquid nitrogen and lysates were prepared by beating in liquid nitrogen (3 min) and clarified by centrifugation at 6,000 × g for 5 min at 4°C. Fifty microliters of this supernatant was set aside as total protein. Fifty microliters was spun at 16,000 × g for 30 min at 4°C. This supernatant was removed and designated the soluble fraction. The pellet was resolubilized by heating in 50 μl 1× SDS sample buffer. Fifty microliters of 4× SDS sample buffer was added to the total-protein and soluble-fraction samples. Equal amounts of each fraction were resolved by SDS-PAGE followed by immunoblot analysis with anti-GFP or anti-Myc antisera. For gel aggregation assays equivalent total protein amounts of lysate were run on SDS–PAGE and both stacking and resolving gels were transferred and analysed by immunoblot as described in (Krobitsch and Lindquist, 2000).

Electron Microscopy

Cells were fixed and processed as described in Mulholland et al. (1994). Briefly:

25 ml cultures of exponentially growing cells (5 X 10^6 cells/ml) in minimal medium were quickly harvested by vacuum filtration over a 0.45 um nitrocellulose membrane; filtration was stopped when the total volume in the filter apparatus was < 5 ml, but not dry. To this concentrated cell suspension, still on the filter membrane, 15 ml of freshly prepared, room temperature fixative [40 mM potassium phosphate, pH 6.7, 0.5 M sorbitol, 4% formaldehyde freshly prepared from paraformaldehyde (Polysciences, Warrington, PA), 0.2% glutaraldehyde (EM grade, Polysciences), 1 mM $MgCl_2$, and 1 mM EGTA, pH 8] was added and mixed rapidly with the cells by pipetting the suspension several times. The cell suspension was then transferred to a 50 ml

polypropylene centrifuge tube and incubated at room temperature for approximately 1 hour.

The fixed cells were then centrifuged at low speed in a clinical centrifuge and the pellet was resuspended in 40 mM potassium phosphate buffer (pH 6.7) containing 0.25 M sorbitol and transferred to eppendorf tubes. The cells were again centrifuged and washed in 40 mM potassium phosphate buffer (pH 6.7). The final pellet of fixed cells was resuspended in 1 ml 1% sodium metaperiodate to make the cell wall more permeable, incubated for 10 min at room temperature, and then centrifuged and resuspended in 1 ml distilled water. Next, to block free aldehyde groups, the cells were centrifuged, resuspended in 1 ml 50 mM ammonium chloride and incubated for 10 min at room temperature.

The cells were then washed once in distilled water, centrifuged at low speed and immediately dehydrated (on ice) by resuspending the cell pellet in 70% (v/v) ice-cold ethanol and incubating on ice for 5 minutes. The cells were similarly centrifuged and sequentially resuspended in 80%, 85%, 90%, 95% ice-cold ethanol and finally once in 100% ice-cold ethanol. A final dehydration and centrifugation in 100% ethanol at room temperature was performed twice. The dehydrated cells then were infiltrated with room temperature L. R. White resin (Polysciences, Warrington, PA) and prepared for polymerization as described by Wright and Rine (1989) except that infiltration of resin into the cells was done without application of vacuum and harvesting of cells was by centrifugation. The resin was polymerized by incubation at 47°C for approximately 48 hours.

Thin sections measuring approximately 60 to 70 nm (as determined by a gray/silver interference color) were cut with a diamond knife and were picked up on 300 mesh nickel grids (Polysciences, Warrington, PA) which had been made sticky with a dilute formvar solution (Wright and Rine, 1989).

Affinity purified rabbit antibodies directed against GFP were a gift to Jon Mulholland (CSIF) from Dr. Pam Silver's lab (Harvard University, MA). The secondary antibodies used were 10 nm gold-conjugated, anti-rabbit IgG (goat) secondary antibodies (BioCell, Ted Pella, CA). Antibody incubations were performed as described previously by Mulholland et al. (1994). Primary and secondary antibodies were diluted

1:50 in PBST (140 mM NaCl, 3 mM KCl, 8 mM Na_2HPO_4, 1.5 mM KH_2PO_4, 0.05% Tween 20) containing 0.5% BSA (bovin serum albumin) and 0.5% ovalbumin (Sigma, St. Louis, MO) and were incubated at room temperature for 1 - 2 hours, with cell sections mounted on grids as described above. In the absence of the primary antibody, the anti-rabbit secondary antibodies did not react with the cell sections. Following immunolocalization cell sections were post-fixed and stained with uranyl acetate and lead citrate as previously described (Mulholland et al., 1994). All observations were made on a JEOL 1230 TEM at an accelerating voltage of 80 kV using a 20-um-diameter objective aperture using a Gatan 967 cooled CCD camera for image acquisition.

Section 2.6: Acknowledgements

We thank R. Tsien for the generous gift of plasmids expressing mCherry and tdTomato fluorescent proteins, S. Michaelis for the gift of the Sec63-GFP plasmid, J. Glover for the gift of the GFP-Hsp104 plasmid, C. Enenkel for strains expressing GFP-tagged proteasomes, and V. Albanese for the gift of B4147 lacking the PDR5 gene; A. Chaudhuri for technical assistance; J. Mulholland for assistance with deconvolution microscopy; S. Yamada for assistance with the photobleaching experiments and W.J. Nelson for access to the live cell microscope and for comments on the manuscript. We thank R. Andino, W. Burkholder, J. England, R. Geller, M. Kaganovich, E. Bennett, and members of the Frydman lab for helpful discussions and comments on the manuscript. This work was supported by grants from NIH to R.K. and J.F.

Figure 2.1 a-c

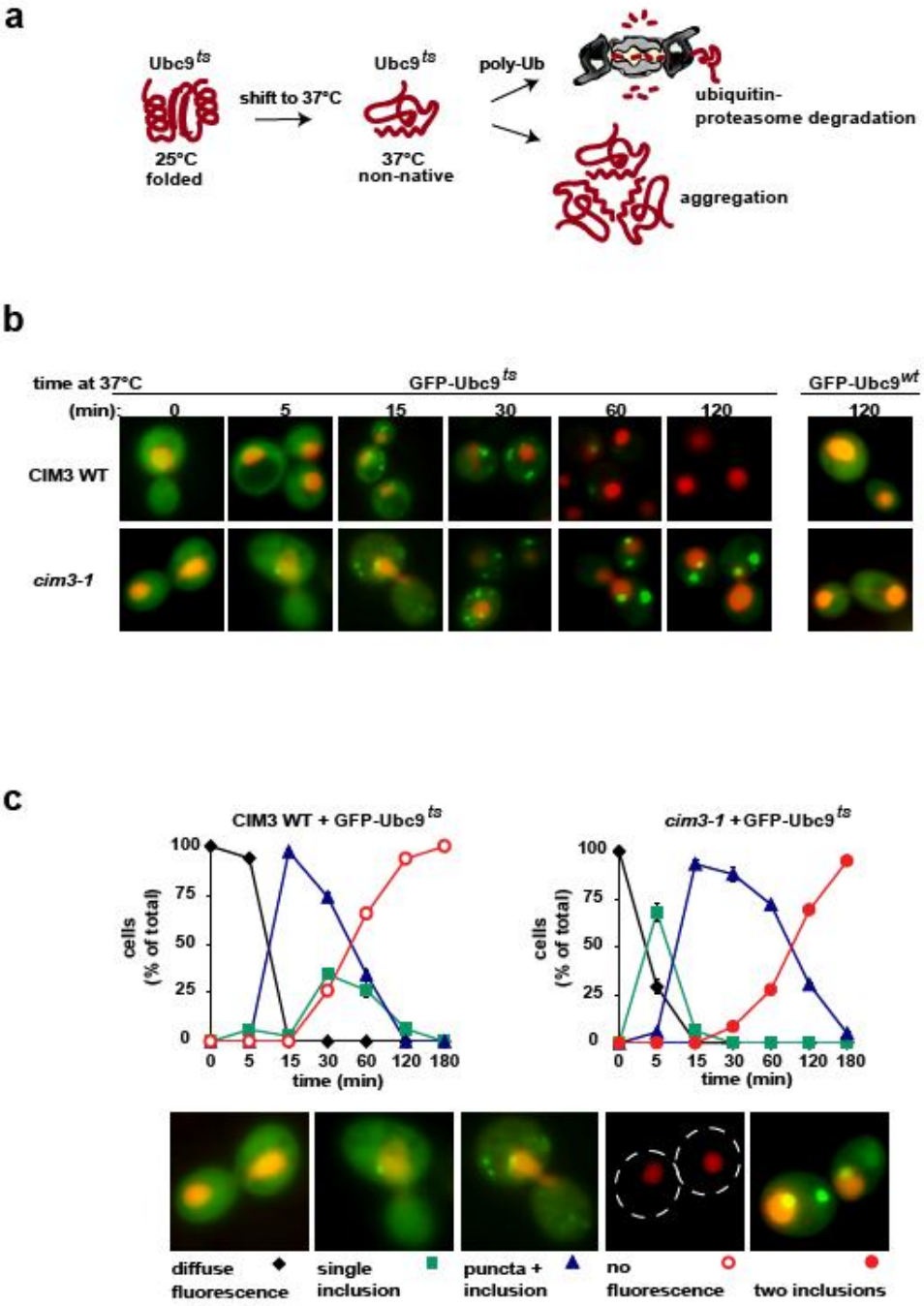
a
Ubc9ts
shift to 37°C
Ubc9ts
poly-Ub
ubiquitin-
proteasome degradation
25°C
folded
37°C
non-native
aggregation
b
time at 37°C
GFP-Ubc9ts
GFP-Ubc9wt
(min):
0
5
15
30
60
120
120
CIM3 WT
cim3-1
c
CIM3 WT + GFP-Ubc9ts
cim3-1 +GFP-Ubc9ts
cells
(% of total)
100
75
50
25
0
0 5 15 30 60 120 180
time (min)
diffuse
fluorescence
single
inclusion
puncta +
inclusion
no
fluorescence
two inclusions

Figure 2.1 d-g

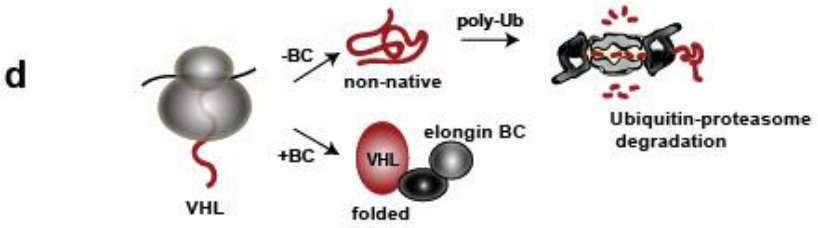
d
-BC
non-native
poly-Ub
Ubiquitin-proteasome
degradation
+BC
VHL
elongin BC
VHL
folded

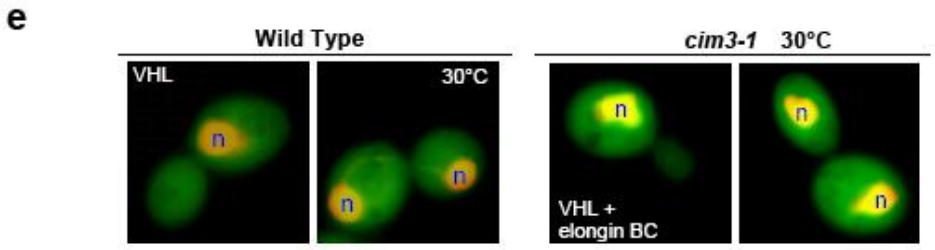
e
Wild Type
cim3-1 30°C
VHL
30°C
VHL +
elongin BC

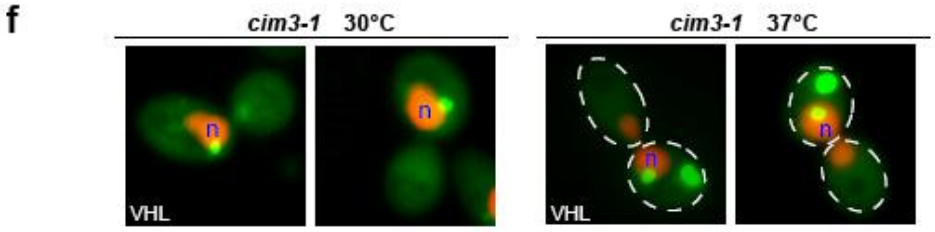
f
cim3-1 30°C
cim3-1 37°C
VHL
VHL

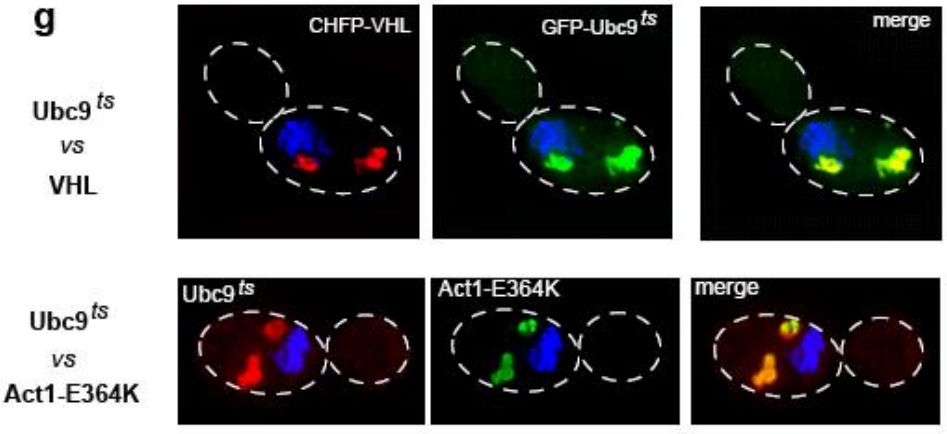
g
Ubc9ts
vs
VHL
CHFP-VHL
GFP-Ubc9ts
merge
Ubc9ts
vs
Act1-E364K
Ubc9ts
Act1-E364K
merge

Figure 2.1 h-j

h

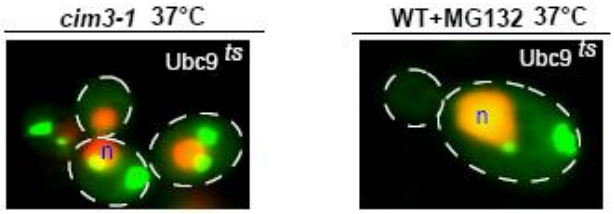

i

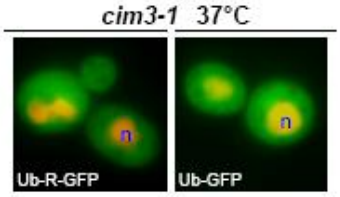

j

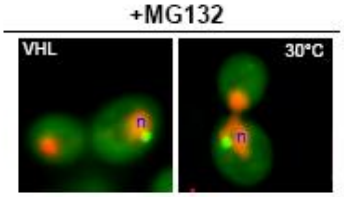

Figure 2.1 k-m

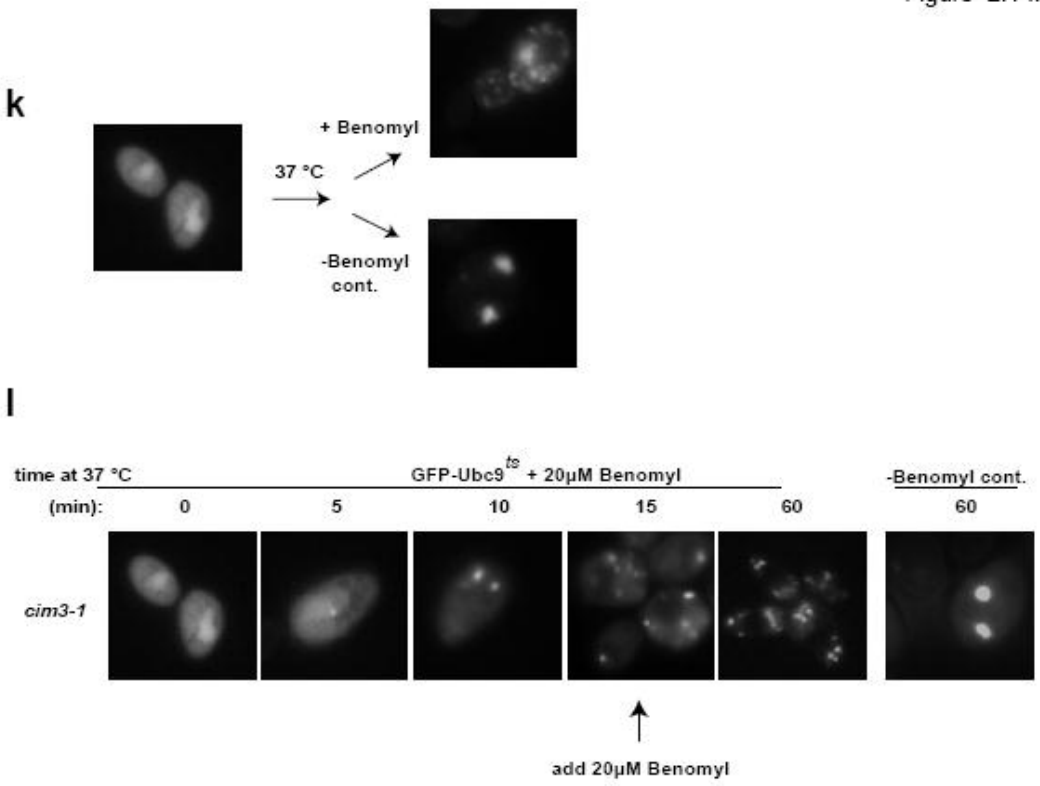
k
+ Benomyl
37 °C
-Benomyl
cont.
l
time at 37 °C
GFP-Ubc9ts + 20μM Benomyl
-Benomyl cont.
(min):
0
5
10
15
60
60
cim3-1
add 20μM Benomyl
m
+ Benomyl
Ubc9ts
folded
37 °C
puncta
wash out Benomyl
two
inclusions
-Benomyl
cont.
two
inclusions
GFP-Ubc9ts
+ 20μM Benomyl
-Benomyl cont.
30min at 37 °C
wash out Benomyl

Figure 2.1: A thermally destabilized QC substrate accumulates in two distinct inclusions upon proteasome impairment

a, The temperature-sensitive mutant of Ubc9 Y68L ($Ubc9^{ts}$) is folded and long-lived at 25 °C. Upon temperature shift to 37 °C, the $Ubc9^{ts}$ protein misfolds and its half-life is decreased from >2 hrs to ~30 min due to turnover by the ubiquitin-proteasome pathway.

b, Localization patterns of folded and misfolded GFP-Ubc9 in wild-type CIM3 cells, detected by direct fluorescence. Folded GFP-Ubc9 shows diffuse fluorescence at 30 °C (0 min). Following a shift to 37 °C, GFP-$Ubc9^{ts}$ initially forms puncta (15 – 30 min) which are eventually cleared (60 -120 min). Wild type GFP-$Ubc9^{wt}$ was monitored for 120 minutes at 37 °C as a control. Nuclei were visualized by co-expressing NLS-tdTomato (Shaner et al., 2004) (NLS-TFP) from the same plasmid as GFP-$Ubc9^{ts}$. Protein expression was shut off by addition of 2% Glucose prior to temperature shift in all experiments. Proteasome inhibition causes accumulation of GFP-$Ubc9^{ts}$ in two inclusions. GFP-$Ubc9^{ts}$ was expressed in the *cim3-1* proteasome mutant strain as above.

c, Quantification of $Ubc9^{ts}$ localization pattern in wild type and proteasome-impaired cells. Graphs represent three separate experiments conducted as in Figs. 1, in which the phenotypes of 100 cells were scored at each timepoint. A representative example of each phenotype scored is shown below.

d, Quality control of the VHL tumor suppressor. Upon co-expression of its binding partners, elongin BC, VHL folds to form the VBC complex. In the absence of elongin BC, VHL is degraded by the ubiquitin-proteasome pathway(McClellan et al., 2005a).

e, VHL localization in wild type and *cim3-1* cells 30 °C. Without proteasome inhibition misfolded VHL shows weak diffuse fluorescence. Folded VHL shows intense diffuse fluorescence upon co-expression of GFP-VHL with elongin BC in *cim3-1* cells.

f, VHL localization in *cim3-1* cells at 30 °C and 37 °C. Upon proteasome inhibition, the diffuse fluorescence of GFP-VHL is re-distributed to a juxtanuclear inclusion. VHL localizes to two inclusions at 37 °C upon proteasome impairment in the *cim3-1* proteasome mutant strain. Two panels are shown for each experiment.

g, Misfolded VHL, Ubc9, and actin co-localize in the same two inclusions. VHL tagged with mCherry(Shaner et al., 2004) (CHFP-VHL, red) co-localizes with GFP-Ubc9^{ts} (green upper panel) and with Act1-E364K-GFP (green lower panel) in *cim3-1* yeast, after 2 hrs at 37 °C. Images were collected as a Z-series and de-convoluted. A 2D projection is shown.

h, Proteasome inhibition causes accumulation of GFP-Ubc9^{ts} in two inclusions. GFP-Ubc9^{ts} was expressed in the *cim3-1* proteasome mutant strain for 1hr at 37 °C. Alternatively, GFP-Ubc9^{ts} was expressed in the YKO (B4147) strains lacking the Pdr5 transporter and treated with 80μM MG132 for 1hr at 37 °C.

i, Native, correctly folded substrates of the ubiquitination pathway Ub-Arg-GFP and Ub-G76A-GFP exhibit diffuse fluorescence at 37 °C upon proteasome impairment in the *cim3-1* proteasome mutant strain.

j, Upon proteasome inhibition with MG132, the diffuse fluorescence of GFP-VHL is re-distributed to a juxtanuclear inclusion.

k, Accumulation of Ubc9^{ts} in two inclusions following misfolding and stress requires microtubule polymerization. When *cim3-1* yeast expressing GFP- Ubc9^{ts} were incubated with or without Benomyl for 2hrs at 37 °C, Benomyl cause inclusion formation to arrest at the puncta stage (Top).

l, Puncta formed by misfolded GFP-Ubc9^{ts} in *cim3-1* yeast require microtubule polymerization to coalesce into inclusions. Benomyl addition after puncta had already formed was equally effective in arresting inclusion formation at the puncta stage.

m, Restoring microtubule polymerization after Benomyl arrest leads to coalescence of puncta into two inclusions.

Figure 2.2 a-f

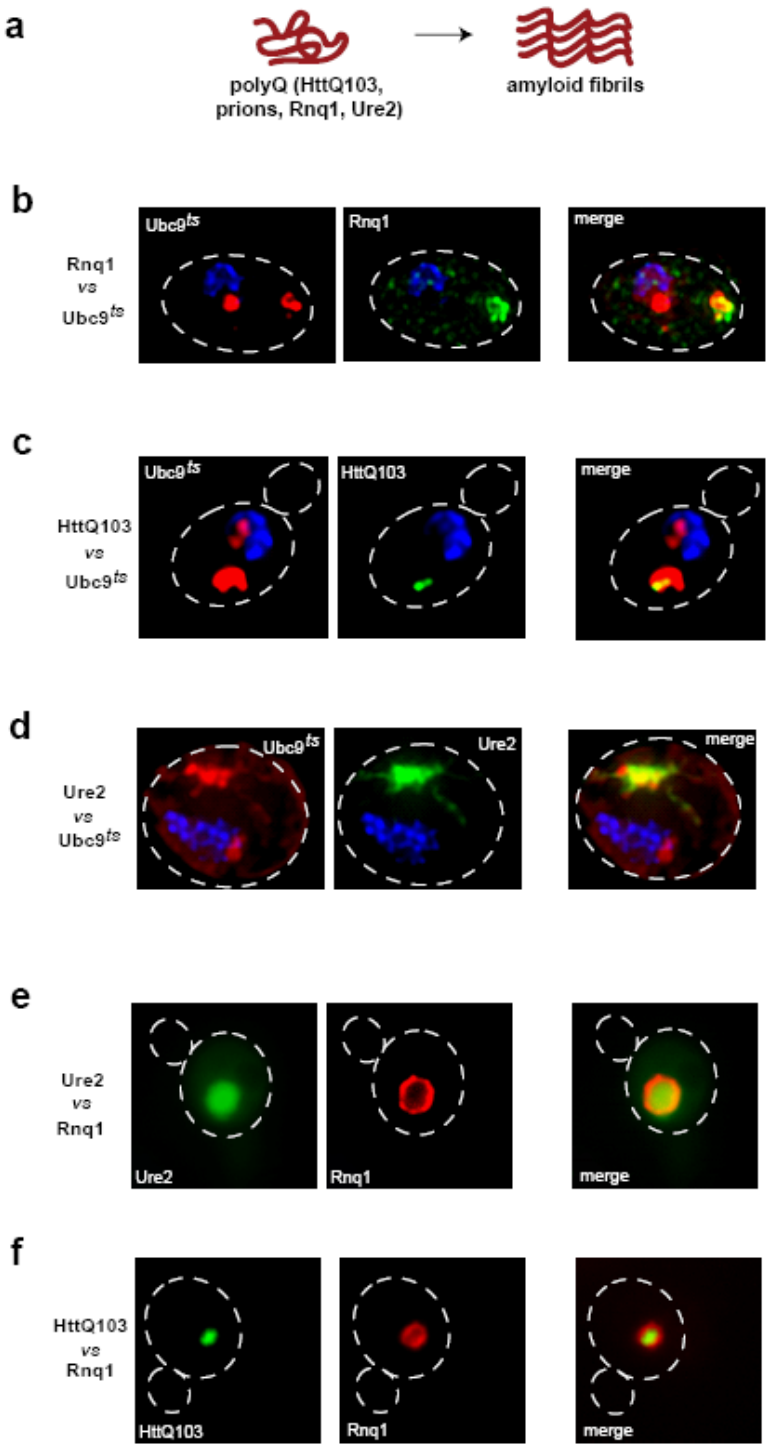
a
polyQ (HttQ103, prions, Rnq1, Ure2)
amyloid fibrils
b
Rnq1 vs Ubc9ts
Ubc9ts
Rnq1
merge
c
HttQ103 vs Ubc9ts
Ubc9ts
HttQ103
merge
d
Ure2 vs Ubc9ts
Ubc9ts
Ure2
merge
e
Ure2 vs Rnq1
Ure2
Rnq1
merge
f
HttQ103 vs Rnq1
HttQ103
Rnq1
merge

Figure 2.2: A panel of QC substrates defines two distinct compartments for the sequestration of misfolded cytosolic proteins

a, A class of amyloidogenic proteins, including HttQ103 and the yeast prions Rnq1 and Ure2, aggregate under normal conditions without proteasome inhibition to form highly ordered insoluble amyloid aggregates.

b, Co-localization of inclusions of the yeast prion Rnq1 (green, tagged with GFP) and misfolded $Ubc9^{ts}$ (red, tagged with CHFP) in *cim3-1* yeast. Images were collected as a Z-series and de-convoluted. A 2D projection is shown for b-d.

c, Co-localization of inclusions of HttQ103-GFP with CHFP-$Ubc9^{ts}$ in *cim3-1* yeast, after 2hrs at 37 °C, examined as in b.

d, Co-localization of inclusions of Ure2-GFP with CHFP-$Ubc9^{ts}$ in *cim3-1* yeast, after 2hrs at 37 °C, examined as in b.

e, Co-localization of the yeast prions Ure2-GFP and Rnq1-CHFP in the peripheral inclusion. A direct fluorescence image is shown for e and f.

f, Co-localization of HttQ103-GFP with Rnq1-CHFP in the peripheral inclusion**.**

Figure 2.3a

a

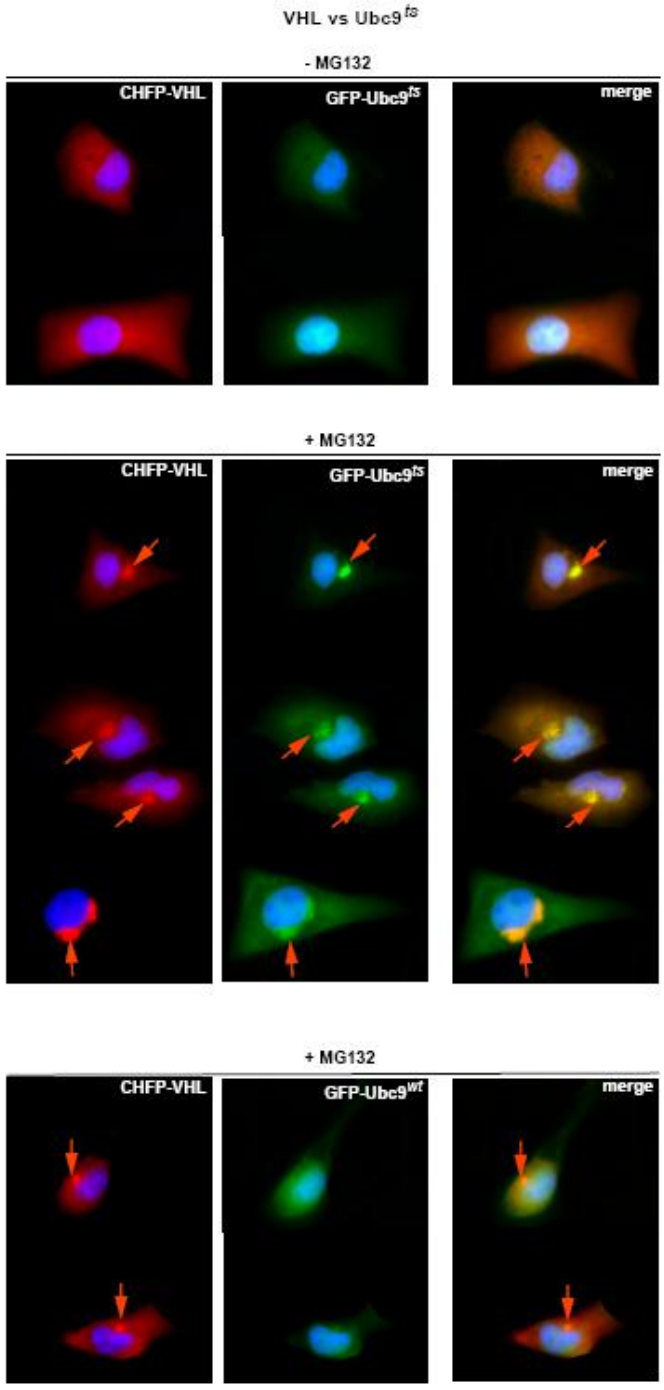
VHL vs Ubc9fs
- MG132
CHFP-VHL
GFP-Ubc9fs
merge
+ MG132
CHFP-VHL
GFP-Ubc9fs
merge
+ MG132
CHFP-VHL
GFP-Ubc9wt
merge

Figure 2.3b

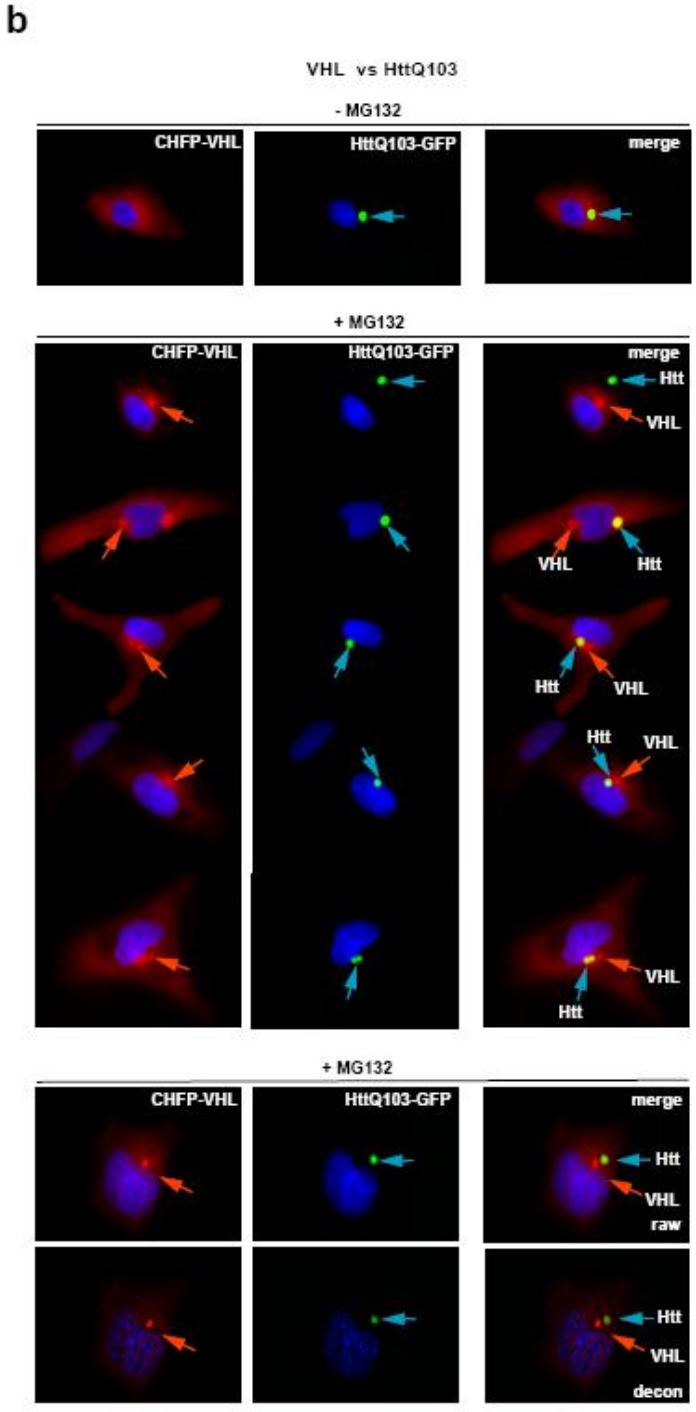
b
VHL vs HttQ103
- MG132
CHFP-VHL
HttQ103-GFP
merge
+ MG132
CHFP-VHL
HttQ103-GFP
merge
Htt
VHL
VHL
Htt
Htt
VHL
Htt
VHL
VHL
Htt
+ MG132
CHFP-VHL
HttQ103-GFP
merge
Htt
VHL
raw
Htt
VHL
decon

Figure 2.3. Mammalian cells differentially sequester misfolded proteins in two distinct compartments.

a, VHL, Ubc9^{ts} and HttQ103 localization in the absence of proteasome inhibition. CHFP-VHL and GFP-Ubc9^{ts} show diffuse localization with enhanced nuclear fluorescence (upper panels), and HttQ103-GFP forms one hyper-fluorescent inclusion per cell (lower panels). A class of amyloidogenic proteins, which includes HttQ103 and the yeast prions Rnq1 and Ure2, aggregate under normal conditions without proteasome inhibition, and form highly oligomeric insoluble amyloid aggregates.

b, VHL, Ubc9^{ts} and HttQ103 localization following 4hr treatment with 10μM MG132. CHFP-VHL and GFP-Ubc9^{ts} form peri-nuclear puncta and inclusions in next to the ER (upper panels). HttQ103-GFP forms a single inclusion that is sometimes peri-nuclear, but oftentimes in other cytosolic locations in the cell. Deconvolution shows that HttQ103 does not co-aggregate with VHL (last panel).

Figure 2.4a-b

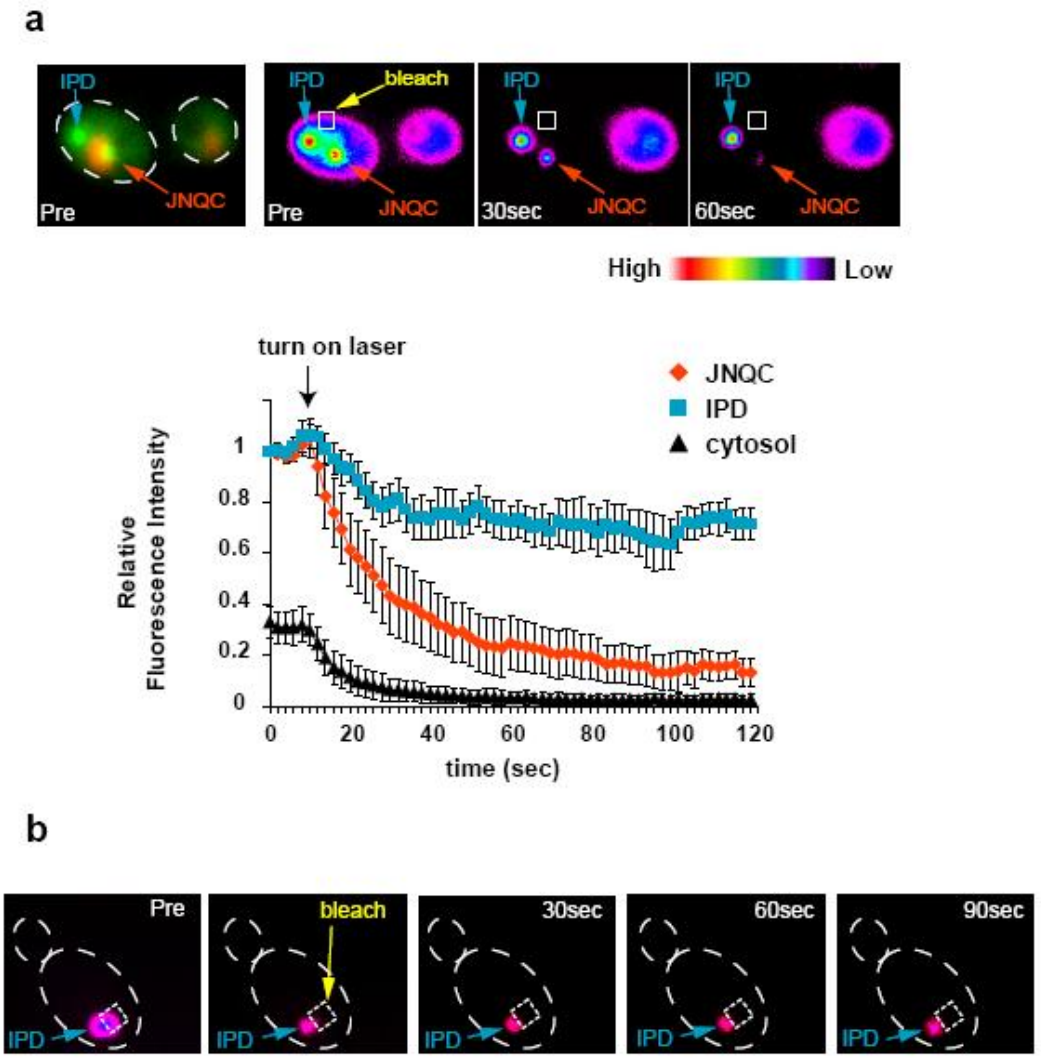
a
IPD
JNQC
Pre
bleach
30sec
60sec
High
Low
turn on laser
JNQC
IPD
cytosol
Relative Fluorescence Intensity
1
0.8
0.6
0.4
0.2
0
0
20
40
60
80
100
120
time (sec)
b
Pre
bleach
30sec
60sec
90sec
IPD

Figure 2.4c-e

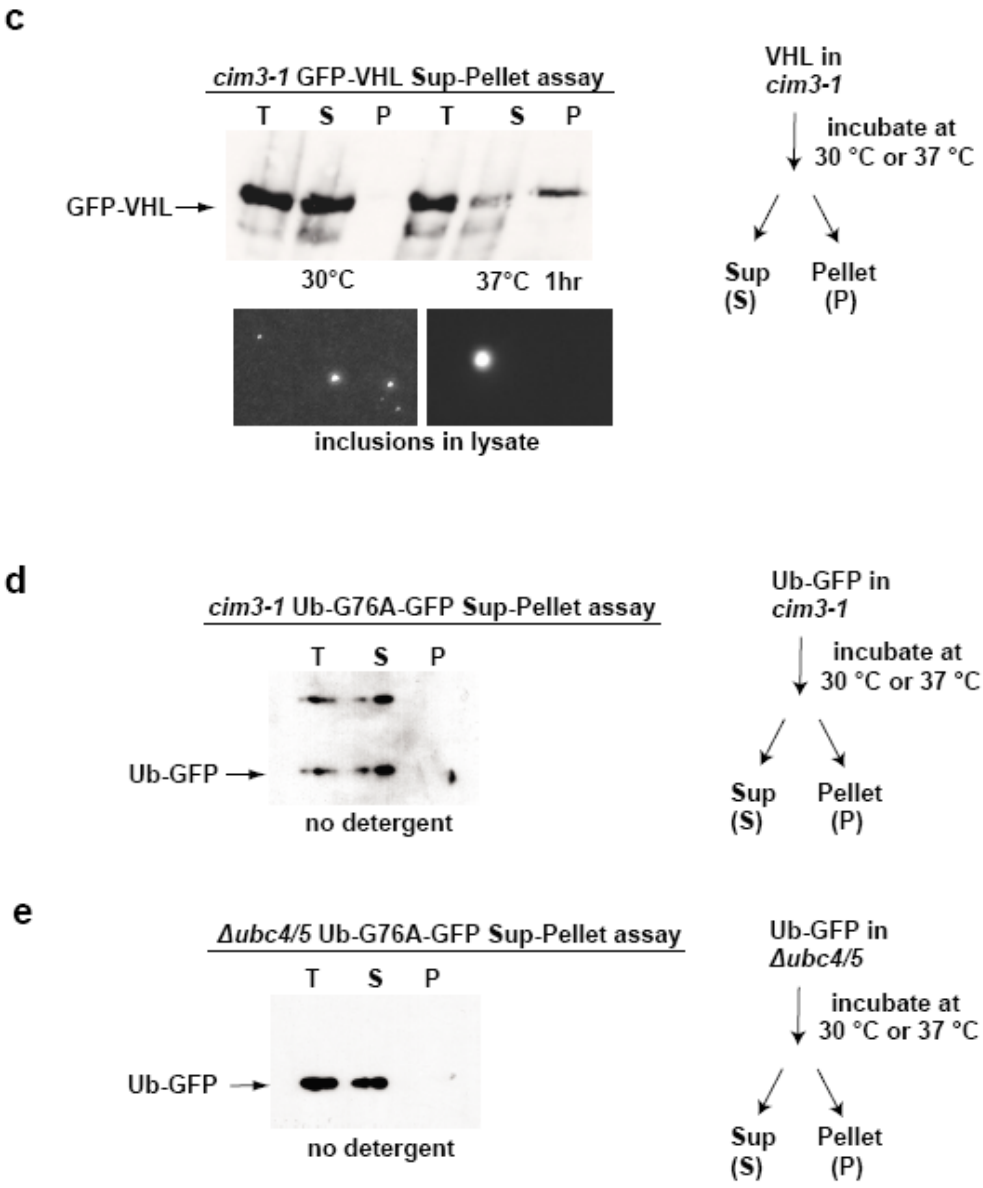
c
cim3-1 GFP-VHL Sup-Pellet assay
T S P T S P
GFP-VHL
30°C
37°C 1hr
inclusions in lysate
VHL in cim3-1
incubate at 30 °C or 37 °C
Sup (S)
Pellet (P)
d
cim3-1 Ub-G76A-GFP Sup-Pellet assay
T S P
Ub-GFP
no detergent
Ub-GFP in cim3-1
incubate at 30 °C or 37 °C
Sup (S)
Pellet (P)
e
Δubc4/5 Ub-G76A-GFP Sup-Pellet assay
T S P
Ub-GFP
no detergent
Ub-GFP in Δubc4/5
incubate at 30 °C or 37 °C
Sup (S)
Pellet (P)

Figure 4. Differential solubility of misfolded substrates in the distinct quality control compartments.

a, Qualitative FLIP analysis indicates that misfolded protein in the JUNQ and IPOD exhibit different relative exchange rates with the cytosolic pool. Pre- and post-bleach images of a representative FLIP experiment with GFP-Ubc9^{ts} are shown. The fluorescence intensity scale is pseudocolored as shown. A square designates the location of the photobleaching laser spot. GFP-Ubc9^{ts} was expressed in *cim3-1* yeast, and expression was shut off by addition of 2% Glucose prior to temperature shift to 37 °C as in Fig. 1.

Relative fluorescence of JUNQ (orange), IPOD (blue), and cytosol (black) from 10 FLIP experiments is shown over time. IPOD has a substantially greater non-exchanging fraction than JUNQ.

b, Protein in the IPOD inclusion is immobile. Shown are pre- and post-bleach images of a representative FRAP experiment and subsequent recovery of GFP-Ubc9^{ts}. GFP-Ubc9^{ts} was expressed in *Δubc4/5* cells and shifted to 37 °C to form the IPOD after addition of 2% Glucose.

c, Accumulation of VHL in the IPOD corresponds to its accumulation in a Triton-insoluble fraction. Proteasome impaired (*cim3-1*) yeast expressing VHL were incubated at 30 °C (where VHL accumulates only in the JUNQ), or at 37 °C (where VHL also accumulates in the IPOD).

d, A native proteasome substrate, Ub-GFP, remains soluble at 37 °C in proteasome-mutant (*cim3-1*) yeast.

e, Ub-GFP remains in the soluble fraction in *Δubc4/5* yeast, where its ubiquitination is blocked.

Figure 2.5a-c

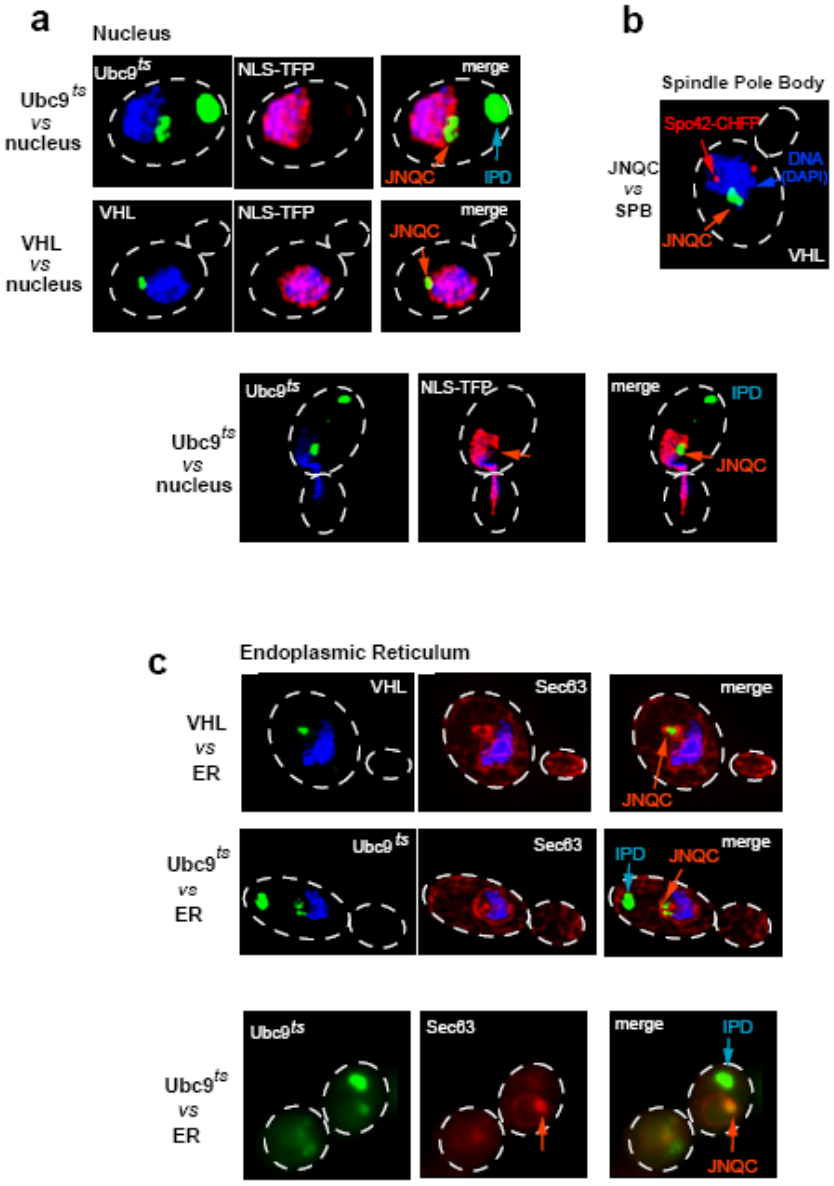
a
Nucleus
Ubc9ts vs nucleus
Ubc9ts
NLS-TFP
merge
JNQC
IPD
VHL vs nucleus
VHL
NLS-TFP
merge
JNQC
b
Spindle Pole Body
JNQC vs SPB
Spc42-CHFP
DNA (DAPI)
JNQC
VHL
Ubc9ts vs nucleus
Ubc9ts
NLS-TFP
merge
IPD
JNQC
c
Endoplasmic Reticulum
VHL vs ER
VHL
Sec63
merge
JNQC
Ubc9ts vs ER
Ubc9ts
Sec63
IPD
JNQC
merge
Ubc9ts vs ER
Ubc9ts
Sec63
merge
IPD
JNQC

Figure 2.5d

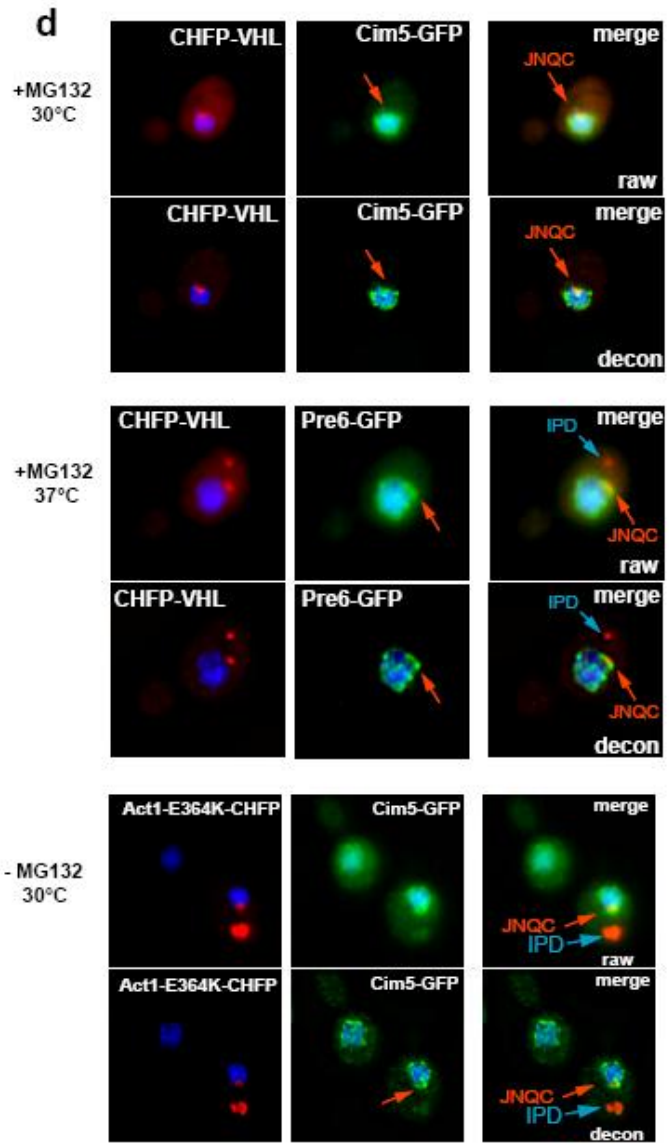
d
+MG132
30°C
CHFP-VHL
Cim5-GFP
merge
JNQC
raw
CHFP-VHL
Cim5-GFP
merge
JNQC
decon
+MG132
37°C
CHFP-VHL
Pre6-GFP
IPD
merge
JNQC
raw
CHFP-VHL
Pre6-GFP
IPD
merge
JNQC
decon
- MG132
30°C
Act1-E364K-CHFP
Cim5-GFP
merge
JNQC
IPD
raw
Act1-E364K-CHFP
Cim5-GFP
merge
JNQC
IPD
decon

Figure 2.5e

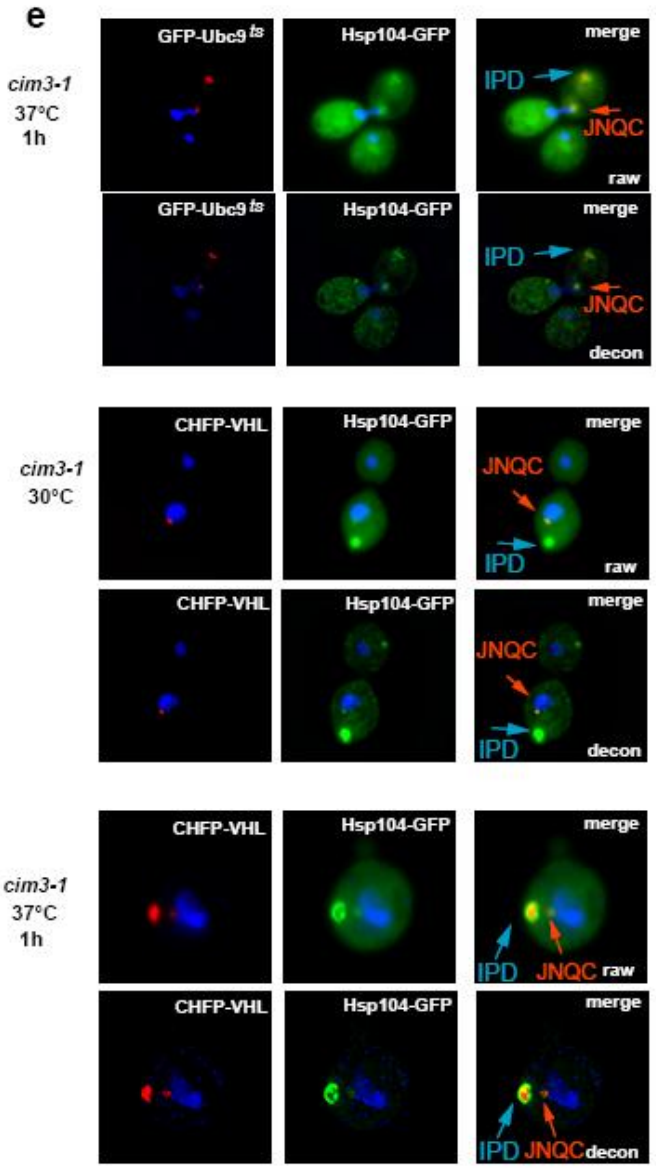
e
cim3-1
37°C
1h
GFP-Ubc9ts
Hsp104-GFP
merge
IPD
JNQC
raw
GFP-Ubc9ts
Hsp104-GFP
merge
IPD
JNQC
decon
cim3-1
30°C
CHFP-VHL
Hsp104-GFP
merge
JNQC
IPD
raw
CHFP-VHL
Hsp104-GFP
merge
JNQC
IPD
decon
cim3-1
37°C
1h
CHFP-VHL
Hsp104-GFP
merge
IPD
JNQC
raw
CHFP-VHL
Hsp104-GFP
merge
IPD
JNQC
decon

Figure 2.5f-g

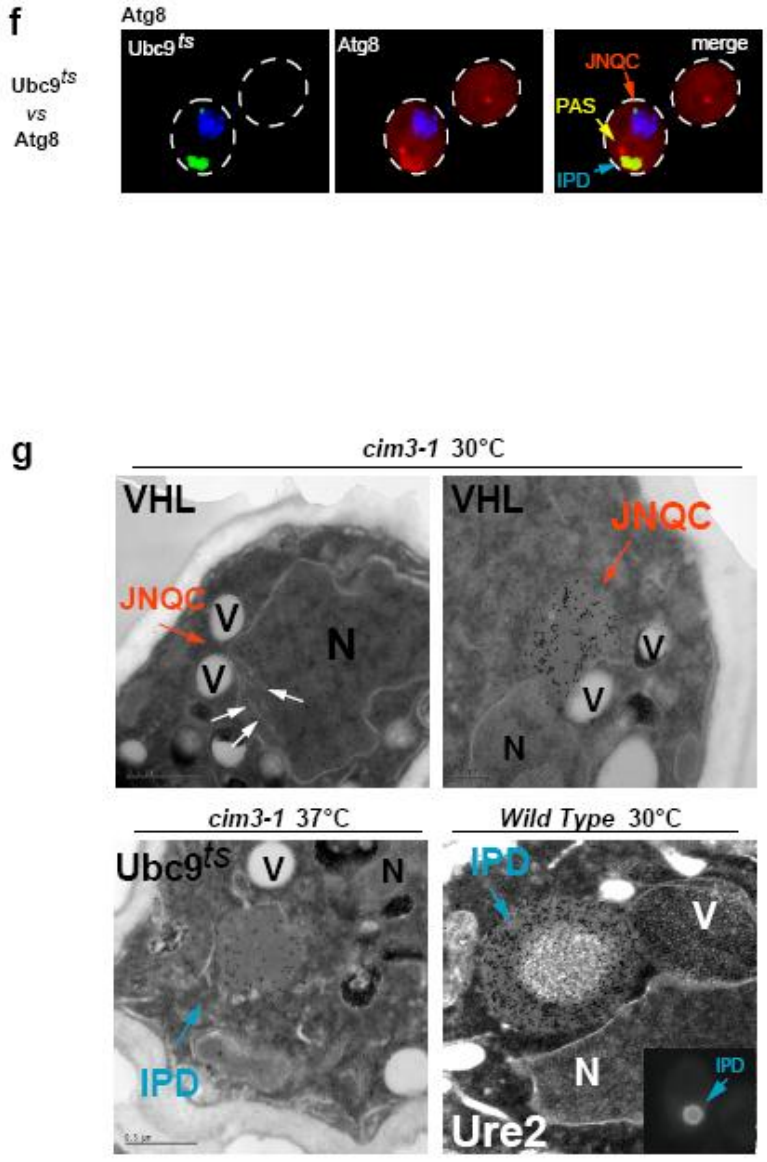
f
Ubc9ts
vs
Atg8
Atg8
Ubc9ts
Atg8
merge
JNQC
PAS
IPD
g
cim3-1 30°C
VHL
JNQC
V
V
N
VHL
JNQC
V
V
N
cim3-1 37°C
Ubc9ts
V
N
IPD
Wild Type 30°C
IPD
V
N
Ure2
IPD

Figure 2.5h-i

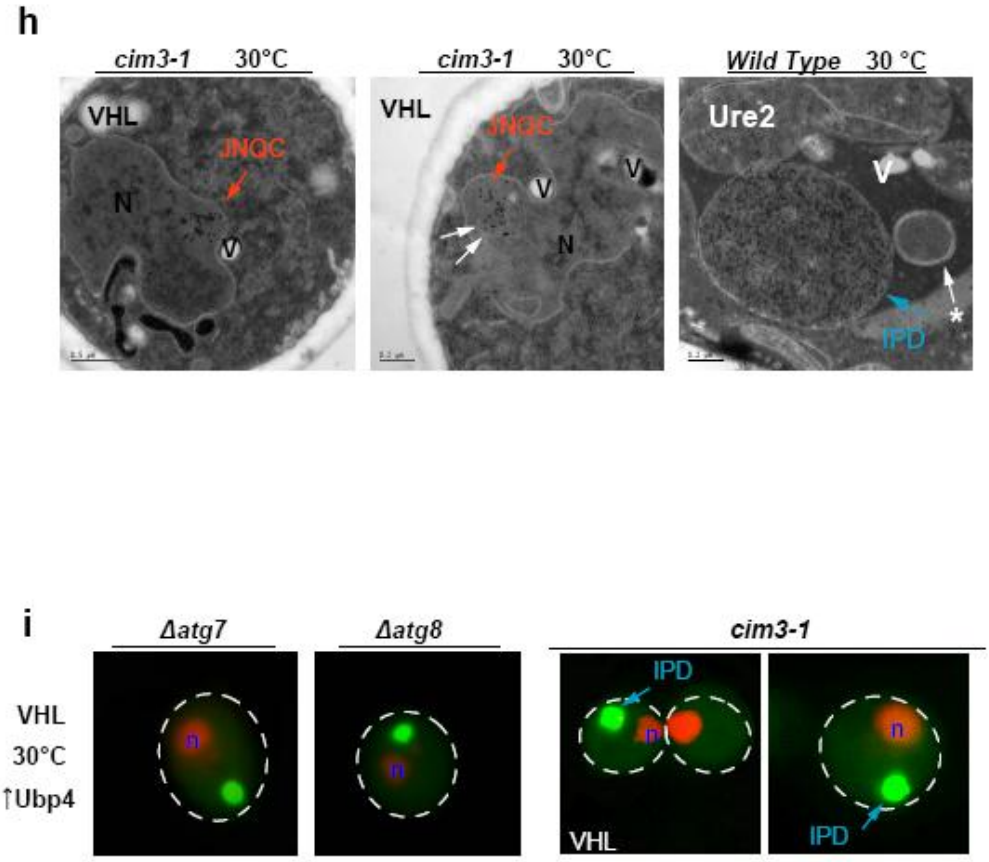
h
cim3-1 30°C
cim3-1 30°C
Wild Type 30 °C
VHL
JNQC
N
V
VHL
JNQC
V
V
N
Ure2
V
IPD
*
i
Δatg7
Δatg8
cim3-1
VHL
30°C
↑Ubp4
n
n
IPD
n
VHL
n
IPD

Figure 2.5: The JUNQ and IPOD are defined subcellular compartments

a, JUNQ compartment tightly co-localizes with nuclear membrane. DNA is visualized with DAPI (blue), and the nucleoplasm is visualized with NLS-TFP (red). GFP-Ubc9^{ts} (Top) localizes to the JUNQ and IPOD after 2hrs at 37 °C in *cim3-1* cells. GFP-VHL (Bottom) accumulates only in the JUNQ at 30 °C in *cim3-1* cells. Images were collected as a Z-series and de-convoluted. A 2D projection is shown.

b, The JUNQ compartment, shown here for GFP-VHL, does not localize to the Spindle Pole Body (marked by Spc42-CHFP).

c, The JUNQ compartment is in close proximity to the ER. ER is visualized by expressing Sec63-CHFP from a low-copy plasmid. Shown for the JUNQ and IPOD formed by GFP-Ubc9^{ts} (Top) and for the JUNQ formed by GFP-VHL (Bottom). A non-deconvoluted image is also shown (lower panel).

d, The JUNQ compartment (upper panel, CHFP-VHL, red), but not the IPOD (middle and lower panels), concentrates 26S proteasomes (visualized with Cim5-GFP for regulatory particle and Pre6-GFP for core particle, green). VHL accumulation in the JUNQ was induced by proteasome inhibition with MG132. In the lower panel both JUNQ and IPOD are formed by Act1-E364K-CHFP over-expression without proteasome inhibition. A direct fluorescence image (Top) and a de-convoluted image (Bottom) are shown for d-e.

e, Hsp104 localizes to both compartments. JUNQ and IPOD were formed by expressing CHFP-Ubc9^{ts} (upper panel) or CHFP-VHL (lower panel) in *cim3-1* cells, followed by 1hr incubation at 37 °C. Note that CHFP-VHL expressed in *cim3-1* cells at 30 °C (middle panel) co-localizes with Hsp104 in JUNQ only, however Hsp104 also accumulates in an IPOD structure independently of any ectopically-expressed aggregating protein (blue arrow).

f, The IPOD, shown here for GFP-Ubc9^{ts}, co-localizes with CHFP-Atg8. Some CHFP-Atg8 can also be seen in the pre-autophagosomal structure (PAS)(Yorimitsu and Klionsky, 2005).

g, The JUNQ, shown in the upper panes with GFP-VHL, is formed in a distinct nuclear-membrane associated compartment. Immuno-gold labeled GFP-VHL consistently accumulates in juxta-nuclear protrusions which are adjacent to vacuolar lobes and contain proliferations of the nuclear membrane (white arrows). The IPOD, shown in the lower panels with GFP-Ubc9^{ts}, often is associated with membrane structures (left), and often contains a non-GFP reactive core of densely aggregated proteins (right). A corresponding GFP-fluorescence image is shown in the inset for Ure2.

h, EM analysis of JUNQ and IPOD

The JUNQ, shown with GFP-VHL, is formed in a distinct nuclear-membrane associated compartment. Immuno-gold labeled GFP-VHL consistently accumulates in juxta-nuclear protrusions which are adjacent to vacuolar lobes and contain proliferations of the nuclear membrane (white arrows). The IPOD, shown with Ure2, often is associated with membrane structures, and often localizes next to vacuoles and autophagic vesicles (white arrow).

i, Autophagic components are not required for IPOD formation

Atg7 and Atg8, essential autophagic components, are not required for IPOD formation. GFP-VHL was induced to accumulate in IPODs by Ubp4 over-expression (control in *cim3-1* cells shown in right panels).

Figure 2.6a-f

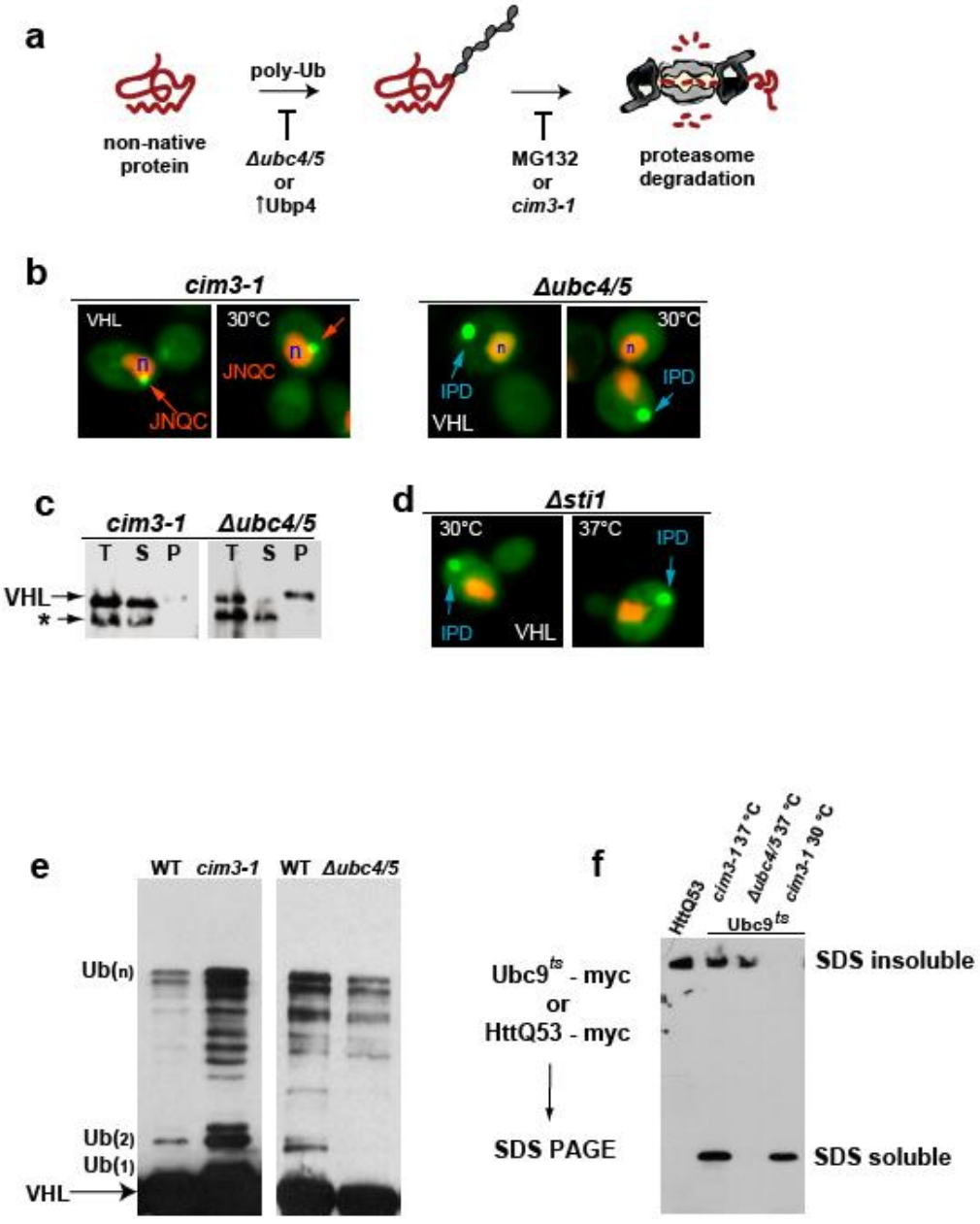
a
non-native protein
poly-Ub
Δubc4/5 or ↑Ubp4
MG132 or cim3-1
proteasome degradation
b
cim3-1
VHL
30°C
JNQC
Δubc4/5
IPD
VHL
30°C
IPD
c
cim3-1
Δubc4/5
T S P
T S P
VHL
*
d
Δsti1
30°C
IPD
VHL
37°C
IPD
e
WT cim3-1
WT Δubc4/5
Ub(n)
Ub(2)
Ub(1)
VHL
f
HttQ53
cim3-1 37 °C
Δubc4/5 37 °C
cim3-1 30 °C
Ubc9ts
Ubc9ts - myc
or
HttQ53 - myc
SDS PAGE
SDS insoluble
SDS soluble

Figure 2.6g-i

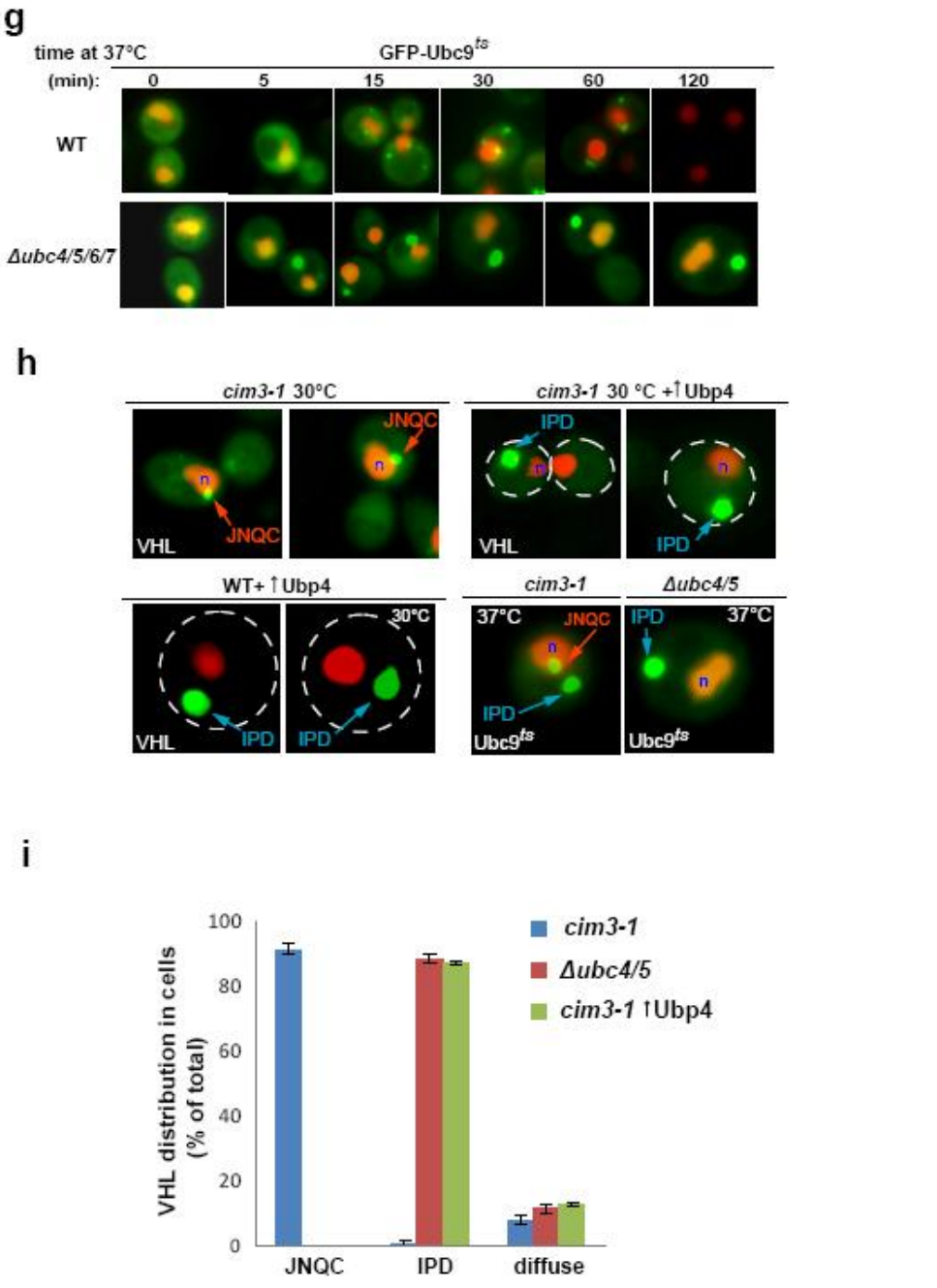
g
time at 37°C
GFP-Ubc9ts
(min):
0
5
15
30
60
120
WT
Δubc4/5/6/7
h
cim3-1 30°C
cim3-1 30 °C +↑Ubp4
JNQC
IPD
VHL
WT+ ↑Ubp4
cim3-1
Δubc4/5
30°C
37°C
Ubc9ts
i
VHL distribution in cells (% of total)
100
80
60
40
20
0
cim3-1
Δubc4/5
cim3-1 ↑Ubp4
JNQC
IPD
diffuse

Figure 2.6j-n

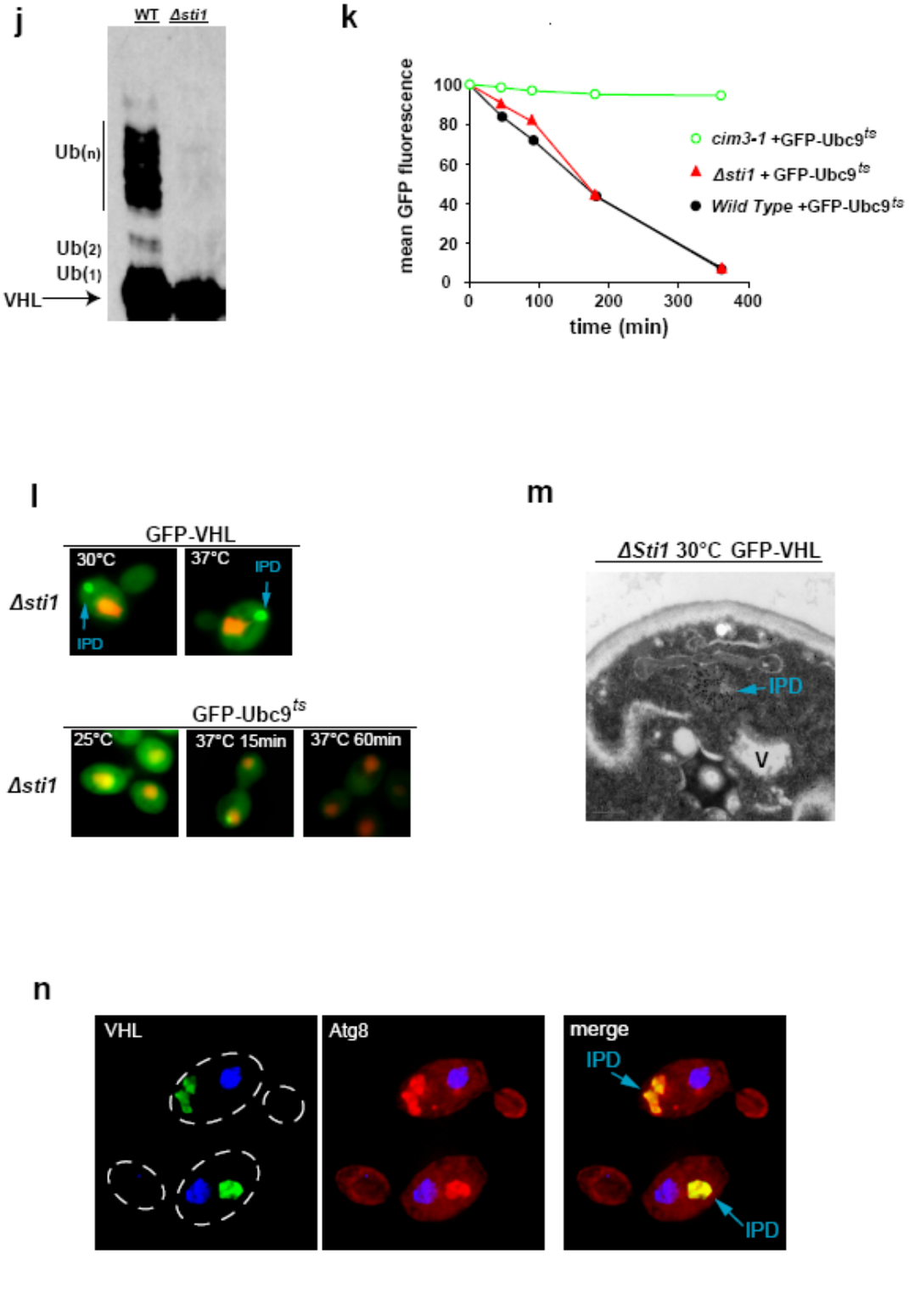
j
WT
Δsti1
Ub(n)
Ub(2)
Ub(1)
VHL
k
mean GFP fluorescence
time (min)
cim3-1 +GFP-Ubc9ts
Δsti1 + GFP-Ubc9ts
Wild Type +GFP-Ubc9ts
l
GFP-VHL
Δsti1
30°C
37°C
IPD
GFP-Ubc9ts
25°C
37°C 15min
37°C 60min
m
Δsti1 30°C GFP-VHL
IPD
V
n
VHL
Atg8
merge
IPD
IPD

Figure 2.6o-r

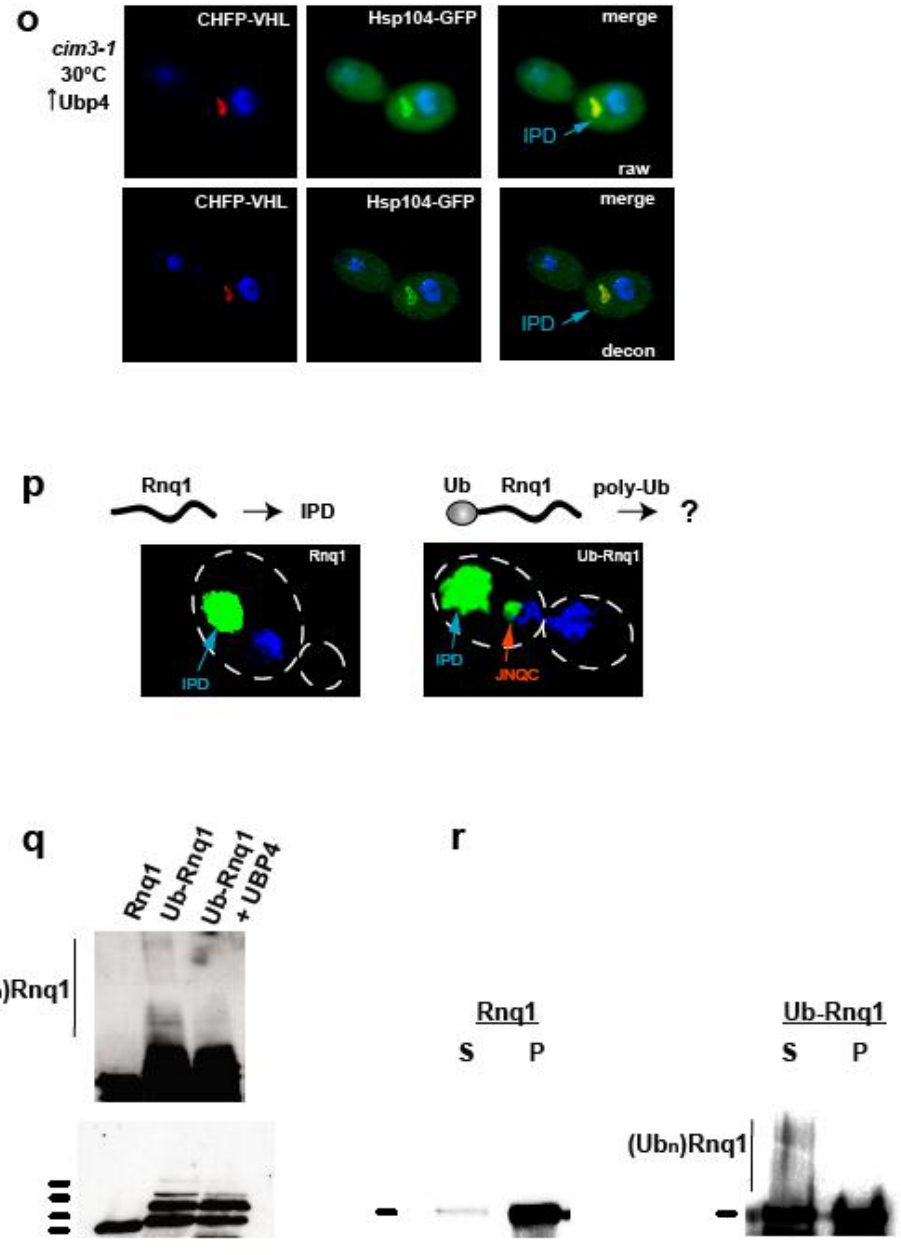
o
cim3-1
30°C
↑Ubp4
CHFP-VHL
Hsp104-GFP
merge
IPD
raw
CHFP-VHL
Hsp104-GFP
merge
IPD
decon
p
Rnq1
IPD
Ub
Rnq1
poly-Ub
?
Rnq1
IPD
Ub-Rnq1
IPD
JNQC
q
Rnq1
Ub-Rnq1
Ub-Rnq1 + UBP4
(Ubn)Rnq1
Ub3-Rnq1
Ub2-Rnq1
Ub-Rnq1
Rnq1
r
Rnq1
S
P
Ub-Rnq1
S
P
(Ubn)Rnq1

Figure 2.6s-t

s

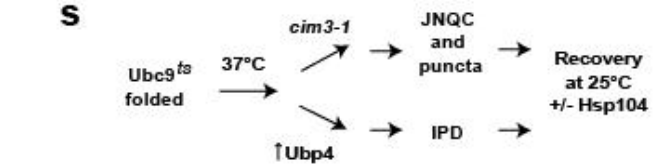

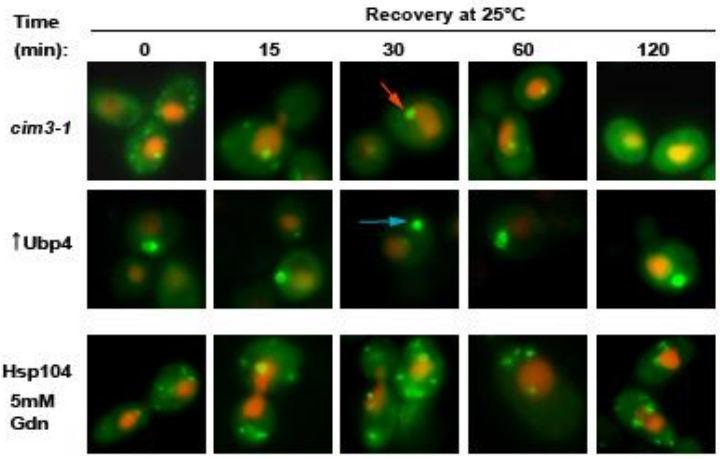

t

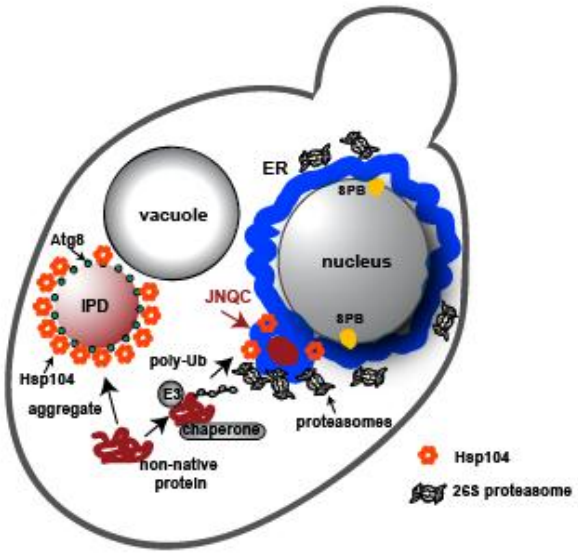

Figure 2.6: Partitioning between JUNQ and IPOD is regulated by ubiquitination

a, Misfolded proteins are ubiquitinated prior to proteasomal degradation. For the QC substrates studied here, ubiquitination can be blocked by over-expression of the Ubp4 ubiquitin hydrolase or by deletion of Ubc4/5. The proteasome can be inhibited by using the *cim3-1* mutant strain or by addition of MG132.

b, Blocking ubiquitination of misfolded VHL prevents its localization to JUNQ, and redirects these proteins to the IPOD. The proteasome was blocked by expression in *cim3-1* cells, ubiquitination was blocked by expression in *Δubc4/5*.

c, Blocking ubiquitination results in VHL accumulation in a Triton-insoluble fraction. Asterisk denotes cross-reacting band unrelated to VHL.

d, Deletion of the Sti1 chaperone, required for VHL degradation(McClellan et al., 2005a), results in re-routing of misfolded VHL to the IPOD.

e, Ubiquitinated VHL accumulates upon expression in proteasome-mutant *cim3-1* cells (left panel). Deletion of *Δubc4/5* drastically decreases the amount of VHL-ubiquitin conjugates as compared to wild-type (right panel).

f, Accumulation of $Ubc9^{ts}$ in the IPOD, after incubation at 37 °C in *cim3-1* cells, or *Δubc4/5* cells corresponds to its accumulation in an SDS-insoluble fraction which fails to fully enter the resolving phase of a 12% SDS gel, similar to HttQ53.

g, Blocking ubiquitination of GFP-$Ubc9^{ts}$ results in its direct targeting to the IPOD. Localization patterns of folded and misfolded GFP-Ubc9 in MHY501 wild-type yeast and *Δubc4/5/6/7* yeast are shown. GFP-$Ubc9^{ts}$ was detected by direct fluorescence for all images as in Figure 1. Nuclei were visualized by co-expressing NLS-TFP from a bi-directional promoter on the same plasmid as GFP-$Ubc9^{ts}$.

h, Blocking ubiquitination of misfolded GFP-VHL and GFP-$Ubc9^{ts}$ prevents their localization to JUNQ, and redirects these proteins to the IPOD. The proteasome was blocked by expression in *cim3-1* cells, ubiquitination was blocked by expression in *Δubc4/5* cells or by over-expression of Ubp4, as indicated.

i, Quantification of VHL aggregation phenotypes. The results of microscopy experiments are represented in the graphs shown. Graphs represent three separate experiments in which 100 cells were counted at each time-point.

j, Expression of VHL in a *Δsti1* strain leads to decreased ubiquitination.

k, Sti1 is not required for $Ubc9^{ts}$ degradation (a timecourse of mean GFP fluorescence as analyzed by FACS sorting is shown). Direct fluorescence images of GFP-$Ubc9^{ts}$ in *Δsti1* cells after shift to 37 °C is shown.

l, Deletion of the Sti1 chaperone, required for VHL degradation, results in re-routing of misfolded VHL to the IPOD.

m, EM analysis shows Immuno-gold labeled GFP-VHL consistently localizing to IPOD in *Δsti1* mutant.

n, Co-localization between GFP-VHL and CHFP-Atg8 is shown in the *Δsti1* strain, lacking a chaperone required for misfolded VHL degradation.

o, VHL directed to IPOD as a result of decreased ubiquitination (due to over-expression of Ubp4) co-localizes with GFP-Hsp104.

p, Ubiquitination suffices to promote prion delivery to the JUNQ. A ubiquitination signal (Ub-G76A) was engineered in the yeast prion Rnq1-GFP to test the effect of ubiquitination on targeting to the JUNQ and IPOD compartments (Fig. 8). Whereas Rnq1-GFP localized exclusively to the IPOD, Ub-G76A-Rnq1-GFP localized to both JUNQ and IPOD in *cim3-1* cells at 30 °C. Nucleus is stained with DAPI.

q, Addition of a ubiquitination signal (Ub-G76A) to Rnq1 results in its increased ubiquitination.

r, Enhancing the ubiquitination of Rnq1 leads to the re-distribution of some of the prion protein to a detergent-soluble fraction. Note that the poly-ubiquitinated Ub-Rnq1 is found entirely in the soluble fraction.

s, Recovery of diffuse cytosolic fluorescence by thermally denatured GFP-$Ubc9^{ts}$ accumulated in the JUNQ (Top) but not in the IPOD (Middle) upon return to the permissive temperature. GFP-$Ubc9^{ts}$ was specifically accumulated in either JUNQ

or the IPOD as schematized. Protein in JUNQ and puncta accumulates reversibly yielding diffuse fluorescence within ~60 min at 25 °C, but the protein in the IPOD persists for >2 hrs at 25 °C. The recovery of GFP-Ubc9^{ts} requires Hsp104 disaggregase activity, which is inhibited by addition of 5 mM GuanidineHCl (Bottom).

t, Sorting of cytosolic misfolded proteins to distinct Quality Control compartments. Cells contain two spatially distinct QC compartments with disparate functions. Proteins that fail to fold or become stress-denatured are recognized by the QC machinery, consisting of chaperones and ubiquitination components such as E3 ubiquitin ligases. Ubiquitination helps direct them to the JUNQ where they remain competent for either refolding or proteasomal degradation, and which concentrates disaggregating chaperones and proteasomes. Aggregated misfolded proteins are directed to the IPOD, which may serve to terminally sequester protein aggregates and, based on the co-localization with Atg8, may deliver them to the autophagy pathway.

Section 2.7: References

Adams, A., Gottschling, D., Kaiser, C., and Stearns, T. (1997). Methods in Yeast Genetics. In Cold Spring Harbor Laboratory Press.

Arrasate, M., Mitra, S., Schweitzer, E.S., Segal, M.R., and Finkbeiner, S. (2004). Inclusion body formation reduces levels of mutant huntingtin and the risk of neuronal death. Nature *431*, 805-810.

Barral, J.M., Broadley, S.A., Schaffar, G., and Hartl, F.U. (2004). Roles of molecular chaperones in protein misfolding diseases. Seminars in cell & developmental biology *15*, 17-29.

Bence, N.F., Sampat, R.M., and Kopito, R.R. (2001). Impairment of the ubiquitin-proteasome system by protein aggregation. Science (New York, NY *292*, 1552-1555.

Betting, J., and Seufert, W. (1996). A yeast Ubc9 mutant protein with temperature-sensitive in vivo function is subject to conditional proteolysis by a ubiquitin- and proteasome-dependent pathway. The Journal of biological chemistry *271*, 25790-25796.

Bucciantini, M., Giannoni, E., Chiti, F., Baroni, F., Formigli, L., Zurdo, J., Taddei, N., Ramponi, G., Dobson, C.M., and Stefani, M. (2002). Inherent toxicity of aggregates implies a common mechanism for protein misfolding diseases. Nature *416*, 507-511.

Bukau, B., Weissman, J., and Horwich, A. (2006). Molecular chaperones and protein quality control. Cell *125*, 443-451.

Cashikar, A.G., Duennwald, M., and Lindquist, S.L. (2005). A chaperone pathway in protein disaggregation. Hsp26 alters the nature of protein aggregates to facilitate reactivation by Hsp104. The Journal of biological chemistry *280*, 23869-23875.

Chen, P., Johnson, P., Sommer, T., Jentsch, S., and Hochstrasser, M. (1993). Multiple ubiquitin-conjugating enzymes participate in the in vivo degradation of the yeast MAT alpha 2 repressor. Cell *74*, 357-369.

Chiti, F., and Dobson, C.M. (2006). Protein misfolding, functional amyloid, and human disease. Annu Rev Biochem *75*, 333-366.

Cohen, E., Bieschke, J., Perciavalle, R.M., Kelly, J.W., and Dillin, A. (2006). Opposing activities protect against age-onset proteotoxicity. Science (New York, NY *313*, 1604-1610.

Duennwald, M.L., Jagadish, S., Giorgini, F., Muchowski, P.J., and Lindquist, S. (2006). A network of protein interactions determines polyglutamine toxicity. Proceedings of the National Academy of Sciences of the United States of America *103*, 11051-11056.

Enenkel, C., Lehmann, A., and Kloetzel, P.M. (1998). Subcellular distribution of proteasomes implicates a major location of protein degradation in the nuclear envelope-ER network in yeast. Embo J *17*, 6144-6154.

Feldman, D.E., Thulasiraman, V., Ferreyra, R.G., and Frydman, J. (1999). Formation of the VHL-elongin BC tumor suppressor complex is mediated by the chaperonin TRiC. Mol Cell *4*, 1051-1061.

Ghislain, M., Udvardy, A., and Mann, C. (1993). S. cerevisiae 26S protease mutants arrest cell division in G2/metaphase. Nature *366*, 358-362.

Gidalevitz, T., Ben-Zvi, A., Ho, K.H., Brignull, H.R., and Morimoto, R.I. (2006). Progressive disruption of cellular protein folding in models of polyglutamine diseases. Science (New York, NY *311*, 1471-1474.

Horwich, A.L., and Weissman, J.S. (1997). Deadly conformations--protein misfolding in prion disease. Cell *89*, 499-510.

Huyer, G., Longsworth, G.L., Mason, D.L., Mallampalli, M.P., McCaffery, J.M., Wright, R.L., and Michaelis, S. (2004). A striking quality control subcompartment in Saccharomyces cerevisiae: the endoplasmic reticulum-associated compartment. Molecular biology of the cell *15*, 908-921.

Iwata, A., Christianson, J.C., Bucci, M., Ellerby, L.M., Nukina, N., Forno, L.S., and Kopito, R.R. (2005). Increased susceptibility of cytoplasmic over nuclear polyglutamine aggregates to autophagic degradation. Proceedings of the National Academy of Sciences of the United States of America *102*, 13135-13140.

Johnston, J.A., Illing, M.E., and Kopito, R.R. (2002). Cytoplasmic dynein/dynactin mediates the assembly of aggresomes. Cell Motil Cytoskeleton *53*, 26-38.

Kamhi-Nesher, S., Shenkman, M., Tolchinsky, S., Fromm, S.V., Ehrlich, R., and Lederkremer, G.Z. (2001). A novel quality control compartment derived from the endoplasmic reticulum. Molecular biology of the cell *12*, 1711-1723.

Kopito, R.R. (2000). Aggresomes, inclusion bodies and protein aggregation. Trends Cell Biol *10*, 524-530.

Krobitsch, S., and Lindquist, S. (2000). Aggregation of huntingtin in yeast varies with the length of the polyglutamine expansion and the expression of chaperone proteins. Proceedings of the National Academy of Sciences of the United States of America *97*, 1589-1594.

Kruse, K.B., Brodsky, J.L., and McCracken, A.A. (2006a). Autophagy: An ER Protein Quality Control Process. Autophagy *2*, 135-137.

Kruse, K.B., Brodsky, J.L., and McCracken, A.A. (2006b). Characterization of an ERAD gene as VPS30/ATG6 reveals two alternative and functionally distinct protein quality control pathways: one for soluble Z variant of human alpha-1 proteinase inhibitor (A1PiZ) and another for aggregates of A1PiZ. Molecular biology of the cell *17*, 203-212.

Lesne, S., Koh, M.T., Kotilinek, L., Kayed, R., Glabe, C.G., Yang, A., Gallagher, M., and Ashe, K.H. (2006). A specific amyloid-beta protein assembly in the brain impairs memory. Nature *440*, 352-357.

Lippincott-Schwartz, J., and Patterson, G.H. (2003). Development and use of fluorescent protein markers in living cells. Science (New York, NY *300*, 87-91.

Mateus, C., and Avery, S.V. (2000). Destabilized green fluorescent protein for monitoring dynamic changes in yeast gene expression with flow cytometry. Yeast *16*, 1313-1323.

Matsumoto, G., Kim, S., and Morimoto, R.I. (2006). Huntingtin and mutant SOD1 form aggregate structures with distinct molecular properties in human cells. The Journal of biological chemistry *281*, 4477-4485.

Matsumoto, G., Stojanovic, A., Holmberg, C.I., Kim, S., and Morimoto, R.I. (2005). Structural properties and neuronal toxicity of amyotrophic lateral sclerosis-associated Cu/Zn superoxide dismutase 1 aggregates. J Cell Biol *171*, 75-85.

McClellan, A.J., Scott, M.D., and Frydman, J. (2005a). Folding and quality control of the VHL tumor suppressor proceed through distinct chaperone pathways. Cell *121*, 739-748.

McClellan, A.J., Tam, S., Kaganovich, D., and Frydman, J. (2005b). Protein quality control: chaperones culling corrupt conformations. Nat Cell Biol *7*, 736-741.

Melville, M.W., McClellan, A.J., Meyer, A.S., Darveau, A., and Frydman, J. (2003). The Hsp70 and TRiC/CCT chaperone systems cooperate in vivo to assemble the von Hippel-Lindau tumor suppressor complex. Mol Cell Biol *23*, 3141-3151.

Muchowski, P.J., and Wacker, J.L. (2005). Modulation of neurodegeneration by molecular chaperones. Nat Rev Neurosci *6*, 11-22.

Outeiro, T.F., and Lindquist, S. (2003). Yeast cells provide insight into alpha-synuclein biology and pathobiology. Science (New York, NY *302*, 1772-1775.

Park, S.H., Bolender, N., Eisele, F., Kostova, Z., Takeuchi, J., Coffino, P., and Wolf, D.H. (2007). The cytoplasmic Hsp70 chaperone machinery subjects misfolded and endoplasmic reticulum import-incompetent proteins to degradation via the ubiquitin-proteasome system. Molecular biology of the cell *18*, 153-165.

Prinz, A., Hartmann, E., and Kalies, K.U. (2000). Sec61p is the main ribosome receptor in the endoplasmic reticulum of Saccharomyces cerevisiae. Biol Chem *381*, 1025-1029.

Rajan, R.S., Illing, M.E., Bence, N.F., and Kopito, R.R. (2001). Specificity in intracellular protein aggregation and inclusion body formation. Proceedings of the National Academy of Sciences of the United States of America *98*, 13060-13065.

Rideout, H.J., Lang-Rollin, I., and Stefanis, L. (2004). Involvement of macroautophagy in the dissolution of neuronal inclusions. Int J Biochem Cell Biol *36*, 2551-2562.

Rubinsztein, D.C. (2006). The roles of intracellular protein-degradation pathways in neurodegeneration. Nature *443*, 780-786.

Rubinsztein, D.C. (2007). Autophagy induction rescues toxicity mediated by proteasome inhibition. Neuron *54*, 854-856.

Rujano, M.A., Bosveld, F., Salomons, F.A., Dijk, F., van Waarde, M.A., van der Want, J.J., de Vos, R.A., Brunt, E.R., Sibon, O.C., and Kampinga, H.H. (2006). Polarised Asymmetric Inheritance of Accumulated Protein Damage in Higher Eukaryotes. PLoS Biol *4*, e417.

Sarkar, S., Perlstein, E.O., Imarisio, S., Pineau, S., Cordenier, A., Maglathlin, R.L., Webster, J.A., Lewis, T.A., O'Kane, C.J., Schreiber, S.L., *et al.* (2007). Small molecules enhance autophagy and reduce toxicity in Huntington's disease models. Nature chemical biology *3*, 331-338.

Schaffar, G., Breuer, P., Boteva, R., Behrends, C., Tzvetkov, N., Strippel, N., Sakahira, H., Siegers, K., Hayer-Hartl, M., and Hartl, F.U. (2004). Cellular toxicity of polyglutamine expansion proteins: mechanism of transcription factor deactivation. Mol Cell *15*, 95-105.

Shaner, N.C., Campbell, R.E., Steinbach, P.A., Giepmans, B.N., Palmer, A.E., and Tsien, R.Y. (2004). Improved monomeric red, orange and yellow fluorescent proteins derived from Discosoma sp. red fluorescent protein. Nat Biotechnol *22*, 1567-1572.

Sherman, M.Y., and Goldberg, A.L. (2001). Cellular defenses against unfolded proteins: a cell biologist thinks about neurodegenerative diseases. Neuron *29*, 15-32.

Siegel, S.J., Bieschke, J., Powers, E.T., and Kelly, J.W. (2007). The oxidative stress metabolite 4-hydroxynonenal promotes Alzheimer protofibril formation. Biochemistry *46*, 1503-1510.

Swaminathan, S., Amerik, A.Y., and Hochstrasser, M. (1999). The Doa4 deubiquitinating enzyme is required for ubiquitin homeostasis in yeast. Molecular biology of the cell *10*, 2583-2594.

Szeto, J., Kaniuk, N.A., Canadien, V., Nisman, R., Mizushima, N., Yoshimori, T., Bazett-Jones, D.P., and Brumell, J.H. (2006). ALIS are Stress-Induced Protein Storage Compartments for Substrates of the Proteasome and Autophagy. Autophagy *2*, 189-199.

Tam, S., Geller, R., Spiess, C., and Frydman, J. (2006). The chaperonin TRiC controls polyglutamine aggregation and toxicity through subunit-specific interactions. Nat Cell Biol *8*, 1155-1162.

Taylor, J.P., Tanaka, F., Robitschek, J., Sandoval, C.M., Taye, A., Markovic-Plese, S., and Fischbeck, K.H. (2003). Aggresomes protect cells by enhancing the degradation of toxic polyglutamine-containing protein. Hum Mol Genet *12*, 749-757.

Tkach, J.M., and Glover, J.R. (2004). Amino acid substitutions in the C-terminal AAA+ module of Hsp104 prevent substrate recognition by disrupting oligomerization and cause high temperature inactivation. The Journal of biological chemistry *279*, 35692-35701.

Tongaonkar, P., Beck, K., Shinde, U.P., and Madura, K. (1999). Characterization of a temperature-sensitive mutant of a ubiquitin-conjugating enzyme and its use as a heat-inducible degradation signal. Anal Biochem *272*, 263-269.

Vang, S., Corydon, T.J., Borglum, A.D., Scott, M.D., Frydman, J., Mogensen, J., Gregersen, N., and Bross, P. (2005). Actin mutations in hypertrophic and dilated cardiomyopathy cause inefficient protein folding and perturbed filament formation. Febs J *272*, 2037-2049.

Webb, J.L., Ravikumar, B., Atkins, J., Skepper, J.N., and Rubinsztein, D.C. (2003). Alpha-Synuclein is degraded by both autophagy and the proteasome. The Journal of biological chemistry *278*, 25009-25013.

Winzeler, E.A., Shoemaker, D.D., Astromoff, A., Liang, H., Anderson, K., Andre, B., Bangham, R., Benito, R., Boeke, J.D., Bussey, H., *et al.* (1999). Functional characterization of the S. cerevisiae genome by gene deletion and parallel analysis. Science (New York, NY *285*, 901-906.

Yorimitsu, T., and Klionsky, D.J. (2005). Autophagy: molecular machinery for self-eating. Cell Death Differ *12 Suppl 2*, 1542-1552.

Chapter 3

Failure to Sequester Amyloidogenic Proteins in Insoluble Inclusion Underlies Toxicity of Aggregated Proteins in Yeast

Section 3.1: Summary

A number of neurodegenerative diseases, including Alzheimer, Huntington's, ALS, and Parkinson's Disease, are characterized by chronic abundance of aggregation prone misfolded proteins. Proteins that cause each disease often have unrelated sequence and function, yet they all accumulate in intracellular inclusions that are associated with the disease pathology. Studies have identified and characterized proteins found in these disease-associated inclusions, such as Huntingtin in Huntington's disease, α-synuclein in Parkinson's, Aβ-peptide in Alzheimers, and SOD-1 mutants in ALS. Although inclusion formation has come to be viewed as the hallmark of disease, presence of inclusions has not always coincided with cytotoxicity. While all amyloidogenic proteins form inclusions, not all inclusions are toxic. Indeed, healthy brains have sometimes been found to contain inclusions, and some cell culture models have observed a reverse correlation between formation of large inclusions and cell death. The molecular basis for toxicity associated with expression of disease-related amyloidogenic proteins has been a topic of many contentious studies, and remains an open question. A better understanding of the relationship between aggregation and toxicity is needed in order to devise pharmacological strategies for curbing the deleterious processes seen in neurodegenerative disease states. Here, we use a yeast model designed to probe the basis for aggregated protein toxicity in order to delineate the differential properties of toxic and non-toxic aggregated species. Our results show that a labile aggregation-prone protein can be rendered toxic by enhancing its ubiquitination. We further show that the molecular basis for this acquired toxicity lies in the altered interaction of the amyloidogenic protein with the quality control system, including the chaperone network and the machinery that partitions misfolded proteins to intracellular inclusions. Using a number of toxic aggregating proteins, we demonstrate that they are inappropriately targeted to the quality control (JUNQ) compartment where soluble misfolded proteins normally accumulate, where these toxic species preferentially interact with Hsp70, perhaps titrating it away from the cytosolic environment. This, in turn, inhibits the processing and degradation of "normal" soluble misfolded intermediates that are generated over the course of normal protein folding quality control. Our data provides

evidence that failure to sequester potentially toxic species in an insoluble compartment (IPOD) results in a harmful interaction of amyloidogenic proteins with the quality control machinery and the inhibition of homeostatic quality control processes.

Section 3.2: Introduction

The formation of aggregated protein deposits in the brain has long been held as common cell-biological feature of neurodegenerative disease states (Caughey and Lansbury, 2003; Dobson, 2006; Kopito, 2000; McClellan et al., 2005b). Numerous amyloidogenic proteins have since been identified as causative agents of the pathology underlying the diseases, with prolonged expression eventually causing neuronal death. These disease-related proteins, whose biochemical and cell-biological features have been extensively analyzed in systems *in vivo* and *in vitro*, and which include Huntingtin, α-synuclein, synphillin, Aβ-peptide, SOD-1, and prion proteins, do not share primary sequence features, or functional characteristics, but do aggregate into insoluble oligomeric super-structures in a generally similar fashion (Chiti and Dobson, 2006; Dobson, 2003; Matsumoto et al., 2006; Outeiro and Lindquist, 2003).

Although the propensity to aggregate is considered to be the primary determinant of toxicity in the context of conformational disorders such as Huntington's, Parkinson's, Alzheimer, and Prion Diseases, several lines of evidence suggest that the ability to aggregate is alone insufficient to cause proteotoxicity. First is the observation that all proteins are capable of forming amyloid aggregates under certain conditions, such as heat denaturation and proteasome inhibition, to which the cytosolic environment is frequently exposed (Chiti and Dobson, 2006). Although the ability to aggregate is common to many, if not all, proteins, only a small subset of aggregation-prone proteins cause amyloidosis and disease (Chiti and Dobson, 2006). This suggests that proteins observed to cause neurotoxicity have a unique feature, besides propensity for aggregation, which leads them to adopt a toxic oligomer conformation. Additionally, a common feature shared by most neurodegenerative diseases provides evidence that aggregation propensity is not sufficient to guarantee cytotoxicity. Typically, individuals affected by these

diseases develop symptoms and evidence of neurodegeneration late in life, despite continuous chronic expression of amyloidogenic proteins (Cohen et al., 2006; Dobson, 2003; Morley et al., 2002; Muchowski, 2002). The fact that toxicity is manifested only in concert with the aging process and is not a linear result of amyloidogenic protein expression, also suggests that the interaction of aggregated species with the cellular quality control machinery, rather than aggregation itself, forms the basis for the deleterious effects of protein aggregation observed in the disease pathology. Thus, any attempt to understand, and eventually treat, conformational disease-associated neurotoxicity must first explain why it is that only certain aggregates are toxic, while most are labile.

A number of biological models for aggregation toxicity in *S. cerevisiae*, *C. elegans*, and mammalian tissue culture systems are consistent with the proposal that unique, aggregation-independent features of toxic aggregated proteins define their toxicity (Arrasate et al., 2004; Meriin et al., 2003; Outeiro and Muchowski, 2004; Rubinsztein, 2007; Sakahira et al., 2002; Sherman and Goldberg, 2001). In particular, the yeast system provides a unique opportunity to characterize the mechanisms of toxicity in a uniform cellular environment, while having readily available tools for genetic dissection and biochemical analysis (Duennwald et al., 2006a). An interesting feature of aggregate toxicity in yeast is that many disease-related proteins that are toxic in mammalian systems are labile in yeast. Recent studies with the Huntingtin fragment Htt exon 1 with a glutamine-expanded region have shown that normal HttQ103 is not toxic in yeast, unlike in mammalian cells (Dehay and Bertolotti, 2006; Duennwald et al., 2006a). However, this protein can be rendered toxic by the deletion of a proline-rich region at its N-terminus (Dehay and Bertolotti, 2006). Although it is not entirely clear why this small sequence alteration rendered a labile protein toxic (though both the normal and proline-deleted (HttQ103ΔP) form have a strong tendency to aggregate *in vivo* and *in vitro*) these studies have yielded a number of interesting insights into the molecular basis of toxicity. The acquired toxicity of the HttQ103ΔP is dependent on the presence of the prion propagation factor, Rnq1, and factors that modulate prion propagation, such as Hsp104 deletion or over-expression, and Hsp70 over-expression, can also suppress its toxicity (Dehay and Bertolotti, 2006; Duennwald et al., 2006a; Duennwald et al., 2006b).

It is thought that aggregation-prone proteins exert a toxic "gain of function" effect that interferes with normal cellular processes, a number of which have been confirmed in different studies. HttQ103ΔP toxicity in yeast has been suggested to result from HttQ103ΔP interference with intracellular trafficking, and possibly with the structure of the actin cytoskeleton (Ganusova et al., 2006; Gokhale et al., 2005). Other yeast studies performed with α-synuclein and synphillin have indicated that toxic aggregates formed by these proteins may inhibit parts of the quality control machinery, including the UPS, as well as the trafficking machinery, as observed with HttQ103ΔP (Outeiro and Lindquist, 2003; Outeiro and Muchowski, 2004).

The *C. elegans* model has also been used in several key studies as a model for protein aggregation, toxicity, and in particular the way that both are modulated by the aging process, which is well understood in worms (Guarente and Kenyon, 2000; Kenyon, 2005; Morley et al., 2002; Morley and Morimoto, 2004; Murphy et al., 2003). A *C. elegans* Huntington's model, for example, showed that inactivation of the worm aging pathway, resulting in up-regulation of certain quality control components, extends the threshold of polyQ aggregation and the resulting toxicity (Morley et al., 2002; Morley and Morimoto, 2004). Over-expression of certain quality control components, particularly chaperones, has itself been shown to alleviate polyQ aggregation toxicity in worms and other systems (Morley and Morimoto, 2004; Warrick et al., 1999). A similar study probed the toxicity of aggregated polyQ in worms, and demonstrated that cell death correlates with the disruption of the cellular protein folding balance, resulting in the co-aggregation of meta-stable proteins present in the cytosol (Gidalevitz et al., 2006). Together these studies suggest that polyQ toxicity in worms results from an adverse interaction of these amyloidogenic proteins with the quality control machinery, likely titrating essential chaperones and degradation factors away from the bulk of the cellular quality control load. Toxicity can hence be modulated by the additional ectopic expression of these quality control components.

While some data has, in the past, supported the notion that inclusions formed by polyQ Htt and other amyloidogenic proteins are themselves harmful, in that they may induce the co-aggregation of factors such as transcription factors or UPS components that are essential for viability, this may not account for all cases of toxicity (Matsumoto et al.,

2005; Sakahira et al., 2002; Schaffar et al., 2004). Indeed, there has also been increasing evidence that far from being the culprits of toxicity, many inclusions formed by aggregating proteins are protective to the cell, while small oligomeric intermediates are the active toxic agents (Arrasate et al., 2004; Cohen et al., 2006). Consistent with this, studies have shown the over-expression of certain cyto-protective quality control components, such as chaperones, rescue the affected cells often without eliminating the protein aggregates themselves (Cohen et al., 2006; Muchowski, 2002; Muchowski et al., 2002; Muchowski et al., 2000; Muchowski and Wacker, 2005). Another recent *C. elegans* study has provided support for the idea that small oligomers rather than large insoluble inclusions are toxic, showing that opposing pathways reduce toxicity of Aβ-peptide aggregates (Cohen et al., 2006). One pathway, regulated by HSF-1, mediates the disaggregation and degradation of toxic oligomeric intermediates, while another pathway, regulated by DAF-16, manages their directed aggregation into larger molecular weight insoluble oligomers (Cohen et al., 2006). Therefore, the bulk of recently obtained evidence indicates that rather than the insoluble amyloids usually found in intracellular inclusions, smaller soluble oligomers are harmful to the cell, and that their disaggregation or direction to inclusions is favorable to the cell.

Finally, recent data has suggested a model that may reconcile conflicting observations from the above studies. A neurodegenerative disease model expressing polyQ Huntingtin and SOD-1 mutants in mammalian cell culture has provided evidence of distinct aggregated structures formed by different disease-related proteins (Matsumoto et al., 2006; Matsumoto et al., 2005). These inclusions had different solubility and permeability properties, with SOD-1 mutants forming porous structures through which Hsp70 and other soluble cytosolic proteins could diffuse freely, and Huntingtin forming completely immobile structures impermeable to other proteins. Hence, the cellular cytosolic environment was exposed to the SOD-1 in the soluble inclusions, whereas aggregated Huntingtin was completely sequestered. The porous SOD-1 aggregates were later observed to recruit and sequester proteasomes, and their appearance correlated with onset of toxicity and eventual cell death (Matsumoto et al., 2006; Matsumoto et al., 2005).

Our previous study, described in Chapter 2, is consistent with the above observation and describes two distinct compartments for cytosolic misfolded proteins in yeast. One inclusion (the JUNQ) serves as the platform for soluble misfolded protein degradation and refolding, while another compartment (the IPOD) sequesters insoluble aggregates from the cytosol. Consistent with the idea that insoluble inclusions are protective, we observed that while "normal" soluble misfolded proteins can, under different conditions, be targeted to either inclusion, amyloidogenic proteins are directed only to the insoluble inclusion. Our yeast model for inclusion formation, therefore, helps to reconcile the conflicting data on the role of inclusions in cytotoxicity. Since there are two inclusions, one accessible to quality control and the cytosol, and one impermeable to other proteins, it follows that toxicity may depend on the type of aggregated species that accumulates in the JUNQ. Our model would predict that if a protein that was meant to be sequestered in the IPOD, were instead mis-targeted to the JUNQ, cytotoxicity would result.

Here we show that, as our model predicts, re-routing the non-toxic amyloidogenic yeast protein, Rnq1, from the IPOD to the JUNQ via the addition of a ubiquitination signal renders it toxic. We show also that another yeast protein that has a toxic and a non-toxic form, HttQ103, is sequestered into the IPOD in its non-toxic form, whereas the toxic form (HttQ103ΔP) inhabits both the cytosol and the JUNQ. Interestingly, toxicity of Ub-Rnq1 correlates with enhanced solubility and ubiquitination, indicating that the increased interaction of the re-routed amyloidogenic protein with the quality control and ubiquitination machinery results in the toxic state. Consistent with this, we observe that for both Ub-Rnq1 and HttQ103ΔP, the toxic but not the labile aggregate co-localizes with Hsp70, and that over-expression of Hsp70 can alleviate toxicity. These data indicate that the increased ubiquitination and solubility causes the aggregated Ub-Rnq1 and HttQ103ΔP to bind essential chaperones, such as Hsp70, possibly titrating them away from the quality control load in the cytosol. To confirm this, we co-expressed the soluble quality control substrate VHL together with labile and toxic forms of Rnq1 and HttQ103, and found that the toxic forms of both proteins inhibit VHL degradation by the quality control machinery, leading to its aggregation. Together, our data provide a model that links toxicity of amyloidogenic aggregates to an increased abundance of soluble species

and their improper sub-cellular compartmentalization, which in turn results in inappropriate interactions with the quality control machinery thus inhibiting it and causing the accumulation of cytosolic quality control substrates. We propose that inappropriate ubiquitination of amyloidogenic proteins is the link between their aggregation and their toxic "gain of function" effect.

Section 3.3: Results

To examine the relationship between protein aggregation and cytotoxicity, we employed a non-toxic yeast amyloidogenic protein which was modified to mis-localize to a compartment normally inhabited by soluble misfolded proteins by the addition of an exogenous ubiquitination signal. Since Ub-Rnq1 was previously shown to localize to both the JUNQ and IPOD, while Rnq1 forms only the IPOD inclusion (Chapter 2 and Fig. 3.1a), we asked whether re-directing an amyloidogenic protein to a compartment for soluble misfolded proteins renders it more soluble, and whether this is detrimental to the cell. Indeed, while Rnq1 was not ubiquitinated and almost entirely detergent insoluble (Fig. 3.1b), enhanced ubiquitination of Ub-Rnq1 correlated with is accumulation in the soluble fraction. Strikingly, this rendered the normally labile Rnq1 protein extremely toxic to the cell (Fig. 3.1d).

We compared Ub-Rnq1 toxicity to that of another yeast protein that can be converted to a toxic form, HttQ103ΔP. Although the expression of both proteins profoundly decreases cell survival, Ub-Rnq1 exhibited higher toxicity than HttQ103ΔP (Fig. 3.2a). Given that both proteins localize exclusively to the IPOD in their labile forms, we asked whether the alteration that renders HttQ103ΔP toxic, also causes it to be re-directed to the JUNQ, as with Ub-Rnq1. We therefore co-expressed HttQ103ΔP with $Ubc9^{ts}$ under conditions of proteasome impairment and stress that cause $Ubc9^{ts}$ to accumulate in both JUNQ and IPOD. As our model predicts, HttQ103ΔP co-localized strongly with $Ubc9^{ts}$ in the JUNQ, while some of it was also observed in cytosolic puncta and around the nuclear envelope (Fig. 3.2b). HttQ103ΔP also showed this localization pattern under non-stressed conditions (Fig. 3.3a and data not shown). Our data indicate,

therefore, that acquired toxicity of amyloidogenic proteins correlates with their re-distribution from the IPOD, where they are labile, to the JUNQ, where they are toxic.

We next asked whether the toxic forms of Rnq1 and HttQ103 exert different affects on the homeostasis of protein quality control than their non-toxic forms. We therefore co-expressed Rnq1, HttQ103, and another yeast amyloidogenic protein Ure2, together with VHL, a soluble misfolded quality control substrate that is normally degraded by the quality control system together with the UPS. These non-toxic proteins had no effect on VHL degradation and localization, which did not accumulate in excess of its normal steady state level and showed diffuse soluble fluorescence (Fig. 3.3b). However, when we expressed VHL in the presence of Ub-Rnq, HttQ103ΔP, and two other toxic aggregating quality control substrates Act1-E364K and Ste6-L1239X, all of which aggregate in the JUNQ as well as the IPOD, we observed massive co-aggregation of VHL (Fig. 3.3c, not shown for Ub-Rnq1). We therefore conclude that the mis-localization of amyloidogenic and highly aggregation prone proteins to the JUNQ inhibits the normal degradation and solubilization of quality control substrates, possibly by titrating essential quality control components away from their cytosolic substrates.

To explore this further, we sought to determine whether Hsp70, an essential chaperone known to interact with protein aggregates, localizes to the JUNQ or the IPOD. While Hsp104, as described previously, predominantly localizes around proteins sequestered in the IPOD, the yeast Hsp70, Ssa1, does not accumulate there (Fig. 3.4a, b). Instead, it is mostly dynamic and soluble, exhibiting diffuse fluorescence. However, we saw that when VHL was induced to accumulate in the JUNQ via proteasome impairment, a small fraction of Ssa1 also re-distributed there (Fig. 3.4b). Since most Ssa1 in the cell is soluble and diffuses rapidly, this suggests that protein trapped in the JUNQ recruits Ssa1. Indeed, whereas non-toxic aggregates formed by Rnq1 and HttQ103 did not co-localize with Ssa1, the toxic forms of these proteins, Ub-Rnq1 and HttQ103ΔP, as well as another toxic aggregate, synphillin, showed strong Ssa1 co-localization (data not shown). Sti1, an Ssa1 co-chaperone required for VHL ubiquitination and degradation remained diffusely localized, even after VHL accumulation in the JUNQ (Fig. 3.4c).

We next asked whether Ssa1 over-expression, known to alleviate HttQ103ΔP cytotoxicity would also rescue Ub-Rnq1-expressing cells. Indeed, while other

chaperones, including Hsp12, Hsp26, Sti1, Hsp82, and Hsp104 had no effect on toxicity of Ub-Rnq1, Ssa1 enhanced the viability of yeast expressing Ub-Rnq1 (Fig. 3.5).

Section 3.4: Discussion

Previous studies have proposed diverse mechanisms for toxicity conferred by intracellular amyloidogenic protein aggregation. These range from destabilization of the cellular membrane, to inhibition of trafficking, irreversible co-aggregation with transcription factors, and perturbation of the cellular protein folding homeostasis (Bence et al., 2001; Chernoff, 2007; Gidalevitz et al., 2006; Matsumoto et al., 2006; Matsumoto et al., 2005; Muchowski, 2002; Muchowski et al., 2002). It has not been clear, however, what aggregated species constitute the toxic "gain of function," and why these aggregates cause toxicity while others are labile. Moreover, the role of inclusion formation in preventing or advancing toxicity has also been a source of controversy, some studies pointing to a protective role while others suggesting that they may be harmful. Here we present data that are consistent with previous findings about aggregate toxicity, and help to integrate them into a wider model for how the cell manages potentially harmful aggregates.

In our study, we were able to turn a labile amyloidogenic protein, Rnq1, into a severely harmful toxic aggregate, Ub-Rnq1, simply by enhancing the ubiquitination of the aggregating protein. It is interesting that enhancing the ubiquitination of Rnq1, also enhances its solubility, with the ubiquitin conjugates re-distributing predominantly to the soluble fraction (Fig. 3.1). This also re-routs the amyloidogenic protein to the JUNQ, instead of the IPOD, where it exerts a toxic effect on the cell. This cytotoxicity is suppressed by the Hsp70 chaperone, suggesting that the basis for toxicity is a titration effect, targeting essential chaperones and quality control components. It is significant that another amyloidogenic protein that can be converted from a labile to a toxic form, HttQ103ΔP behaves nearly identically to Rnq1/Ub-Rnq1. The labile HttQ103 form inhabits only the IPOD, whereas the HttQ103ΔP is re-localized to the JUNQ.

A striking finding in our study is the direct evidence demonstrating that the molecular basis for aggregate toxicity is the perturbation of the cellular quality control homeostasis. All of the toxic amyloidogenic or aggregation prone substrates we texted inhibited the turnover of a model soluble misfolded protein, VHL, and caused its aggregation under conditions where normally it would be remain and would eventually be degraded.

In summary, we propose a model for how the cell manages potentially toxic aggregates, based on our results. When amyloidogenic proteins are expressed and begin to oligomerize, they are either disaggregated by Hsp104 and its co-chaperones, or are targeted directly to the IPOD where they are sequestered from the cytosolic environment and other quality control components. Cytosolic proteins do not have access to the aggregates inside the IPOD because it is completely insoluble, and possibly protected by Hsp104 which localizes around it. Since ubiquitination determines partition between the JUNQ and the IPOD, when amyloidogenic proteins are ubiquitinated in excess of the cells' ability to disaggregate or degrade them, they accumulate also in the JUNQ where they irreversibly bind chaperones and other quality control components including the UPS, thereby causing cytotoxicity. This is consistent with our previous finding that proteasomes re-distribute heavily to the JUNQ upon accumulation of misfolded proteins there, and suggests that proteasome sequestration may also play a role in toxicity.

An interesting facet of this model, supported by our data, is that the sequestration of potentially toxic amyloidogenic aggregates in the IPOD is a normal part of cellular protein folding homeostasis. In preliminary work, we observed that IPOD-like inclusions, surrounded by Hsp104, are present in a fraction of all wild type cells under normal conditions, and that the deletion of certain chaperones like Sti1, or the induction of global de-ubiquitination via Ubp4 over-expression, drastically increases the percentage of cells that have an Hsp104, or Atg8 stained IPOD (Fig. 3.6). This is an interesting finding because it could explain why most aggregation is not toxic. Although many proteins are capable of forming aggregates and amyloids, potentially harmful intermediates are targeted directly to the IPOD, where they are unable to interact with quality control components and exert their toxic effects. These findings enhance our

understanding of the toxicity observed in neurodegenerative disease states, and offer interesting insights into how toxicity can be suppressed or prevented.

Section 3.5: Methods

Yeast Media, Plasmids, and Strains

Yeast media preparation, growth, transformations, and manipulations were performed according to standard protocols(Adams et al., 1997). The protein substrates used in this study were visualized as fusions to fluorescent proteins derived from Green Fluorescent Protein (GFP). GFP-Ubc9^{ts}, GFP-Ubc9^{wt}, GFP-VHL, Act1-E364K-GFP, Rnq1-GFP, Ure2-GFP, Ub-G76A-GFP, Ub-Arg-GFP, Ub-G76A-Rnq1-GFP, CHFP-Apg8, NLS-tdTomato (Shaner et al., 2004) (TFP) were cloned into pESC (GAL1 *URA3*; Stratagene, La Jolla, California). Each of the above was also cloned into pESC GAL1 LEU2 vectors, and identical fusion proteins were made with mCherry (Shaner et al., 2004) Fluorescent Protein (CHFP) instead of GFP. The pESC plasmid expressing elongin B and elongin C from a GAL-inducible promoter is described elsewhere(McClellan et al., 2005a; Melville et al., 2003). All proteins were cloned by PCR from yeast genomic DNA or a template plasmid and verified by sequencing. GFP-Hsp104 (Tkach and Glover, 2004) was a generous gift from John Glover.

The yeast strains used in this study are as follows: wt *CIM3* (YPG499; MAT**a** *ura3-52 leu2-Δ1 his3-Δ200 trp1-Δ63 lys2-801 ade2-101*) and *cim3-1* (CMY762; *ura3-52 leu2-Δ1 his3-Δ200 cim3-1*)(Ghislain et al., 1993); W303 (*MATα can1-100 ade2-1 his3-11, 15 trp1-1 ura3-1 leu23,112*); YKO wt, *Δsti1*, (MAT**a**/MATα *orfΔ::kanMX4/orfΔ::kanMX4 ura3Δ0/ura3Δ0 leu2Δ0/leu2Δ0 his3Δ1/his3Δ1 met15Δ0/MET15 lys2Δ0/LYS2* (*Saccharomyces* Genome Project)(Winzeler et al., 1999). For all experiments, expression was shut off prior to temperature shift and microscopy by addition of 2% Glucose.

Fluorescence Microscopy

Conventional epifluorescence micrographs were obtained from live yeast cells on a Zeiss Axiovert microscope with a 100× oil lens (NA1.4; Zeiss). Digital (12-bit) images were acquired with a cooled CCD (Princeton Instruments, Trenton, NJ) and processed by using

METAMORPH software (Universal Imaging, Media, PA). The excitation filters used for conventional microscopy were 500DF20 (GFP), 540DF20 (Rhodamine), and 570DF20 (Texas red). Emission filters were 535DF20 (GFP), 560DF20 (Rhodamine), and 630DF25 (Texas red). The dichroics were: 505 DCLP (GFP), and 595 DCLP (Texas red).

For deconvolution microscopy, yeast cells were fixed on glass coverslips in 4% paraformaldehyde. Deconvoluted images were acquired by using an Olympus microscope with 436 DF10 (CFP) and 500DF20 (YFP) filters for excitation and 470 DF30 (CFP) and 535 DF30 (YFP) filters for emission. Digital images (12 bit) were digitally deconvoluted by using DELTAVISION hardware and software (Applied Precision, Issaquah, WA). Live-cell imaging was performed using the Marianas system from Intelligent Imaging Innovations equipped with the MicroPoint FRAP laser system (Photonic Instruments, Inc.).

Rnq1 Solubility and Ubiquitination Assay

Yeast were grown, collected, and lysed according to standard protocols as described in (McClellan et al., 2005a). Cells expressing Rnq1 or Ub-Rnq1 were grown at 30 °C, harvested, washed once with sterile double-distilled H_2O, and resuspended in 1X native yeast lysis buffer (30 mM HEPES [pH 8.0], 150 mM NaCl, 1% glycerol, 1 mM DTT, 1 mM PMSF, and 1 μg/ml pepstatin-A; and 1mM NEM for ubiquitination assays). Where indicated, lysis buffer also contained 0.1% SDS. Pellets were frozen in liquid nitrogen and lysates were prepared by beating in liquid nitrogen (3 min) and clarified by centrifugation at 6,000 × g for 5 min at 4°C. Fifty microliters of this supernatant was set aside as total protein. Fifty microliters was spun at 16,000 × g for 30 min at 4°C. This supernatant was removed and designated the soluble fraction. The pellet was resolubilized by heating in 50 μl 1× SDS sample buffer. Fifty microliters of 4× SDS sample buffer was added to the total-protein and soluble-fraction samples. Equal amounts of each fraction were resolved by SDS-PAGE followed by immunoblot analysis with anti-GFP antisera.

Ub-Rnq1 Toxicity Assay

Yeast transformants were grown overnight in selective media with raffinose (2%) as a sole carbon source. After the OD_{600} was determined, cultures were diluted to equal concentrations (OD_{600} 0.8). 10 µl of cells were spotted onto selective media in four 10-fold dilutions with the most concentrated spot containing ≈100,000 cells. Cells were spotted on glucose (which repressed expression of the transformed plasmid) and galactose (which induced expression) in parallel to ensure equal spotting.

Section 3.6: Acknowledgements

We thank R. Tsien for the generous gift of plasmids expressing mCherry and tdTomato fluorescent proteins, S. Michaelis for the Ste6-L1239X-GFP plasmid, J. Glover for the gift of the GFP-Hsp104 plasmid, S. Lindquist for the synphillin-GFP plasmid, and S. Tam for the HttQ103ΔP-GFP plasmid; A. Chaudhuri for technical assistance, and J. Mulholland for assistance with deconvolution microscopy. We thank J. England, R. Geller, M. Kaganovich, and members of the Frydman lab for helpful discussions and comments.

Figure 3.1a-d

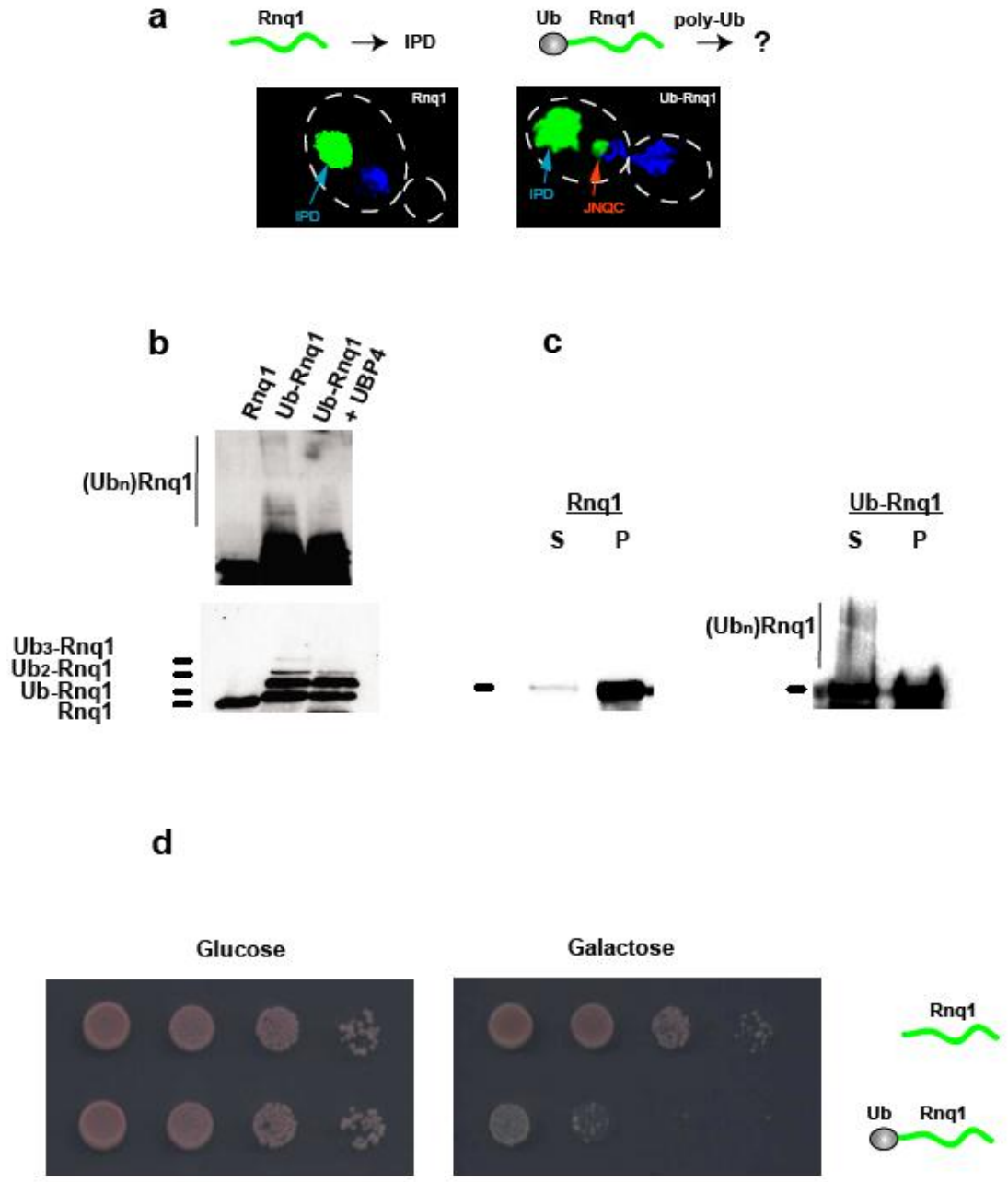
a
Rnq1
IPD
Ub
Rnq1
poly-Ub
?
Rnq1
IPD
Ub-Rnq1
IPD
JNQC
b
Rnq1
Ub-Rnq1
Ub-Rnq1 + UBP4
(Ubn)Rnq1
Ub3-Rnq1
Ub2-Rnq1
Ub-Rnq1
Rnq1
c
Rnq1
S
P
Ub-Rnq1
S
P
(Ubn)Rnq1
d
Glucose
Galactose
Rnq1
Ub
Rnq1

Figure 3.1: Ubiquitination re-routs Rnq1 to the JUNQ where it causes cytotoxicity

a, Ubiquitination suffices to promote amyloidogenic prion delivery to the JUNQ. A ubiquitination signal (Ub-G76A) was engineered in the yeast prion Rnq1-GFP to test the effect of ubiquitination on targeting to the JUNQ and IPOD compartments (Fig. 8). Whereas Rnq1-GFP localized exclusively to the IPOD, Ub-G76A-Rnq1-GFP localized to both JUNQ and IPOD in *cim3-1* cells at 30 °C. Nucleus is stained with DAPI.

b, Addition of a ubiquitination signal (Ub-G76A) to Rnq1 results in its increased ubiquitination.

c, Enhancing the ubiquitination of Rnq1 leads to the re-distribution of some of the prion protein to a detergent-soluble fraction. Note that the poly-ubiquitinated Ub-Rnq1 is found entirely in the soluble fraction.

d, Addition of a ubiquitination signal (Ub-G76A) to Rnq1 renders it toxic to the cell. Rnq1 (Top) and Ub-Rnq1 (Bottom) are expressed under a Gal promoter that is repressed by glucose addition (left panel).

Figure 3.2

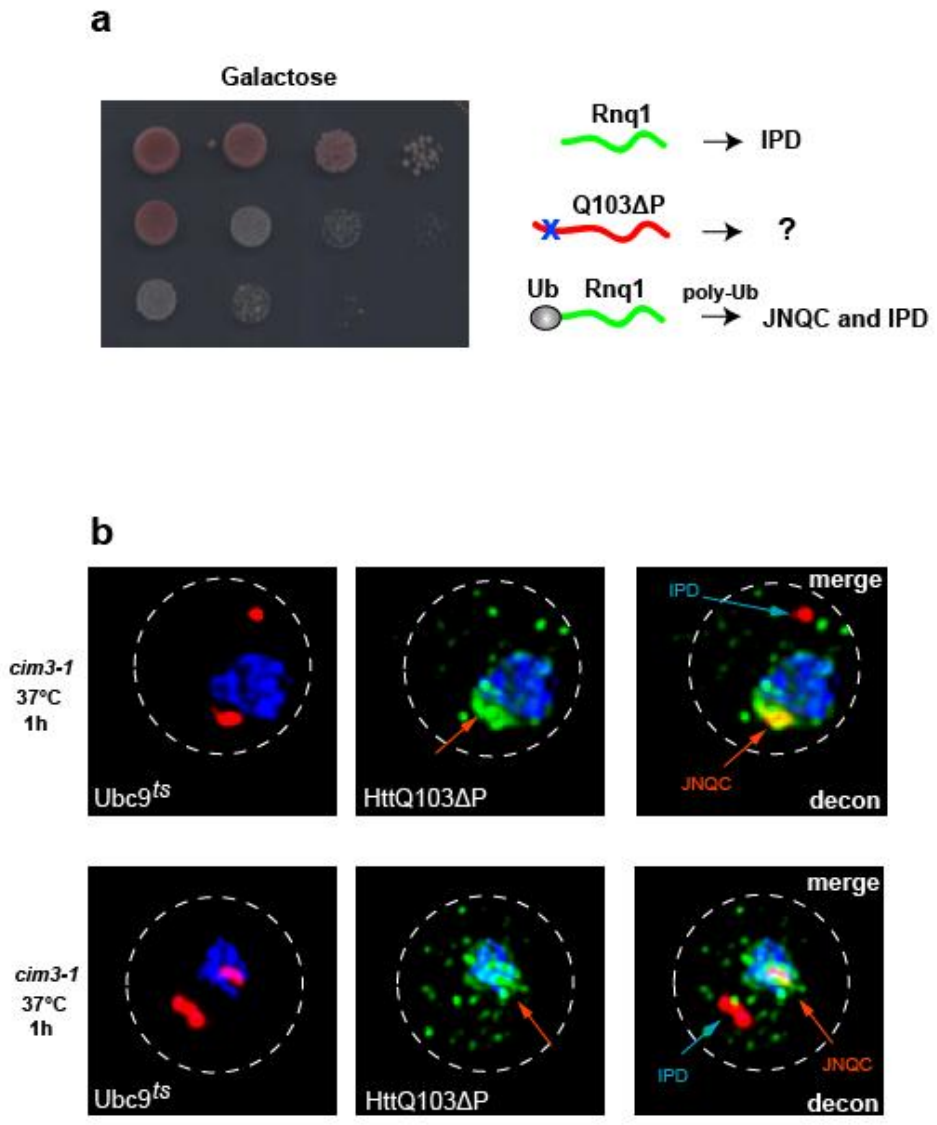
a
Galactose
Rnq1
IPD
Q103ΔP
?
Ub
Rnq1
poly-Ub
JNQC and IPD
b
cim3-1
37°C
1h
Ubc9ts
HttQ103ΔP
IPD
merge
JNQC
decon
cim3-1
37°C
1h
Ubc9ts
HttQ103ΔP
merge
IPD
JNQC
decon

Figure 3.2: HttQ103ΔP toxicity correlates to its redistribution from IPOD to the JUNQ

a, Both Ub-Rnq1 and HttQ103ΔP, but not Rnq1 and HttQ103 (not shown) are toxic to yeast. Addition of a ubiquitination signal (Ub-G76A) to Rnq1 results in its increased ubiquitination.

b, Co-localization of HttQ103ΔP-GFP (Green) with CHFP-Ubc9^{ts} (Red) in the JUNQ, in *cim3-1* yeast, after 1 hr at 37 °C. The nucleus was stained with DAPI (Blue). Images were collected as a Z-series and de-convoluted. A 2D projection is shown.

Figure 3.3a, b

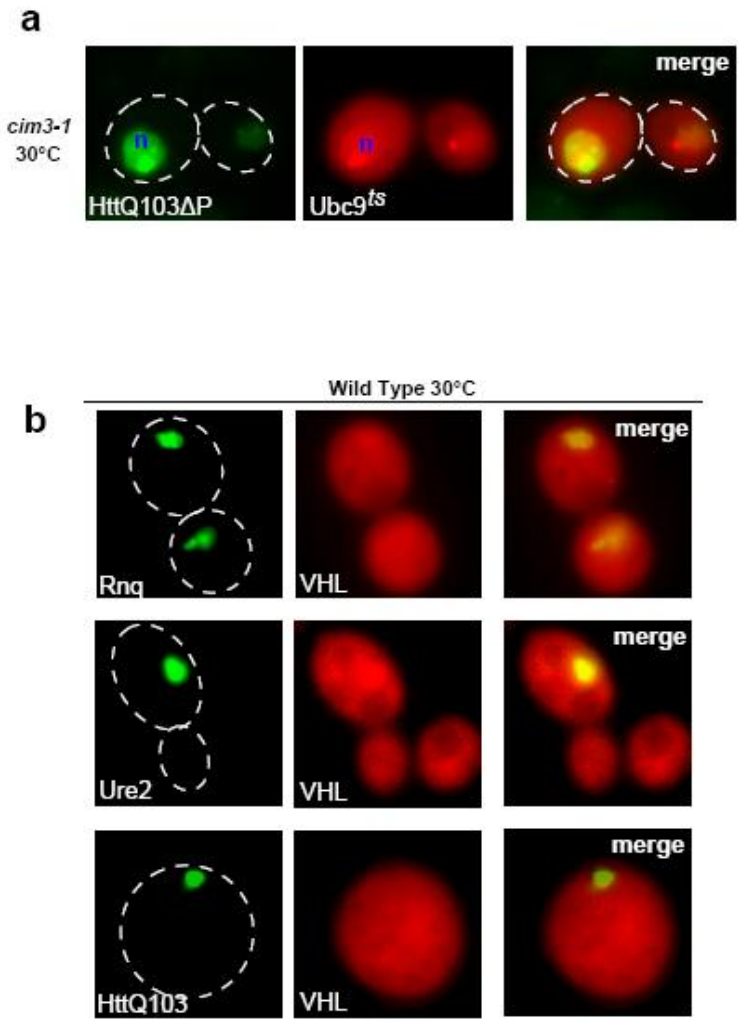
a
cim3-1
30°C
HttQ103ΔP
Ubc9ts
merge
b
Wild Type 30°C
Rnq
VHL
merge
Ure2
VHL
merge
HttQ103
VHL
merge

Figure 3.3c

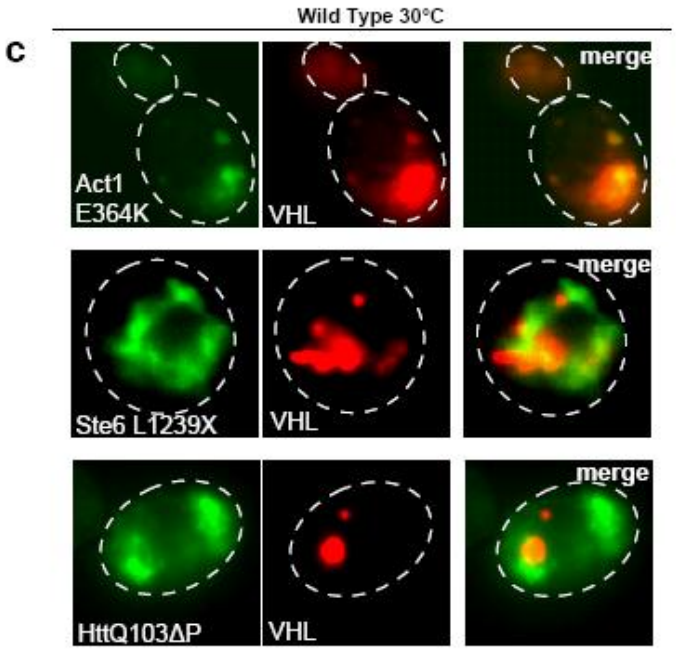
Wild Type 30°C
C
merge
Act1
E364K
VHL
merge
Ste6 L1239X
VHL
merge
HttQ103ΔP
VHL

Figure 3.3: Toxic aggregation-prone proteins inhibit VHL degradation, while labile aggregates do not.

a, Co-localization of HttQ103ΔP-GFP (Green) with CHFP-Ubc9^{ts} (Red) in the JUNQ, in *cim3-1* yeast at 30 °C. The nucleus was stained with DAPI (Blue). Images were collected as a Z-series and de-convoluted. A 2D projection is shown.

b, Rnq1-GFP (Green) expression does not affect turnover of soluble misfolded CHFP-VHL (Red), and does not co-aggregate with VHL. Direct microscopy images are shown.

c, Expression of toxic aggregation-prone proteins (Shown in green) Act1-E364K-GFP, Ste6-L1239X-GFP, HttQ103ΔP-GFP, and Ub-Rnq1 (not shown), blocks VHL (Red) degradation and causes it to aggregate in trans.

Figure 3.4

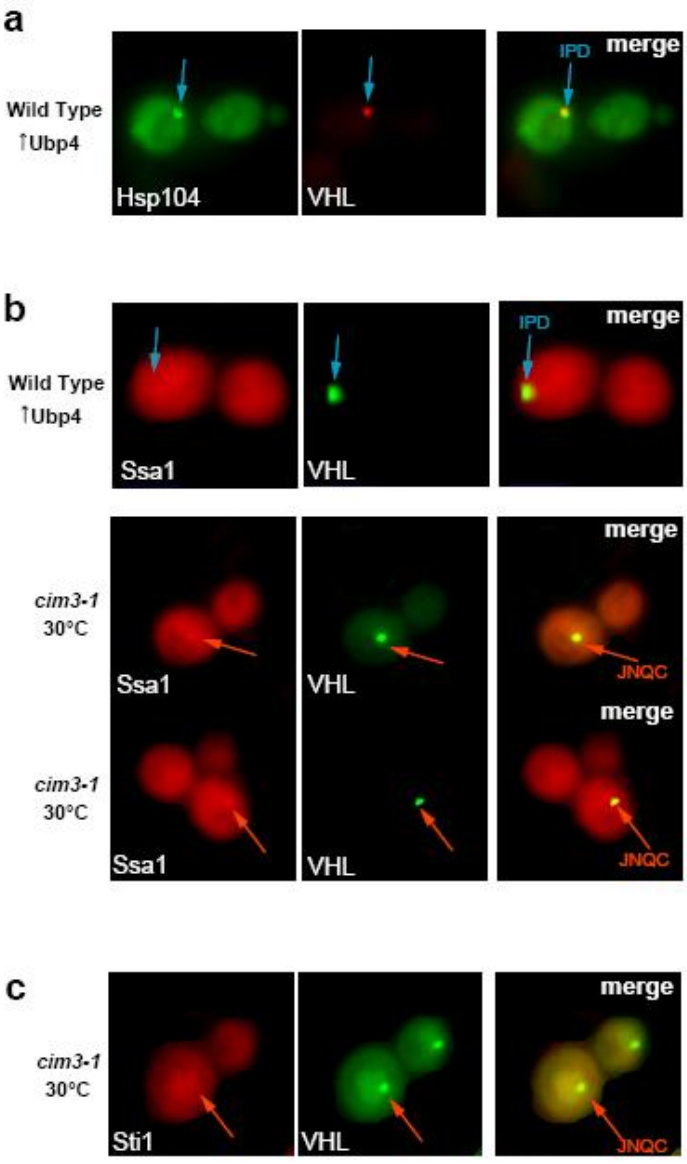
a
Wild Type
↑Ubp4
Hsp104
VHL
IPD
merge
b
Wild Type
↑Ubp4
Ssa1
VHL
IPD
merge
cim3-1
30°C
Ssa1
VHL
merge
JNQC
cim3-1
30°C
Ssa1
VHL
merge
JNQC
c
cim3-1
30°C
Sti1
VHL
merge
JNQC

Figure 3.4: The JUNQ and IPOD show differential interaction with cellular chaperones.

a, Hsp104 (Green) localizes predominantly to the IPOD, around VHL (Green). Upb4 was over-expressed to induce VHL accumulation in the IPOD. Direct microscopy images are shown in a-c.

b, Ssa1 (Red) is predominantly soluble and diffuse, and does not co-localize with IPOD. When VHL is induce to accumulate in the JUNQ, by proteasome impairment in cim3-1 cells, a small but discernable fraction of Ssa1 is recruited to the JUNQ.

c, The Sti1 chaperone is soluble and diffuse and does not co-localize with JUNQ or IPOD.

Figure 3.5

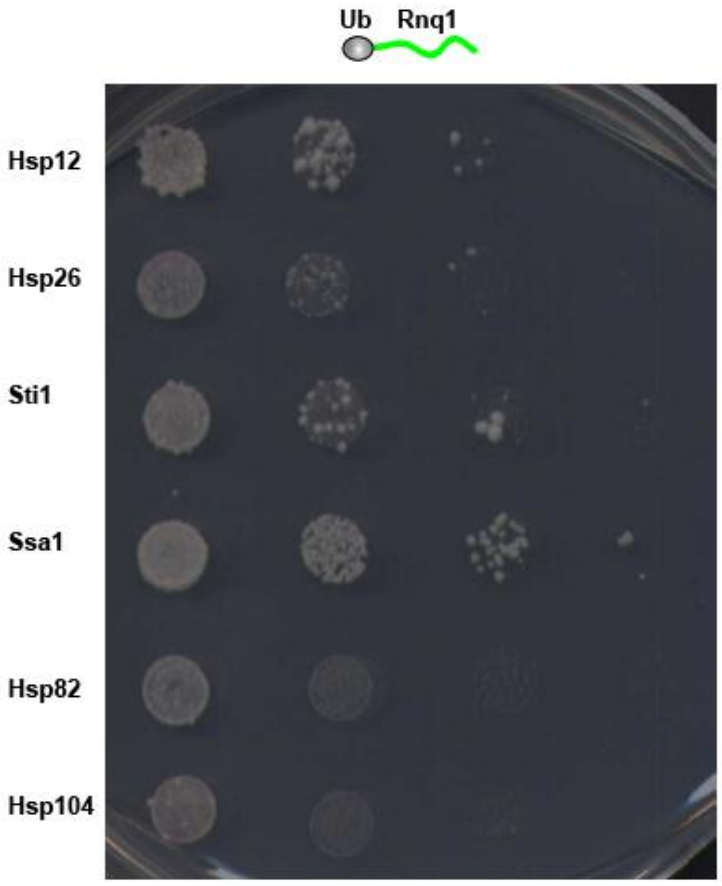

Figure 3.5: Hsp70 suppresses Ub-Rnq1 toxicity.

Over-expression of un-tagged chaperones, together with Ub-Rnq1. Ssa1 rescues grown of yeast co-expressing Ub-Rnq1.

Figure 3.6

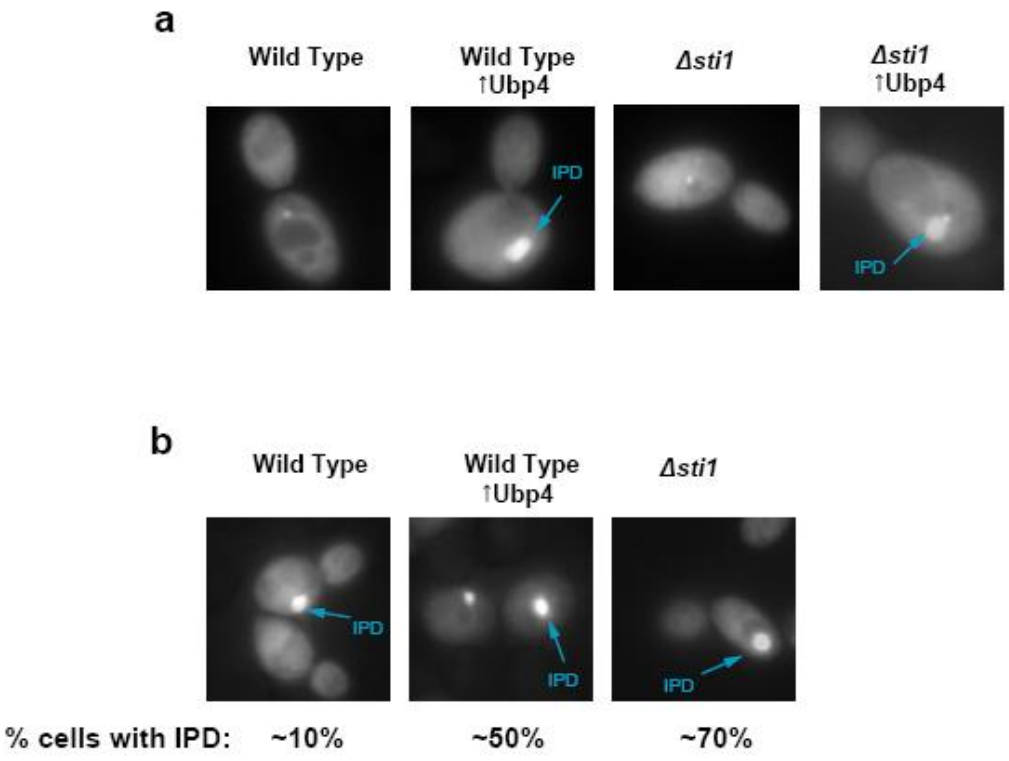
a
Wild Type
Wild Type
↑Ubp4
Δsti1
Δsti1
↑Ubp4
IPD
IPD
b
Wild Type
Wild Type
↑Ubp4
Δsti1
IPD
IPD
IPD
% cells with IPD:
~10%
~50%
~70%

Figure 3.6: Hsp104 and Atg8 localize to an IPOD-like structure in the absence of ectopic expression of an aggregation-prone protein.

a, Atg8 accumulates in an IPOD-like structure upon global protein de-ubiquitionation. CHFP-Atg8 was expressed in wild-type cells (left-panel), ΔSti1 (right panels) or was co-expressed in Ubp4. Direct microscopy images are shown in a-b.

b, Hsp104 accumulates in an IPOD-like structure upon protein de-ubiquitination and increased protein misfolding (in ΔSti1).

Section 3.7: References

Adams, A., Gottschling, D., Kaiser, C., and Stearns, T. (1997). Methods in Yeast Genetics. In Cold Spring Harbor Laboratory Press.

Arrasate, M., Mitra, S., Schweitzer, E.S., Segal, M.R., and Finkbeiner, S. (2004). Inclusion body formation reduces levels of mutant huntingtin and the risk of neuronal death. Nature *431*, 805-810.

Bence, N.F., Sampat, R.M., and Kopito, R.R. (2001). Impairment of the ubiquitin-proteasome system by protein aggregation. Science *292*, 1552-1555.

Caughey, B., and Lansbury, P.T. (2003). Protofibrils, pores, fibrils, and neurodegeneration: separating the responsible protein aggregates from the innocent bystanders. Annu Rev Neurosci *26*, 267-298.

Chernoff, Y.O. (2007). Stress and prions: lessons from the yeast model. FEBS letters *581*, 3695-3701.

Chiti, F., and Dobson, C.M. (2006). Protein misfolding, functional amyloid, and human disease. Annu Rev Biochem *75*, 333-366.

Cohen, E., Bieschke, J., Perciavalle, R.M., Kelly, J.W., and Dillin, A. (2006). Opposing activities protect against age-onset proteotoxicity. Science *313*, 1604-1610.

Dehay, B., and Bertolotti, A. (2006). Critical role of the proline-rich region in Huntingtin for aggregation and cytotoxicity in yeast. J Biol Chem *281*, 35608-35615.

Dobson, C.M. (2003). Protein folding and misfolding. Nature *426*, 884-890.

Dobson, C.M. (2006). Protein aggregation and its consequences for human disease. Protein Pept Lett *13*, 219-227.

Duennwald, M.L., Jagadish, S., Giorgini, F., Muchowski, P.J., and Lindquist, S. (2006a). A network of protein interactions determines polyglutamine toxicity. Proc Natl Acad Sci U S A *103*, 11051-11056.

Duennwald, M.L., Jagadish, S., Muchowski, P.J., and Lindquist, S. (2006b). Flanking sequences profoundly alter polyglutamine toxicity in yeast. Proc Natl Acad Sci U S A *103*, 11045-11050.

Ganusova, E.E., Ozolins, L.N., Bhagat, S., Newnam, G.P., Wegrzyn, R.D., Sherman, M.Y., and Chernoff, Y.O. (2006). Modulation of prion formation, aggregation, and toxicity by the actin cytoskeleton in yeast. Mol Cell Biol *26*, 617-629.

Ghislain, M., Udvardy, A., and Mann, C. (1993). S. cerevisiae 26S protease mutants arrest cell division in G2/metaphase. Nature *366*, 358-362.

Gidalevitz, T., Ben-Zvi, A., Ho, K.H., Brignull, H.R., and Morimoto, R.I. (2006). Progressive disruption of cellular protein folding in models of polyglutamine diseases. Science *311*, 1471-1474.

Gokhale, K.C., Newnam, G.P., Sherman, M.Y., and Chernoff, Y.O. (2005). Modulation of prion-dependent polyglutamine aggregation and toxicity by chaperone proteins in the yeast model. J Biol Chem *280*, 22809-22818.

Guarente, L., and Kenyon, C. (2000). Genetic pathways that regulate ageing in model organisms. Nature *408*, 255-262.

Kenyon, C. (2005). The plasticity of aging: insights from long-lived mutants. Cell *120*, 449-460.

Kopito, R.R. (2000). Aggresomes, inclusion bodies and protein aggregation. Trends Cell Biol *10*, 524-530.

Matsumoto, G., Kim, S., and Morimoto, R.I. (2006). Huntingtin and mutant SOD1 form aggregate structures with distinct molecular properties in human cells. J Biol Chem *281*, 4477-4485.

Matsumoto, G., Stojanovic, A., Holmberg, C.I., Kim, S., and Morimoto, R.I. (2005). Structural properties and neuronal toxicity of amyotrophic lateral sclerosis-associated Cu/Zn superoxide dismutase 1 aggregates. J Cell Biol *171*, 75-85.

McClellan, A.J., Scott, M.D., and Frydman, J. (2005a). Folding and quality control of the VHL tumor suppressor proceed through distinct chaperone pathways. Cell *121*, 739-748.

McClellan, A.J., Tam, S., Kaganovich, D., and Frydman, J. (2005b). Protein quality control: chaperones culling corrupt conformations. Nat Cell Biol *7*, 736-741.

Melville, M.W., McClellan, A.J., Meyer, A.S., Darveau, A., and Frydman, J. (2003). The Hsp70 and TRiC/CCT chaperone systems cooperate in vivo to assemble the von Hippel-Lindau tumor suppressor complex. Mol Cell Biol *23*, 3141-3151.

Meriin, A.B., Zhang, X., Miliaras, N.B., Kazantsev, A., Chernoff, Y.O., McCaffery, J.M., Wendland, B., and Sherman, M.Y. (2003). Aggregation of expanded polyglutamine domain in yeast leads to defects in endocytosis. Mol Cell Biol *23*, 7554-7565.

Morley, J.F., Brignull, H.R., Weyers, J.J., and Morimoto, R.I. (2002). The threshold for polyglutamine-expansion protein aggregation and cellular toxicity is dynamic and influenced by aging in Caenorhabditis elegans. Proc Natl Acad Sci U S A *99*, 10417-10422.

Morley, J.F., and Morimoto, R.I. (2004). Regulation of longevity in Caenorhabditis elegans by heat shock factor and molecular chaperones. Mol Biol Cell *15*, 657-664.

Muchowski, P.J. (2002). Protein misfolding, amyloid formation, and neurodegeneration: a critical role for molecular chaperones? Neuron *35*, 9-12.

Muchowski, P.J., Ning, K., D'Souza-Schorey, C., and Fields, S. (2002). Requirement of an intact microtubule cytoskeleton for aggregation and inclusion body formation by a mutant huntingtin fragment. Proc Natl Acad Sci U S A *99*, 727-732.

Muchowski, P.J., Schaffar, G., Sittler, A., Wanker, E.E., Hayer-Hartl, M.K., and Hartl, F.U. (2000). Hsp70 and hsp40 chaperones can inhibit self-assembly of polyglutamine proteins into amyloid-like fibrils. Proc Natl Acad Sci U S A *97*, 7841-7846.

Muchowski, P.J., and Wacker, J.L. (2005). Modulation of neurodegeneration by molecular chaperones. Nat Rev Neurosci *6*, 11-22.

Murphy, C.T., McCarroll, S.A., Bargmann, C.I., Fraser, A., Kamath, R.S., Ahringer, J., Li, H., and Kenyon, C. (2003). Genes that act downstream of DAF-16 to influence the lifespan of Caenorhabditis elegans. Nature *424*, 277-283.

Outeiro, T.F., and Lindquist, S. (2003). Yeast cells provide insight into alpha-synuclein biology and pathobiology. Science *302*, 1772-1775.

Outeiro, T.F., and Muchowski, P.J. (2004). Molecular genetics approaches in yeast to study amyloid diseases. J Mol Neurosci *23*, 49-60.

Rubinsztein, D.C. (2007). Autophagy induction rescues toxicity mediated by proteasome inhibition. Neuron *54*, 854-856.

Sakahira, H., Breuer, P., Hayer-Hartl, M.K., and Hartl, F.U. (2002). Molecular chaperones as modulators of polyglutamine protein aggregation and toxicity. Proc Natl Acad Sci U S A *99 Suppl 4*, 16412-16418.

Schaffar, G., Breuer, P., Boteva, R., Behrends, C., Tzvetkov, N., Strippel, N., Sakahira, H., Siegers, K., Hayer-Hartl, M., and Hartl, F.U. (2004). Cellular toxicity of polyglutamine expansion proteins: mechanism of transcription factor deactivation. Mol Cell *15*, 95-105.

Shaner, N.C., Campbell, R.E., Steinbach, P.A., Giepmans, B.N., Palmer, A.E., and Tsien, R.Y. (2004). Improved monomeric red, orange and yellow fluorescent proteins derived from Discosoma sp. red fluorescent protein. Nat Biotechnol *22*, 1567-1572.

Sherman, M.Y., and Goldberg, A.L. (2001). Cellular defenses against unfolded proteins: a cell biologist thinks about neurodegenerative diseases. Neuron *29*, 15-32.

Tkach, J.M., and Glover, J.R. (2004). Amino acid substitutions in the C-terminal AAA+ module of Hsp104 prevent substrate recognition by disrupting oligomerization and cause high temperature inactivation. The Journal of biological chemistry *279*, 35692-35701.

Warrick, J.M., Chan, H.Y., Gray-Board, G.L., Chai, Y., Paulson, H.L., and Bonini, N.M. (1999). Suppression of polyglutamine-mediated neurodegeneration in Drosophila by the molecular chaperone HSP70. Nature genetics *23*, 425-428.

Winzeler, E.A., Shoemaker, D.D., Astromoff, A., Liang, H., Anderson, K., Andre, B., Bangham, R., Benito, R., Boeke, J.D., Bussey, H., *et al.* (1999). Functional characterization of the S. cerevisiae genome by gene deletion and parallel analysis. Science (New York, NY *285*, 901-906.

Chapter 4

Conclusion and Future Directions

Section 4.1: Summary

The formation of intracellular inclusions containing aggregated proteins has long been understood to be a hallmark of neurodegenerative disease (Dobson, 2006). More recently, inclusion formation has been identified as a highly regulated pathway that is essential for proper management of the cellular protein misfolding load and suppression of aggregate-induced toxicity (Arrasate et al., 2004; Cohen et al., 2006; Matsumoto et al., 2006; Matsumoto et al., 2005; Taylor et al., 2003). The data presented in this study argue for a general model explaining the role of misfolded protein inclusion formation in cytosolic quality control. We show that inclusions observed previously with different aggregation-prone substrates correspond to two quality control compartments, conserved in yeast and mammalian cells, each with a particular function in maintaining cellular protein folding homeostasis. One compartment, the JUNQ, which interacts with the nuclear envelope/ER network, concentrates chaperones and proteasomes and serves as a degradation and re-folding platform for soluble misfolded proteins that are not harmful to the cell, and are productively dealt with by the cellular quality control machinery. When the capacity of the quality control or degradative machinery is exceeded, or stressful conditions generate an abundance of potentially toxic aggregates, misfolded proteins are routed to another compartment, the IPOD, which is completely isolated from the cytosol and which houses insoluble aggregates which are sequestered there or are eventually degraded by autophagy.

An interesting finding presented in our results, is that the ubiquitination state of a misfolded protein determines whether it is routed to the soluble JUNQ compartment, or the insoluble IPOD "sequestration" compartment. Blocking the ubiquitination of a soluble misfolded protein that would normally accumulate in the JUNQ upon proteasome inhibition re-routs it entirely to the IPOD. Conversely, enhancing the ubiquitination of a protein that normally is found only in the IPOD "rescues" some of it to the JUNQ. What is quite striking, is that enhancing the ubiquitination of an insoluble protein destined for sequestration in the IPOD, causes the ubiquitinated fraction to be solubilized, and this process is toxic to the cell. Although it is not clear whether ubiquitination itself results in increased solubility of the amyloidogenic protein, or whether the ability to ubiquitinate a

misfolded protein is coupled to its interaction with chaperones and other quality control machinery, ubiquitination clearly partitions misfolded proteins between a "productive" degradation /refolding pathway, and a terminal path to aggregation and sequestration.

Our data helps to explain previous observations of different types of aggregated protein inclusions observed in different organisms from yeast to mammals, and provides a way of understanding why only a select number of amyloidogenic proteins accumulate in disease associated inclusions and cause toxicity, while most proteins capable of aggregating are not harmful. We suggest that amyloidogenic disease associated proteins and prions have a unique property that results in their decreased interaction with the cellular quality control machinery and preferential targeting to the IPOD insoluble compartment. This would explain why these proteins in particular cause disease and lead to amyloidosis. We cannot at present determine whether the inefficient interaction of prions and amyloidogenic disease-related proteins is what makes them toxic, or whether they are not recognized by the quality control machinery in the same way as other misfolded substrates are, precisely because accumulation of these proteins in the JUNQ would be toxic. The results we observed after rendering a normally insoluble prion a more efficient ubiquitination substrate would argue for the latter model. Enhancing ubiquitination of a prion made it accumulate in the JUNQ, and also rendered it more soluble. This, in turn, lead to inappropriate interactions between the ubiquitinated prion and the cellular quality control machinery, including Hsp70. This eventually resulted in the inhibition of soluble misfolded protein degradation, and cell death. It is important to note that none of the toxic aggregated species tested in our study appeared to cause direct proteasome inhibition, as assayed using native model proteasome substrates (data not shown). This suggests that toxic aggregates inhibit or titrate away quality control components required for misfolded protein ubiquitination and delivery to the proteasome, rather than the UPS itself. However, given our observation that proteasomes re-distribute heavily around the JUNQ upon misfolded protein accumulation there, it is also possible that excessive accumulation of aggregates in the JUNQ could also eventually inhibit parts of the UPS.

We propose that the JUNQ and IPOD are general quality control compartments that are always present in cells and are essential for efficient quality control of protein

folding and cell survival. Consistent with this, we observed pre-existing insoluble protein deposits forming the core of IPODs we observed with ectopically expressed aggregation-prone proteins. Additionally, Hsp104, which is localized predominantly to the IPOD, can be seen there in normal cells, not expressing model aggregating proteins. It is possible, therefore, that a certain subset of misfolded proteins is always sequestered in the IPOD, rather than be exposed to the quality control machinery, where these proteins may cause damage. When one of these potentially toxic proteins is inappropriately engaged by the quality control machinery, it inhibits it and causes cytotoxicity. Alternatively, some basic property of amyloidogenic proteins causes them to interact poorly with the quality control ubiquitination machinery, and they are sequestered to the IPOD so as not to inhabit the cytosol where the quality control machinery would be unable to degrade them. When this process becomes disregulated, these toxic aggregates accumulate in the cytosol and eventually cause toxicity by irreversibly binding chaperones.

Section 4.2: Future Directions

The results described here provide the basis for several exciting avenues of inquiry into the basis for neurotoxicity of aggregates, and the functioning of cellular quality control. The toxic effect of enhancing Rnq1 ubiquitination, suggests that Hsp70 may be a limiting factor in cytosolic quality control and that its titration by toxic aggregating species like Ub-Rnq1 and HttQ103ΔP results in the inhibition or misfolded protein degradation, as evidence by the subsequent accumulation and co-aggregation of VHL. If this is the case, over-expression of Hsp70 would be expected to reverse the inhibition of VHL degradation, as it rescues toxicity. Since the toxic effect of aggregates has been ascribed to their inhibition of a number of sub-cellular processes, the system we have developed offers a unique opportunity to test these models. For example, toxicity has been linked to proteasome inhibition, perturbation of the protein folding homeostasis, and titration of essential quality control components (Bence et al., 2001; Gidalevitz et al., 2006; Matsumoto et al., 2005; Schaffar et al., 2004). In future experiments, model proteins

used in our study will be used as reporters of these different aspects of quality control (Fig. 4.1). Ubc9^{ts} is a meta-stable thermo-sensitive protein that can serve as a reporter of protein folding homeostasis and the function of the cellular chaperone network. VHL is a soluble misfolded protein that is constantly turned over by the quality control/UPS machinery, and can therefore serve as a reporter of misfolded protein degradation (as described in Chapter 3). Finally, Ub-Arg-GFP can be used as native reporters of the UPS, since it is efficiently ubiquitinated and degraded but does not require chaperones for degradation. These experiments will determine whether any or all of these pathways are affected by toxic aggregates.

Since ubiquitination is a requirement for partitioning to the JUNQ compartment, and since even soluble quality control substrates are re-routed to the IPOD when their ubiquitination is blocked, the IPOD formation phenotype can be used to score for components essential for misfolded protein ubiquitination. To date, there have been no E3 enzymes identified for cytosolic quality control in yeast, as described in Chapter 1. In addition to E3s, other factors, such as chaperones may be required for efficient soluble misfolded protein degradation. In future studies, the genome-wide yeast deletion library expressing Ubc9^{ts} or VHL will be screened for IPOD formation using high-throughput microscopy. Deletion strains lacking an essential factor for misfolded protein ubiquitination will form an IPOD, which will be scored for using GFP for the misfolded protein and NLS-TFP for the nucleus. The advantage of this approach is that it not only scores for inhibition of misfolded protein degradation, but also the qualitative localization of the misfolded protein, indicative of a defect machinery required for its ubiquitination.

Other studies will focus on identifying the components required for delivery of proteins to the JUNQ and the IPOD. The easily scorable puncta or IPOD formation phenotypes can be used to screen for components required for delivery to the JUNQ, using microscopy as the readout. Alternatively, both the puncta, JUNQ, and IPOD can be purified biochemically, and mass-spectroscopy can be used to determine what factors co-purify with them. This will lead to the identification of candidates for aggregate delivery to the IPOD, which can then be tested using a number of previously described model quality control substrates. The JUNQ and puncta can most easily be purified using sucrose gradient fractionation, whereas the IPOD can be purified using FACS sorting,

due to its large size, insolubility, and high GFP fluorescence (when a GFP-tagged protein localizes to the IPOD).

Purification of the IPOD will yield a number of other important sets of data. In addition to components required for transport of proteins to the IPOD or the JUNQ, both inclusions will also contain quality control components that are sequestered in each compartment, and knowing which proteins bind to which inclusion will help characterized the essential or limiting factors titrated out by the inclusions. Additionally, if the IPOD indeed has an autophagic role as suggested by data shown in Chapter 2, this will also be confirmed by its purification and mass-spec analysis. IPODs formed from different amyloidogenic proteins will be compared by mass-spec, as well as toxic vs non-toxic inclusions, to better assess the molecular basis for toxicity.

Finally, our findings suggest that the IPOD compartment is continually present in some normal cells, as evidenced by Hsp104 localization to IPOD-like inclusions. The idea that a subset of proteins in any given cell is always more likely to aggregate over the course of stressful events, or just cellular homeostasis, is exciting and bares further investigation. It could be that these proteins share structural features that lead them to preferentially form amyloids, or that some proteins simply misfold more readily and therefore a fraction of them is routed to the IPOD over the course of normal quality control and exposure to stress. Determining whether the same proteins are always present in IPODs, and which proteins these are, will be invaluable for understanding the basis for conformational disorders and toxicity of protein aggregation.

Figure 4.1

Using reporters to assess which stages of the quality control pathway are inhibited by toxic misfolded proteins.

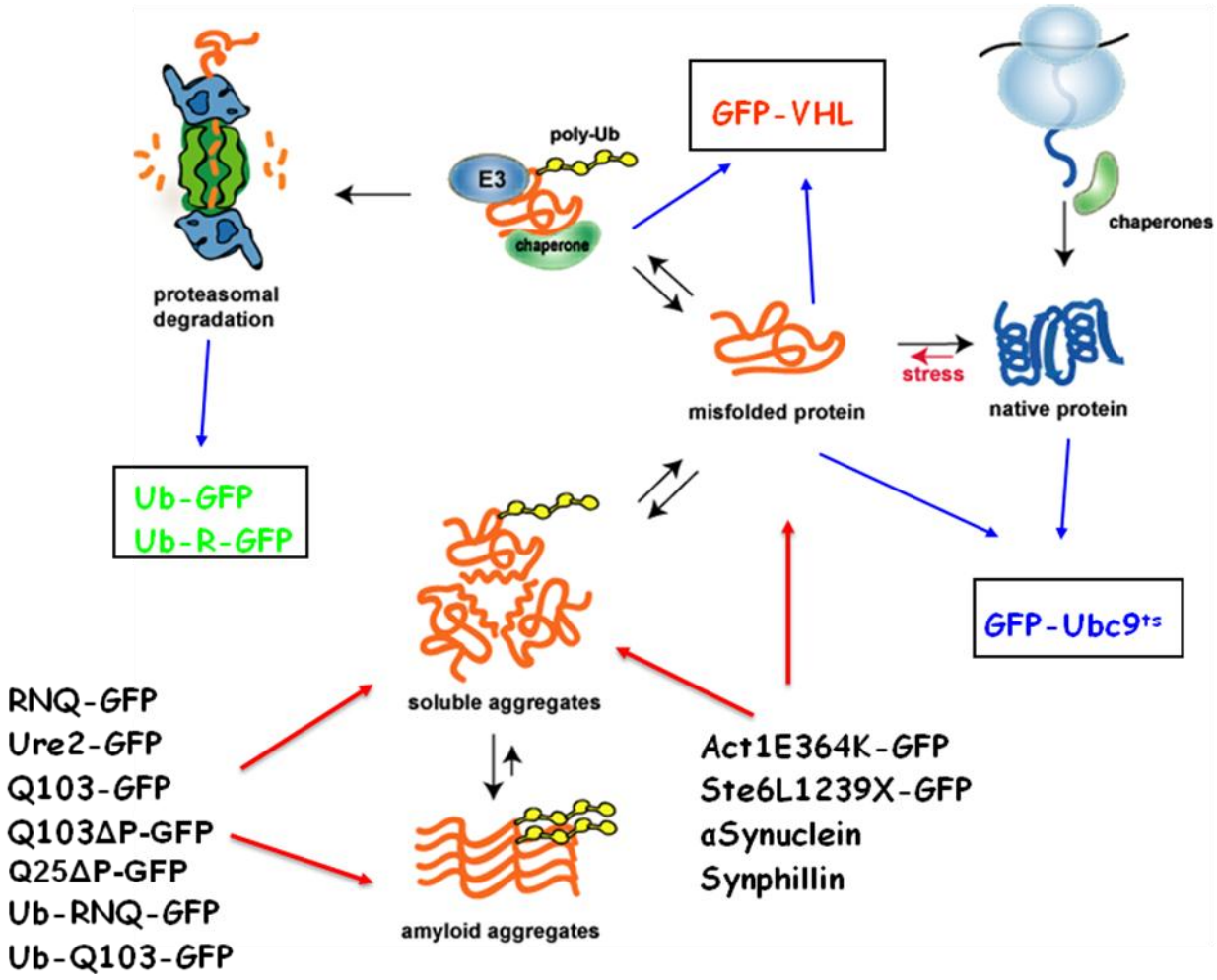

Section 4.3: References

Arrasate, M., Mitra, S., Schweitzer, E.S., Segal, M.R., and Finkbeiner, S. (2004). Inclusion body formation reduces levels of mutant huntingtin and the risk of neuronal death. Nature *431*, 805-810.

Bence, N.F., Sampat, R.M., and Kopito, R.R. (2001). Impairment of the ubiquitin-proteasome system by protein aggregation. Science *292*, 1552-1555.

Cohen, E., Bieschke, J., Perciavalle, R.M., Kelly, J.W., and Dillin, A. (2006). Opposing activities protect against age-onset proteotoxicity. Science *313*, 1604-1610.

Dobson, C.M. (2006). Protein aggregation and its consequences for human disease. Protein Pept Lett *13*, 219-227.

Gidalevitz, T., Ben-Zvi, A., Ho, K.H., Brignull, H.R., and Morimoto, R.I. (2006). Progressive disruption of cellular protein folding in models of polyglutamine diseases. Science *311*, 1471-1474.

Matsumoto, G., Kim, S., and Morimoto, R.I. (2006). Huntingtin and mutant SOD1 form aggregate structures with distinct molecular properties in human cells. J Biol Chem *281*, 4477-4485.

Matsumoto, G., Stojanovic, A., Holmberg, C.I., Kim, S., and Morimoto, R.I. (2005). Structural properties and neuronal toxicity of amyotrophic lateral sclerosis-associated Cu/Zn superoxide dismutase 1 aggregates. J Cell Biol *171*, 75-85.

Schaffar, G., Breuer, P., Boteva, R., Behrends, C., Tzvetkov, N., Strippel, N., Sakahira, H., Siegers, K., Hayer-Hartl, M., and Hartl, F.U. (2004). Cellular toxicity of polyglutamine expansion proteins: mechanism of transcription factor deactivation. Mol Cell *15*, 95-105.

Taylor, J.P., Tanaka, F., Robitschek, J., Sandoval, C.M., Taye, A., Markovic-Plese, S., and Fischbeck, K.H. (2003). Aggresomes protect cells by enhancing the degradation of toxic polyglutamine-containing protein. Hum Mol Genet *12*, 749-757.